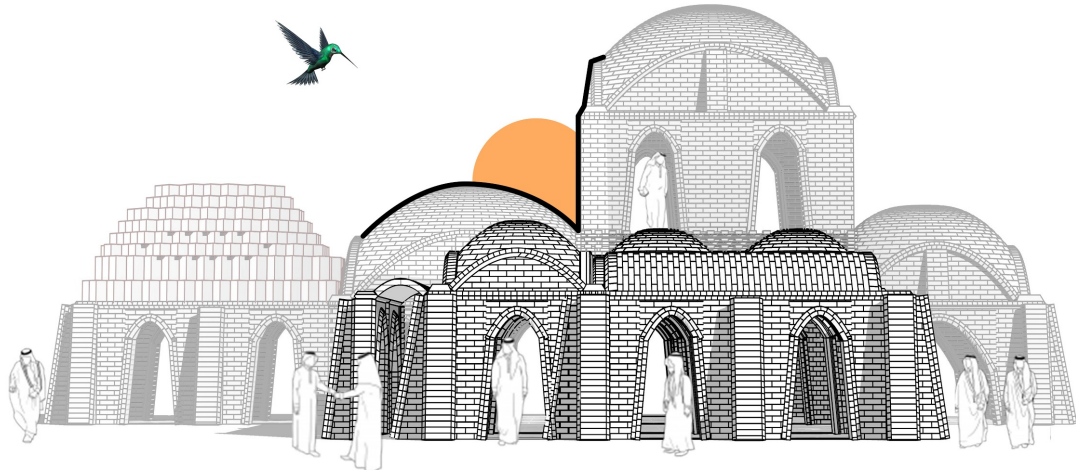


MODUL_ABILITY

AR3B011 Earthy



Flexible Housing

Mentors

Dr. Pirouz Nourian

Ir. Hans Hoogenboom

Ir. Shervin Azadi

Dr. Fred Veer

Ir. Dirk Rinse Visser

Group 6

Alessandro Passoni	4949838
Alessio Vigorito	4946219
Fredy Fortich	4821858
Kiana Mousavi	4878736
Stephanie Moumdjian	4907663



Contents

1 Introduction

- 1.1 Zaatari refugee camp
- 1.2 Context
- 1.3 Design goals and principles
- 1.4 Flowchart

2 Configuring

- 2.1 Cultural analysis

- 2.2 Bubble diagrams

- 2.3 Rel Charts

- 2.4 Concept diagrams

- 2.5 Program of requirements

- 2.6 Units and modules

- 2.7 Game rules

- 2.8 Architecture translation to domino code

- 2.9 Documentation

- 2.10 Computational urban growth

- 2.10.1 Introduction

- 2.10.2 Goals

- 2.10.3 Plug-in “WASP” and Software

- 2.10.3.1 Tools and Platform

- 2.10.3.2 Role of each Tools in the Aggregation

- 2.10.3.3 About Wasp

- 2.10.4 Methodology of Work

- 2.10.4.1 Preparation of the Wasp setting in Grasshopper

- 2.10.4.1 Modeling Phase of the Geometries

- 2.10.5 Inputs Adaptation

- 2.10.5.1 Association of Functions to Connection Points

- 2.10.5.2 Connection Points Location

- 2.10.6 Adaptation of Corner Modules

- 2.10.7 Collider as Non-Built Spaces

- 2.10.8 Visualization

- 2.10.8.1 Geometry Alteration

- 2.10.8.2 Color Coding
- 2.10.9 Limitations
 - 2.10.9.1 Control of Ratio Parts
 - 2.10.9.2 Scattered Collider
 - 2.10.9.3 Corner System
- 2.10.10 Future Developments
 - 2.10.10.1 Second Storey Level
 - 2.10.10.2 Dominant Rule
 - 2.10.10.3 Closed Connection Possibilities
- 2.11 Physical model

3 Forming

4 Structuring

- 4.1 Introduction
- 4.2 Methodology
 - 4.2.1 Geometry design and mesh refinement
 - 4.2.2 Form-finding
 - 4.2.3 Karamba settings
 - 4.2.4 Loadcases
 - 4.2.5 Evolutionary solver
- 4.3 Evaluation and discussion of results
 - 4.3.1 Four dome unit
 - 4.3.2 Large dome unit
 - 4.3.3 Riwaq unit
- 4.4 Conclusion and limitations

5 Bibliography

Appendix A

Appendix B - Analysis of adobe bricks



1 Introduction

1.1 Zaatari refugee camp

Located in Jordan, Al Zaatri camp has been home to Syrian refugees since the summer of 2012 as masses of refugees crossed the border. Supported by The UN Refugee Agency, the camp offers different facilities including health facilities, youth centers, schools and kindergartens, water facilities, recreational areas, playgrounds, mosques, community offices and recycling facilities (UNHCR, 2019).

Since the emergence of the camp, the population started to increase dramatically until 2013. As of today, almost 80000 people live on the camp from which around 56% of them are children and teenagers (UNHCR, 2018).

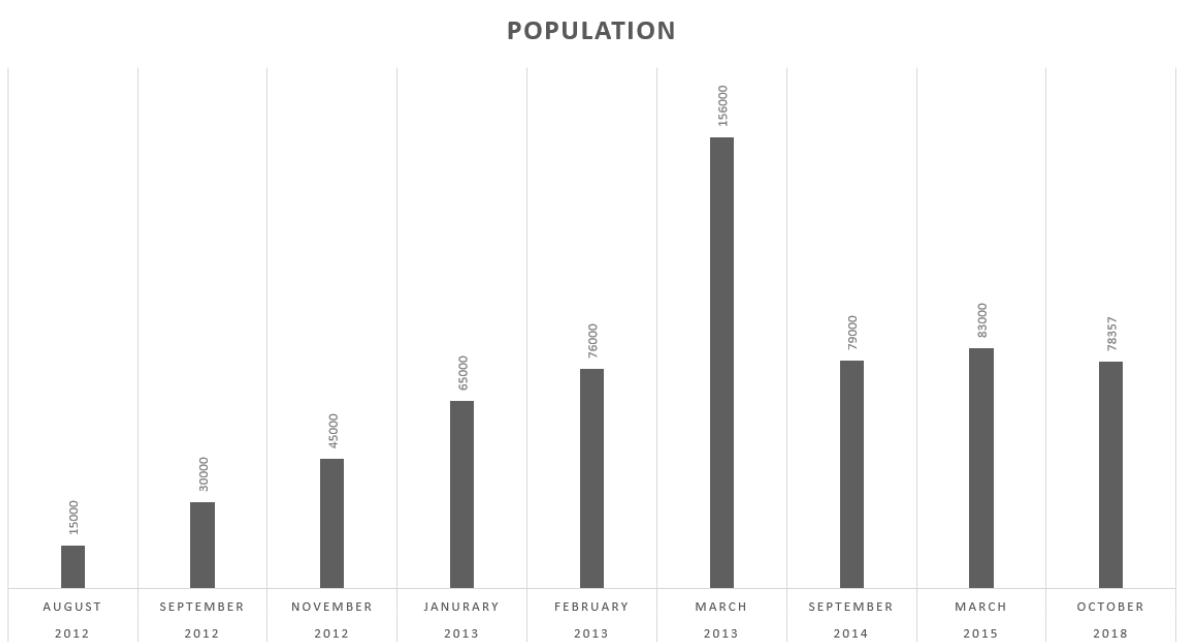


Figure 1.1: Demographic evolution of the camp (source: own work)

Currently, the camp has 12 districts. However, it is important to mention that the emergence of the camp started from district 1 and 2 and expanded in several stages.

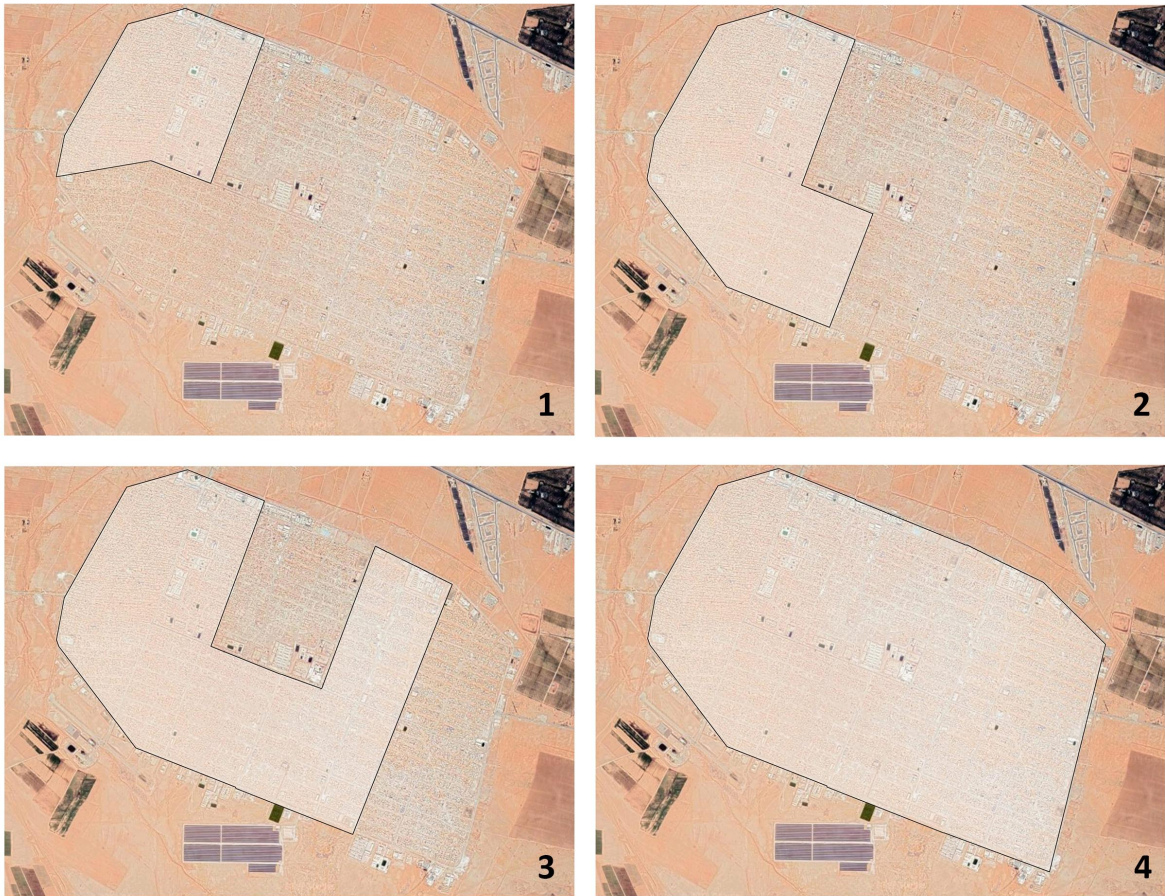


Figure 1.2: Order of the emergence of the camp (source: Timár, 2016)

At first, refugees were accommodated in tents. In 2015, the shelter type of households were 79.7% caravans, 9.5% tents and the rest, a combination of caravans and tents (Unicef, 2015).

1.2 Context

To be able to analyze the quality of life in the camp, to understand the daily struggles of the refugees there and to accurately determine the problems and needs, we looked into the documentary, Salam Neighbor (2015), which was specifically made about the Al Zaatri camp in Jordan. Salam Neighbor depicted how the people have adapted themselves to the life in the camp and how they were thriving to make it a home away from home. Many small and intricate details shown in the documentary gave us various leads on what people were expecting from the housing in the camp and that they had hope to rebuild their lives.

“People showed us that they had a different concept of space; of how their settlement should look like. We were building a camp, they were building a city. Nonprofits and The UN don’t have the expertise to set up a city, they need support from city planners, etc. Currently Zaatri remains a short term solution for a long term problem”

As a first step of the design process, a location had to be chosen. During the site analysis, it was noticed that the household density per hectare per each district was different and districts 1 and 2 had the highest density compared to the other districts (Unicef, 2015).

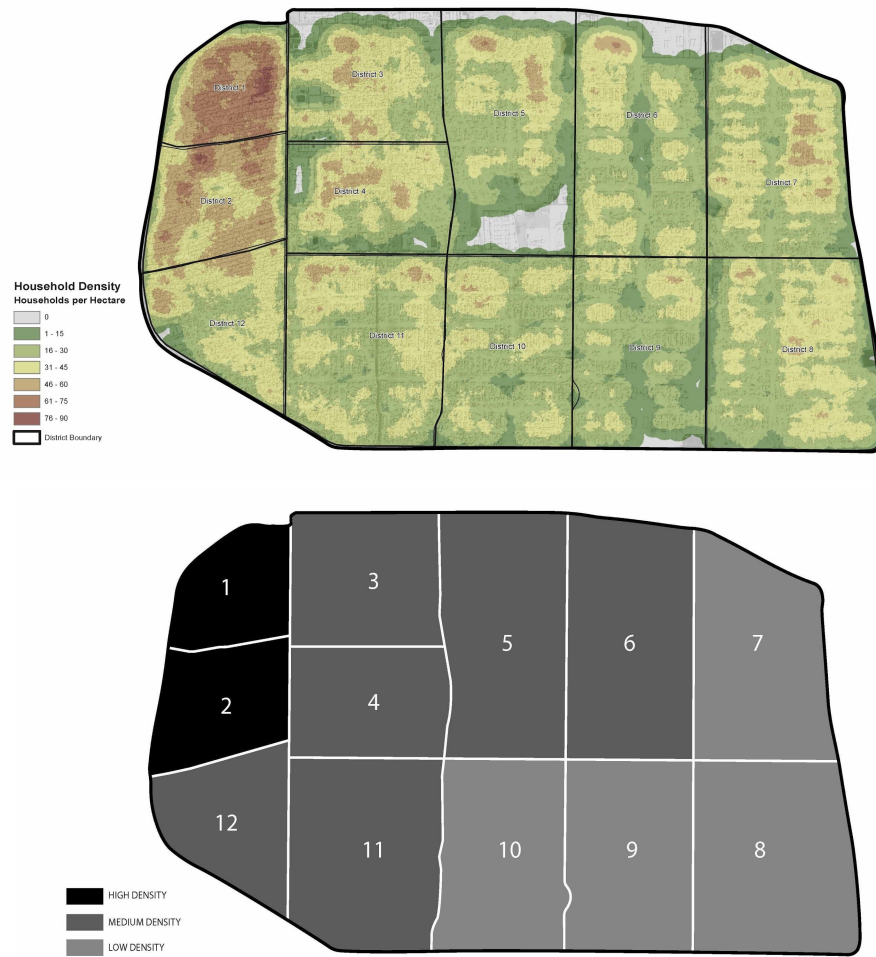


Figure 1.3: Comparison of household density per hectare in different districts (Source up: Unicef, 2015. Source bottom: own work)

Also, in district 2, more than 80% of the area was built, while in the other districts this number was less than 60%. So as a team, we decided to focus on district 2 and make a balance between the built area percentage of this district and the others. However, it has to be mentioned that the resulted design is applicable to all the other districts too as it is a rule-based system.

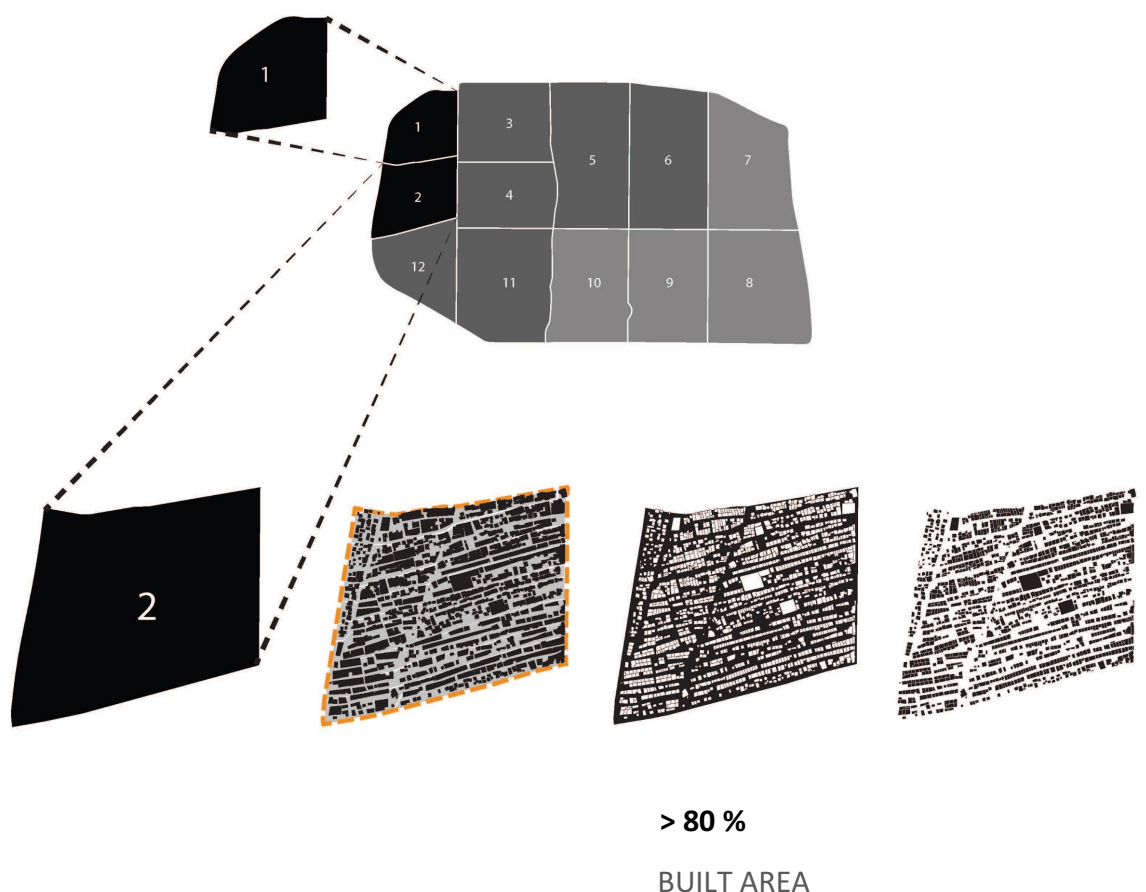


Figure 1.4: Density district analysis (source: own work)

1.3 Design goals and principles

The dynamic population of the camp was the first motivation to design an adaptive and flexible housing. The context analysis made it clear that people wanted to be more engaged in the activities of the camp which could also develop and enhance the sense of ownership of the space in them. This sense of belonging could be actuated by living in a house that has a similar type of architecture and responds to the cultural needs of the people. As a result, the following points were set as the goals of the project:

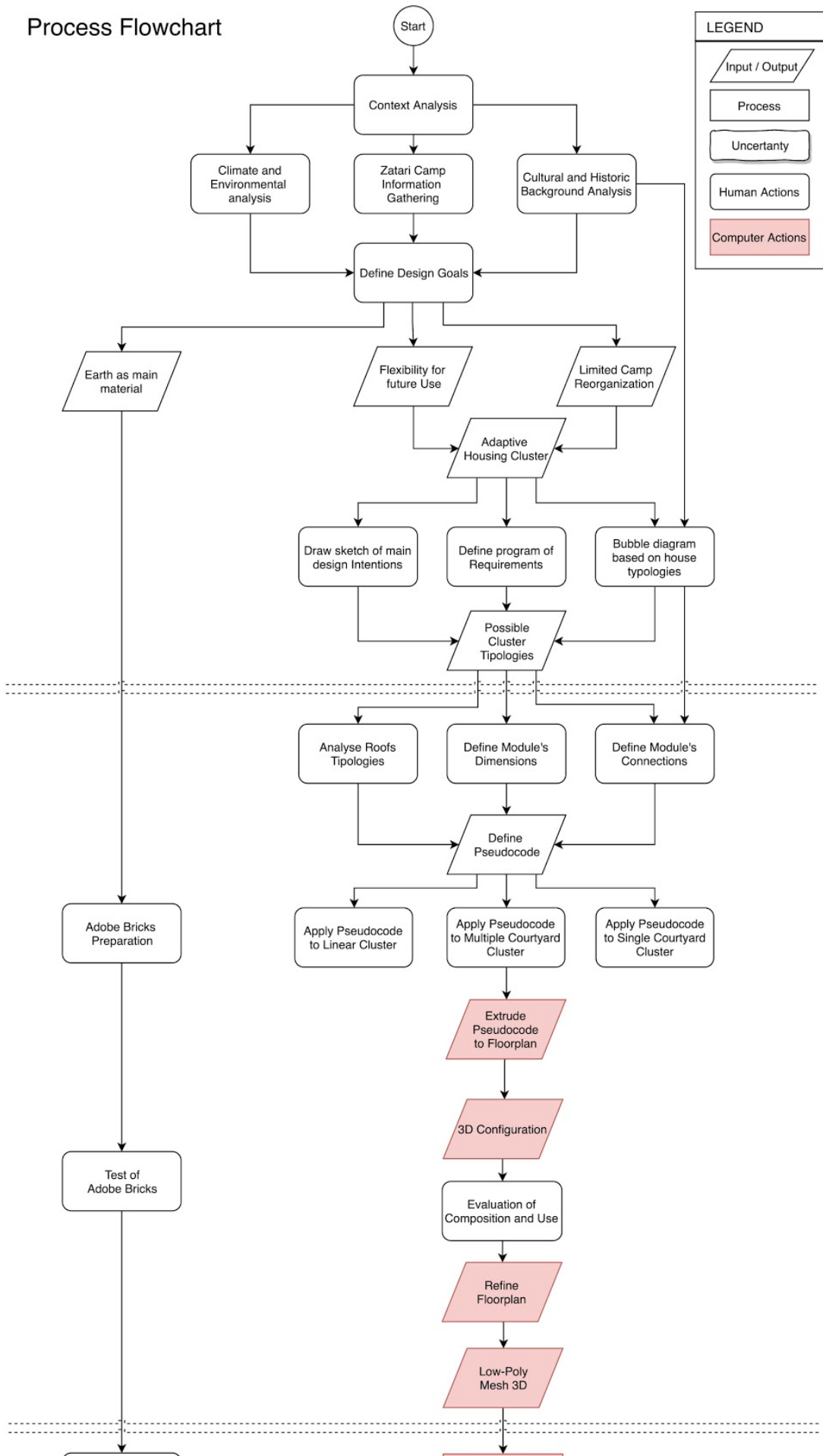
- To devise an **affordable and fast earth-based** housing
- Housing that stays true to the **cultural** and climatic background and typology
- Housing with access to **open spaces**
- Designing a **community integrated** district to improve the social interactions and values
- **Flexibility of usage** for future growth and functions.
- **Flexible configurations** that can serve multiple or different uses in the future
- **Feasibility of construction**; allowing people to participate in the construction process

To achieve the mentioned goals, the following principles were defined:

- **Modular** pieces for ease of construction and simplicity, thus; creating a construction catalog that includes the instructions on how to build the housing
- **Rule-Based** design for compliance with communal and cultural typology
- **Rule-Based** design to allow for the concept of flexibility and modularity and to enable the possibility of future growth according to the defined rules
- Proper **orientation** of spaces for passive climate control

1.4 Flowchart

Process Flowchart



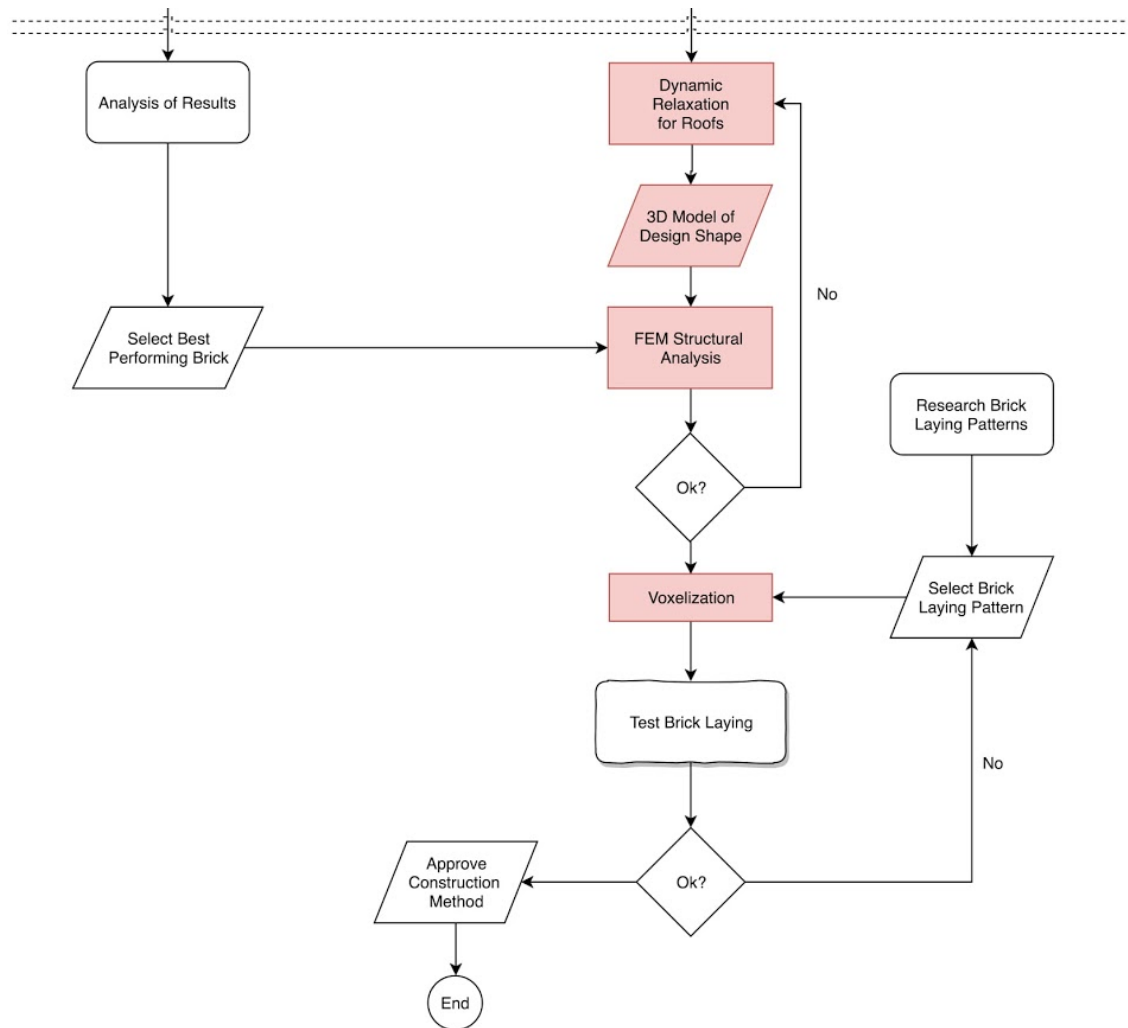


Figure 1.5: Process flowchart (source: own work)



2 Configuring

2.1 Cultural analysis

According to CORPUS Levant (2004), there are seven different types of housing in Syria:

- The Tent
- The Basic House
- The House with a Riwaq
- The House with a Liwan
- The Rural House with Courtyard
- The Urban House with Courtyard
- The Lebanese House

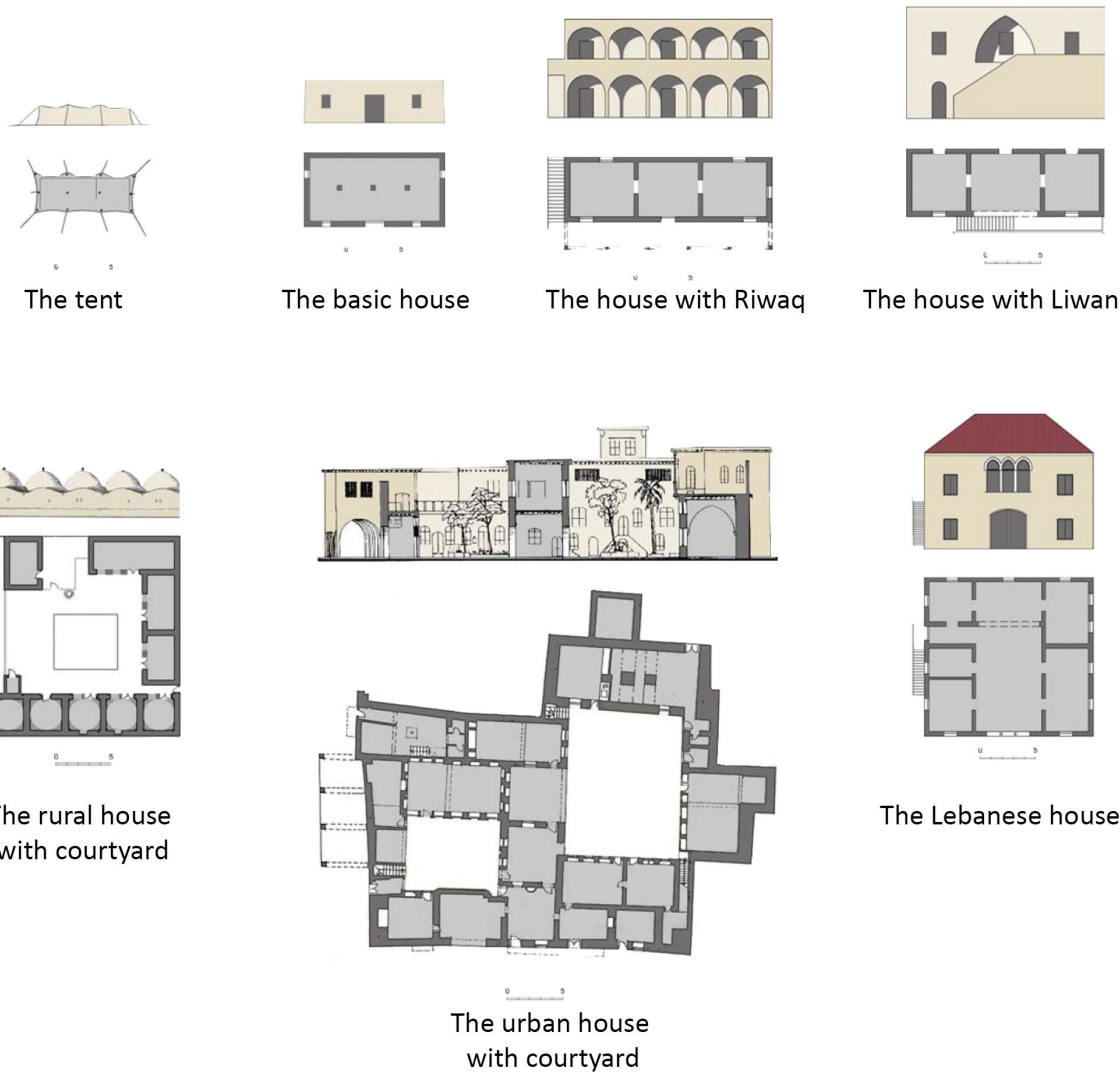
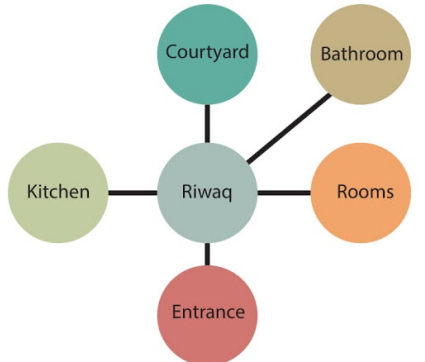


Figure 2.1: Different Syrian housing typologies (source: CORPUS Levant, 2004)

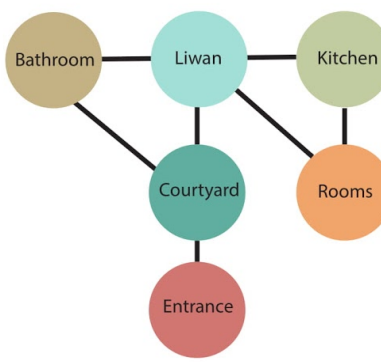
By looking into each of these typologies, their primary spaces were identified, and the connections between the spaces and the general architectural impression was analyzed which lead to the different bubble diagrams.

2.2 Bubble diagrams

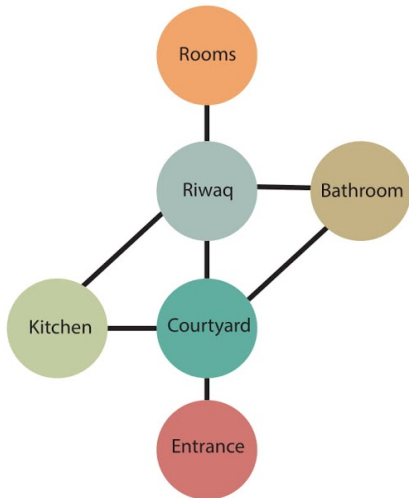
Based on the cultural analysis, four housing typology bubble diagrams were designed and some of their possible configurations as clusters were explored. In the designed bubble diagrams, bathrooms are considered as shared spaces inside the house due to the lack of infrastructure. Kitchen and courtyard are also considered as shared to allow people to communicate and socialize.



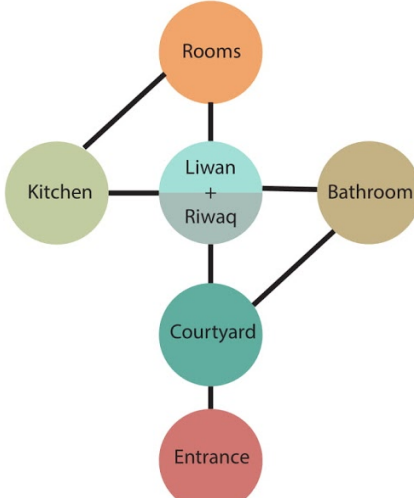
Typology 1



Typology 2

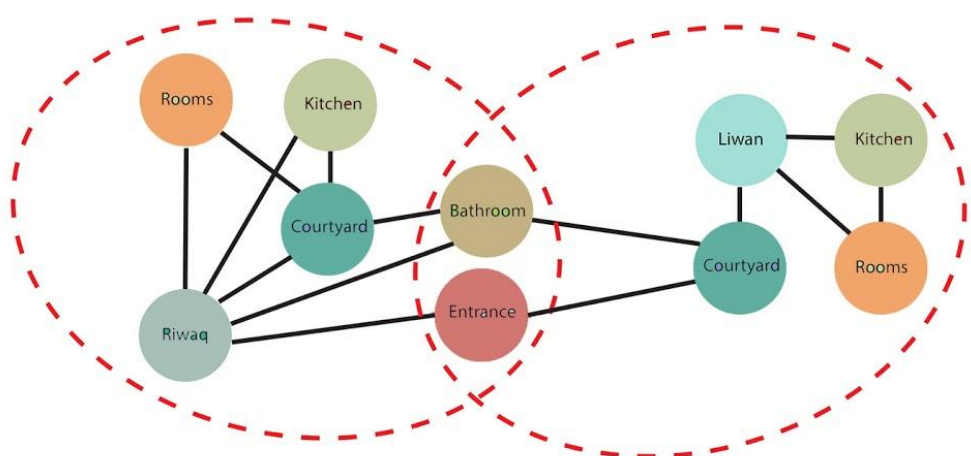
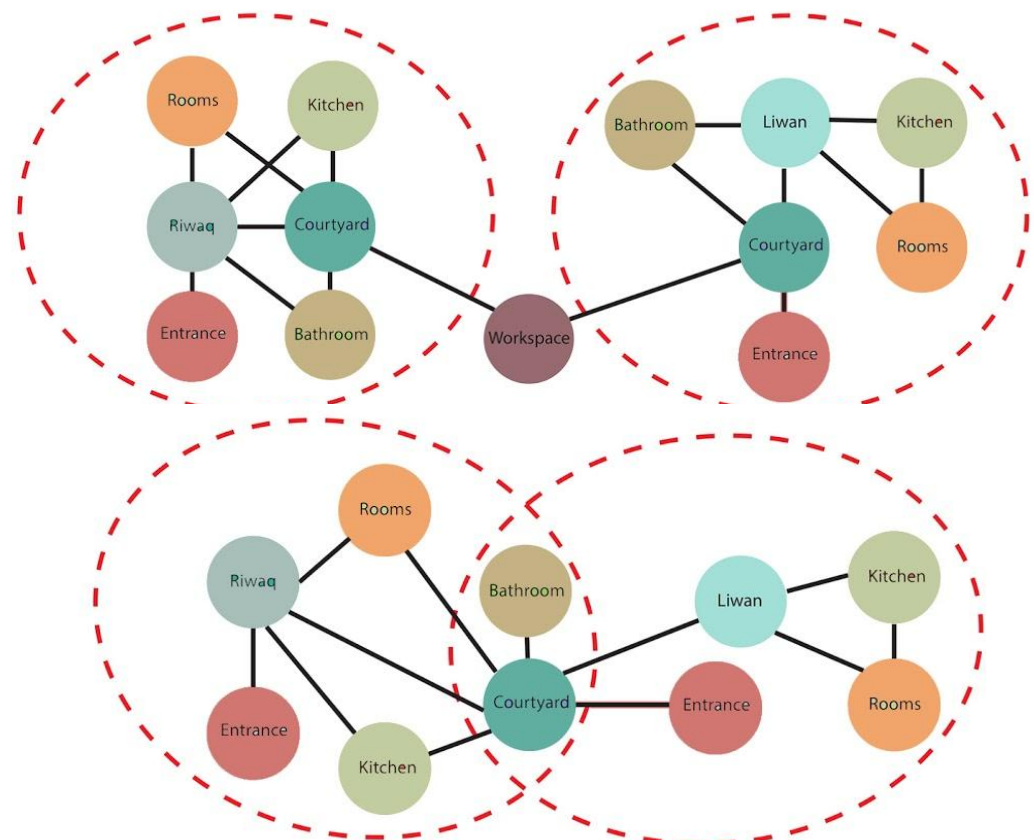


Typology 3



Typology 4

Figure 2.2: Bubble diagrams of the four designed typologies (source: own work)



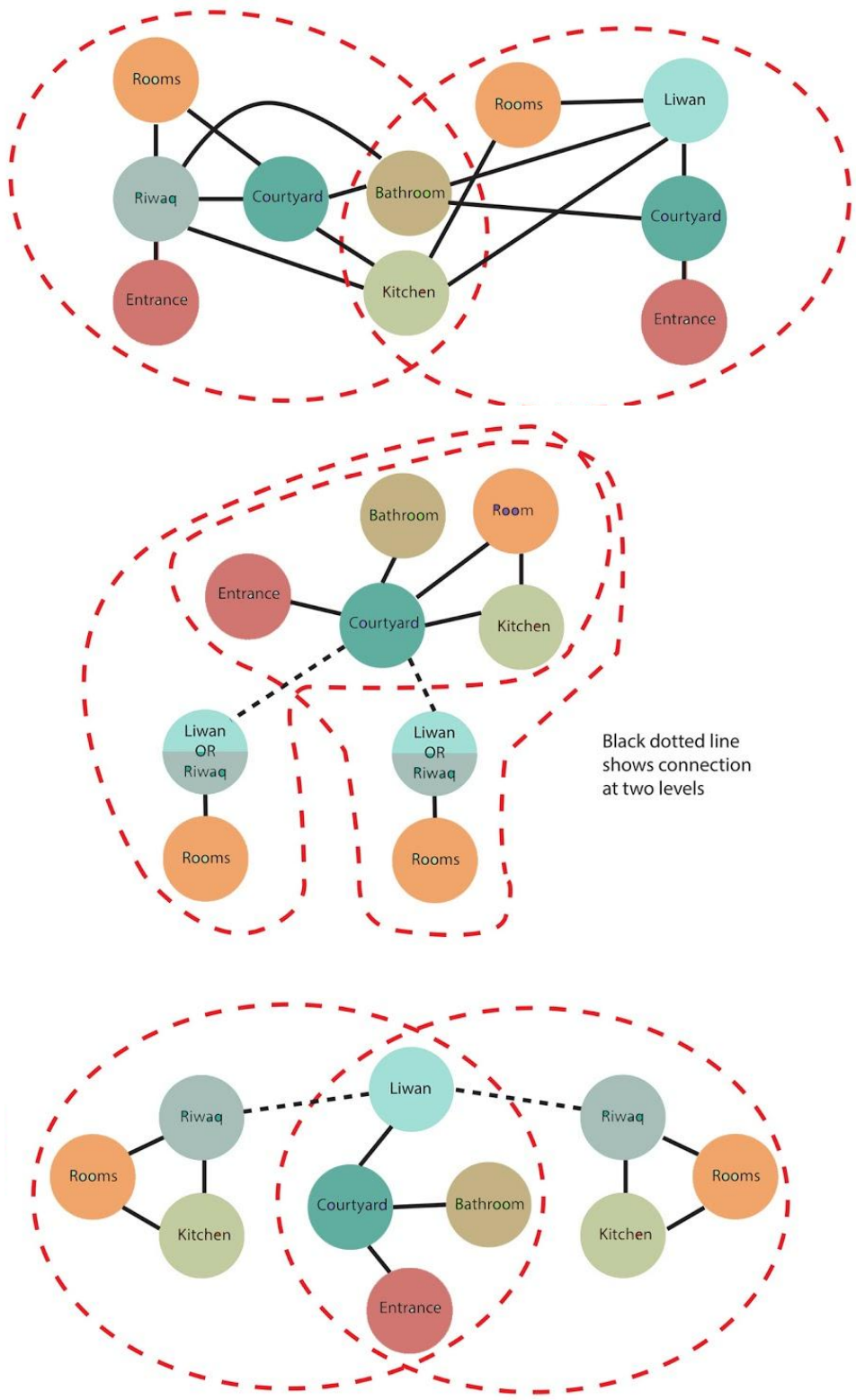


Figure 2.3: Bubble diagrams of the possible clusters (source: own work)

2.3 Rel Charts

Room		Entrance	Riwaq	Kitchen	Courtyard	Rooms	Bathroom
Typology 1	Room						
Entrance	Entrance	1					
Riwaq	Riwaq	0	1				
Kitchen	Kitchen	0	0	1			
Courtyard	Courtyard	0	0	1	0		
Rooms	Rooms	0	0	1	0	0	
Bathroom	Bathroom	0	0	1	0	0	1

Room		Entrance	Liwan	Courtyard	Kitchen	Rooms	Bathroom
Typology 2	Room						
Entrance	Entrance	1					
Liwan	Liwan	0	1				
Courtyard	Courtyard	1	0	1			
Kitchen	Kitchen	0	0	1	0		
Rooms	Rooms	0	0	1	0	1	
Bathroom	Bathroom	0	1	0	1	0	0

Room		Entrance	Riwaq	Courtyard	Kitchen	Rooms	Bathroom
Typology 3	Room						
Entrance	Entrance	1					
Riwaq	Riwaq	0	1				
Courtyard	Courtyard	1	0	1			
Kitchen	Kitchen	0	0	1	1		
Rooms	Rooms	0	0	1	0	0	
Bathroom	Bathroom	0	1	0	1	0	1

Room		Entrance	Riwaq/Liwan	Courtyard	Kitchen	Rooms	Bathroom
Typology 4	Room						
Entrance	Entrance	1					
Riwaq/Liwan	Riwaq/Liwan	0	1				
Courtyard	Courtyard	1	0	1			
Kitchen	Kitchen	0	0	1	0		
Rooms	Rooms	0	0	1	0	1	
Bathroom	Bathroom	0	1	0	1	0	0

Direct Connection	1
No Connection	0

Figure 2.4: Rel charts of the four designed typologies (source: own work)

2.4 Concept diagrams

In order to have a flexible housing that can accommodate the fluctuating population of the camp over time, the main goal is to have an adaptive and modular system that can grow and extend organically.

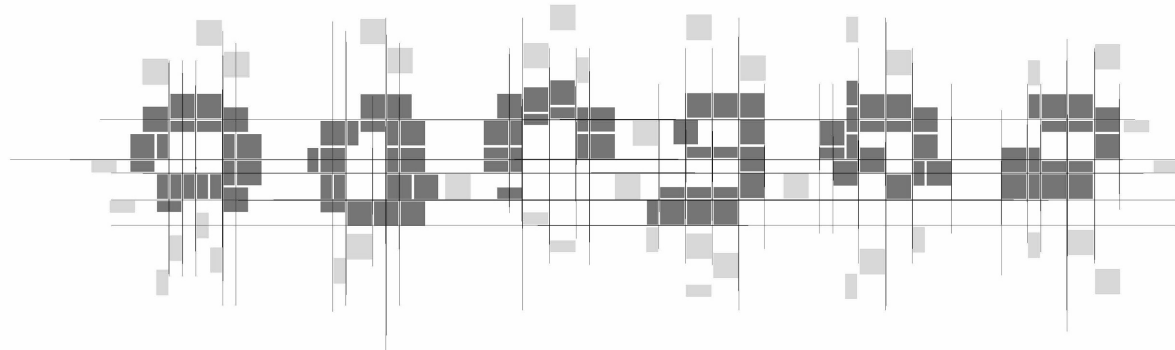


Figure 2.5: Designing an adaptive and modular system (source: own work)

In this system, houses have communal open spaces which follows the traditional Syrian architecture of having inner courtyards. For further flexibility, configurations can serve for different uses in the future.

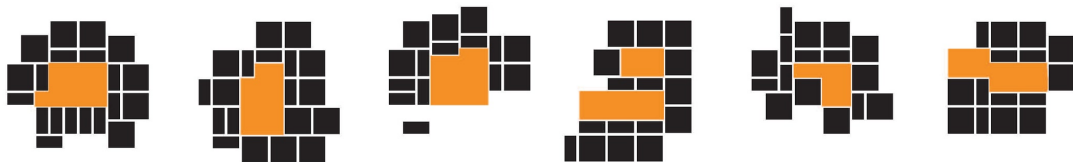


Figure 2.6: Housing with communal open spaces (source: own work)

To achieve a community-integrated district, clusters are created by merging the families together and sharing the facilities between them. Kitchen, bathroom and courtyard are shared between the families of one cluster. Shared kitchens would allow for women to communicate and shared bathrooms would require less water sewage system and infrastructure compared to one bathroom per family.



Figure 2.7: Creating clusters by sharing the facilities (source: own work)

In order to have a flexible built area and to lower the density of the built area in district 2, second stories are built which allows for future construction if needed.

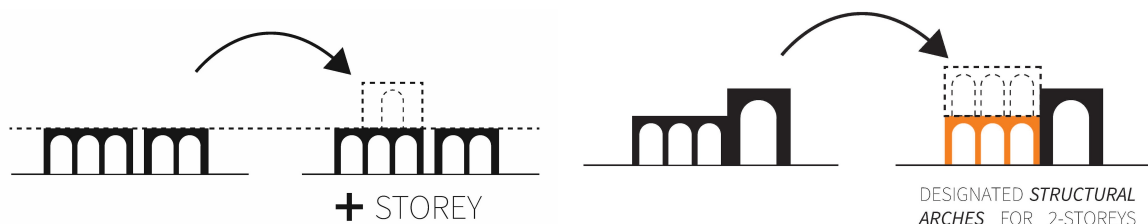


Figure 2.8: Design of second stories to provide adaptability and future growth (source: own work)

For the feasibility of construction which is a crucial part of the concept, a construction catalog is designed in which the components' list for all the modules is available.

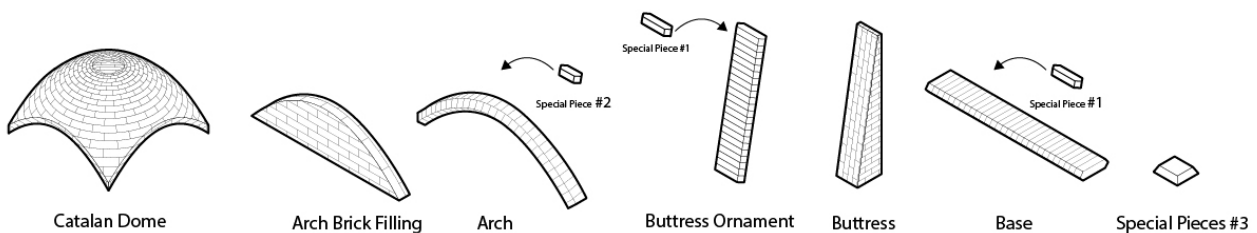


Figure 2.9: Components' list for the corner Riwaq module (source: own work)

2.5 Program of requirements

The spaces used in the design of the clusters have different requirements such as the amount of privacy they need, whether they need a roof on top and how much daylight they require.

Name of Space	Abbreviation	Privacy	Roof	Desired Area (m2)	Max No. of Occupants	Free Height (m)	Daylight Requirement
Entrance	E	Med	No	8	1	-	Low
Courtyard	C	Med	No	Varies	8	-	High
Riwaq (Open Gallery)	R	Med	Yes	8	4	3	Med
Bathroom	WC	High	Yes	8	1	2.5	Low
Kitchen	K	Med	Yes	16	4 - 8	3	Med
Bedroom	B	High	Yes	4 or 16	1-2	2.5	High

Figure 2.10: Program of requirements (source: own work)

2.6 Units and modules

The smallest piece, which is a unit, has the dimensions of 1.25m*125m. This unit makes up all the modules, which are 2, 4, 8, 9 and 16 units.

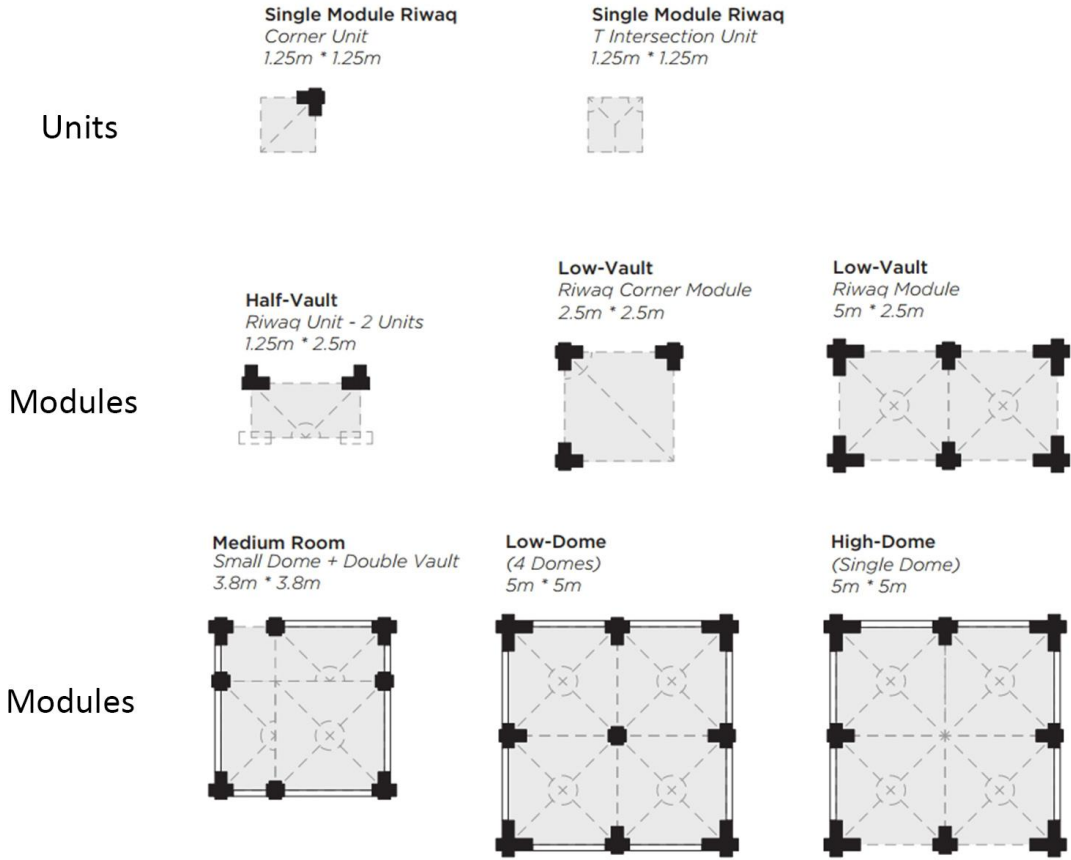


Figure 2.11: Units and modules (source: own work)

2.7 Game rules

After defining the modules, it was necessary to determine how their connections would work. Hence, a code was developed according to the evaluation ran on the connections among the spaces of the typical houses which were previously analyzed. Therefore, 8 main connections are defined: 5 on a 2D level and 3 on the 3D level.

On the 2D level, the A connection represents the main connection type. It connects the distribution spaces such as the big and small Riwaqs to each other and to the entrances of each module in correspondence to the doors. Connection B and C are similar, but still different. These two connections are designed as closed, meaning that it is not possible to pass from one module to another one if these connections are present. However, connection B can become a connection type A if it is required for the planning of the cluster (due to dual identity, it can create two scenarios). Therefore, the main entrance of each module is flexible and can be easily arranged in the allowed positions by the user. Lastly, connection type COURT connects the modules to an open space inside the cluster (a private courtyard) and EXT connect the modules to the outside environment (public space of the refugee camp and the urban area).

On the 3D level, the PLUS connection informs the user that is allowed to build on top of the module. For example, if 3 families are already living in the cluster and another family moves in, they can build their rooms on the second floor, on top of the rooms that allow for a construction on top. However, the TRIANGLE connection allows only the possibility of walking on top of the module. The CIRCLE connection exclude both possibilities. For instance, the entrance module and the kitchen do not allow for construction and walking on top of these modules.

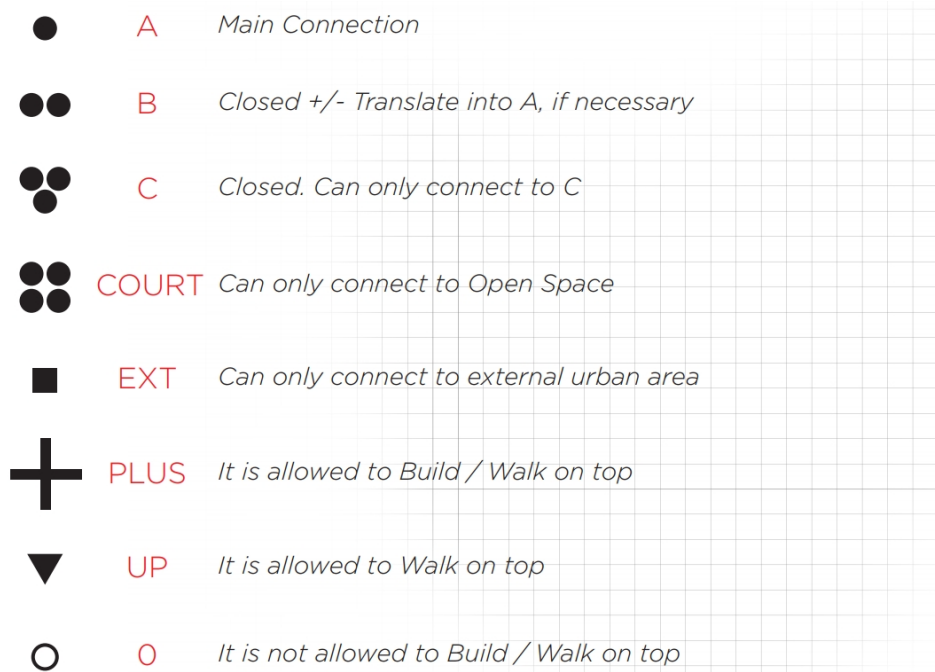


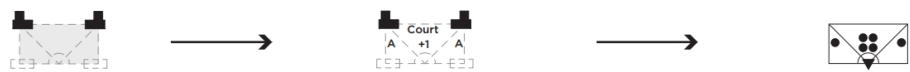
Figure 2.12: Game rules of the domino code (source: own work)

2.8 Architecture translation to domino code

The developed code applies to all the modules and it is therefore possible to translate it to architecture. Indeed, the relation between the code and the architectural expression of each module constitutes a method which can be easily interpreted and utilized by the refugees to create their own cluster of housing in complete safety. Indeed, the modules are all structurally independent from the others and can be connected safely by following the rules of the developed domino code.

To conclude, the code is designed in order to allow its transcription into a computational script to generate various clusters to reorganize the complete camp.

Half-Vault Unit



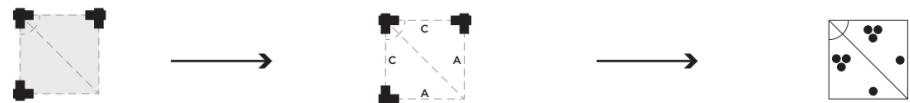
Corner Unit



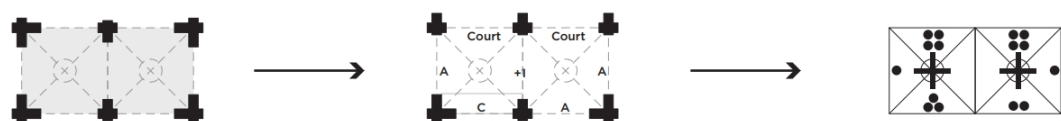
T Intersection Unit



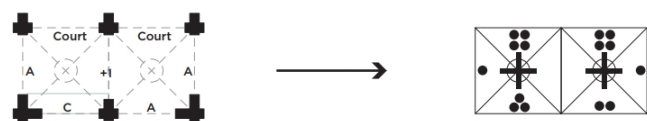
Riwaq Corner Module



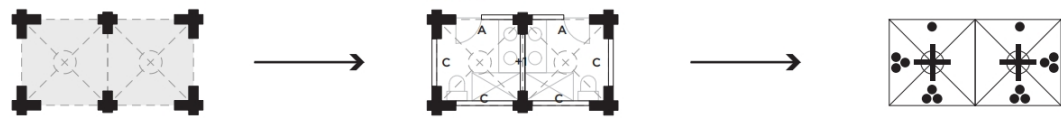
Low-Vault Module



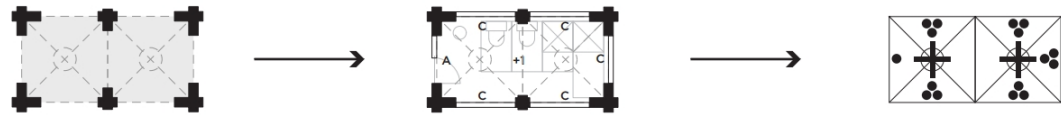
Riwaq Module



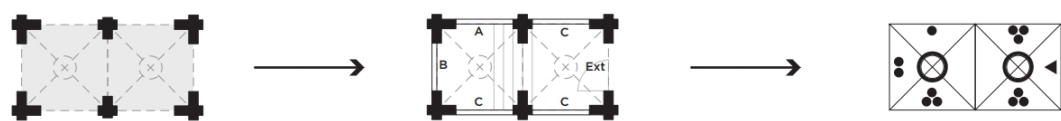
Bathroom Module
Type 1



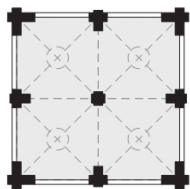
Bathroom Module
Type 2



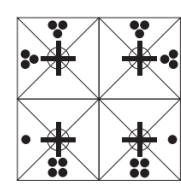
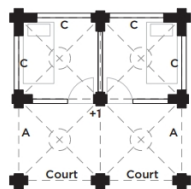
Entrance Module



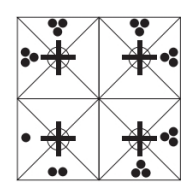
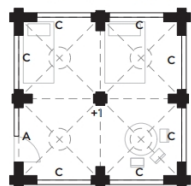
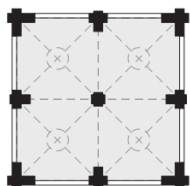
4 Low-Domes Module



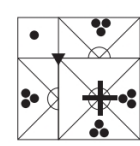
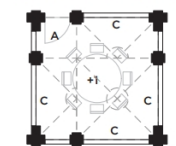
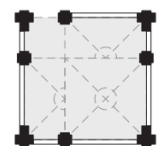
2 Small Rooms + Riwaq



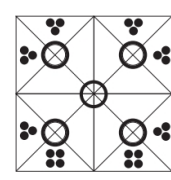
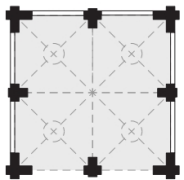
Large Room
with Central Column



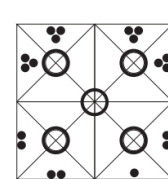
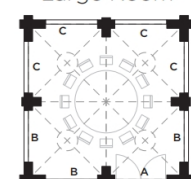
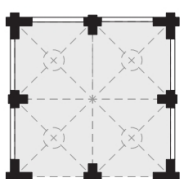
Medium Room



High - Dome



Large Room



Stairs Module

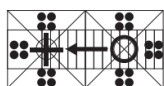


Figure 2.13: Architecture translation of the modules to domino pieces (source: own work)

In the example below, a possible connection of the modules is created which is based on the mentioned rules. Each module is translated to its domino piece and it can be seen that the architectural configuration and the

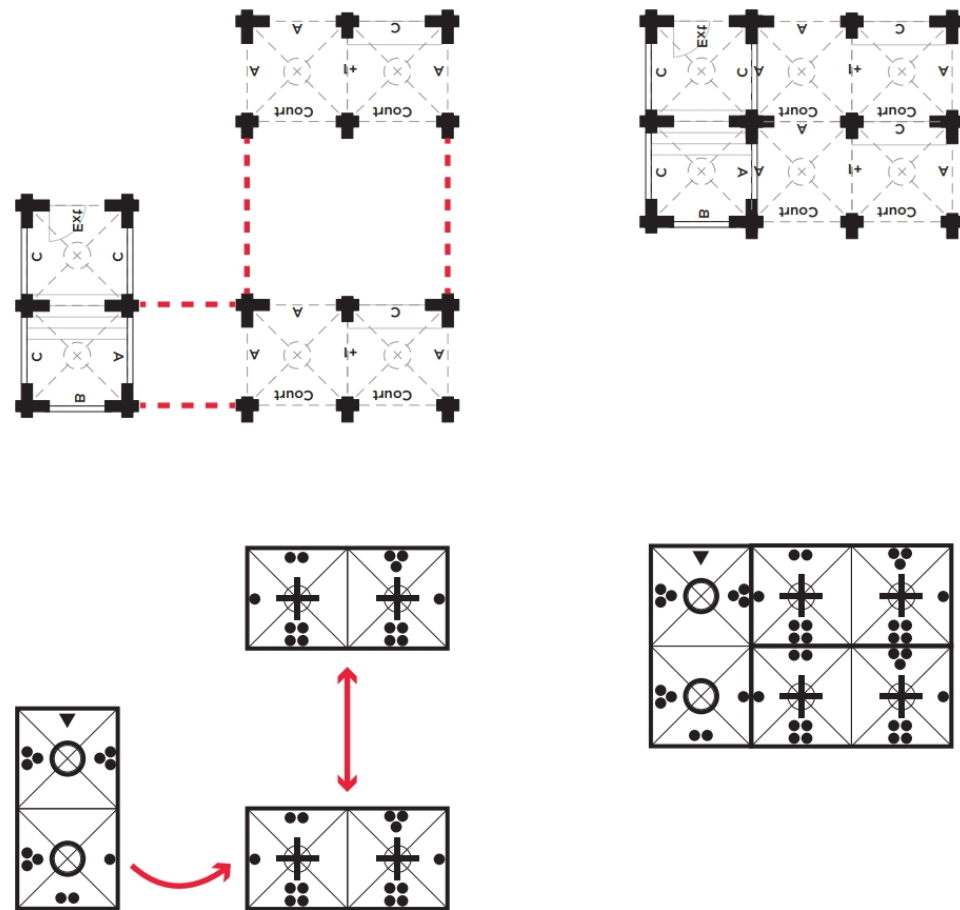


Figure 2.14: An example showing the connection of the modules and their translation to domino codes

(Source: own work)

As can be seen in the example below, all the modules that are connected to the courtyard are always 4 dots, as they can only be connected to an open space.

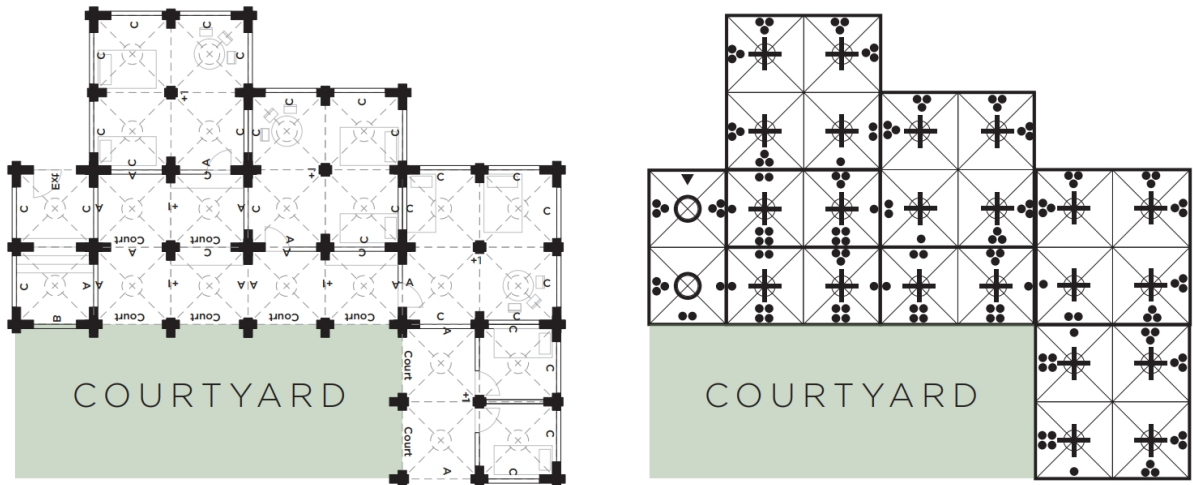


Figure 2.15: Connection of Court (4 dots) is always to an open space (source: own work)

2.9 Documentation

In this report, a cluster based on the developed rules is proposed to show the potential of the proposed system. The designed house consists of a ground floor level and a first floor level. It is notable that on the first floor, the Riwaqs are not allowed to be built. Nevertheless, the cloth provided by the refugee camp can be utilized as a shading element and to highlight the distribution area. Moreover, since the first floor is not provided with a common courtyard, terraces are created to provide open space and private terraces to the families which may live on this level.

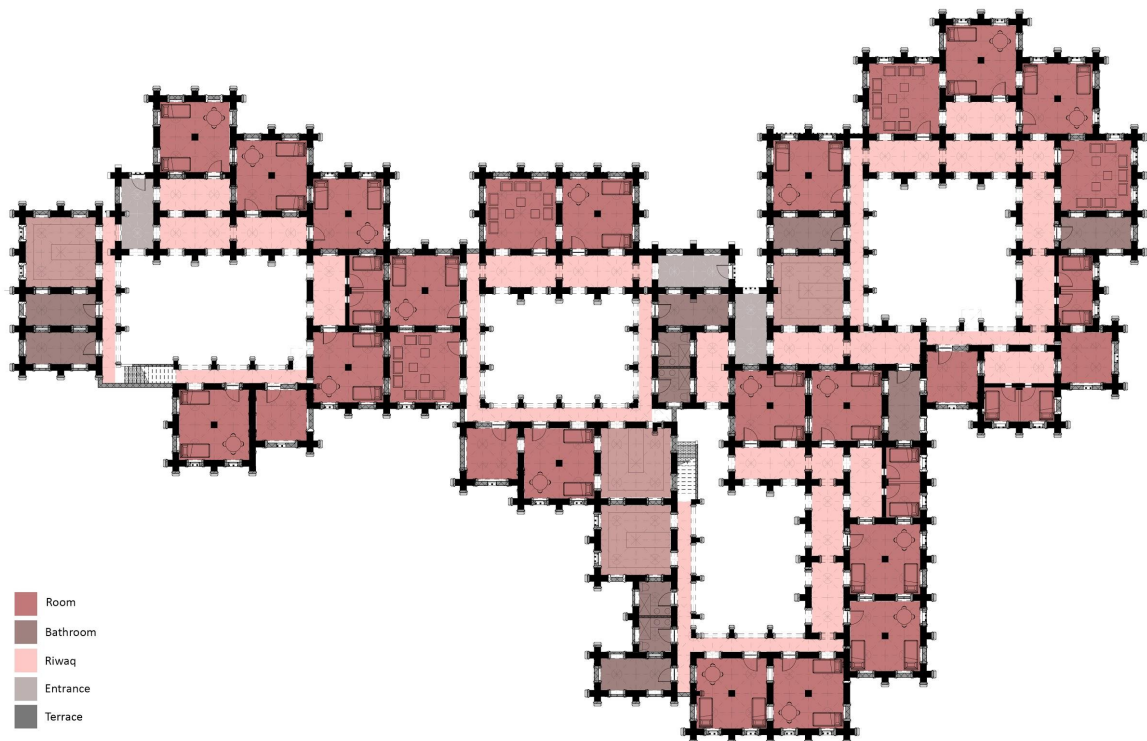


Figure 2.16: Floor plan level 0 (source: own work)

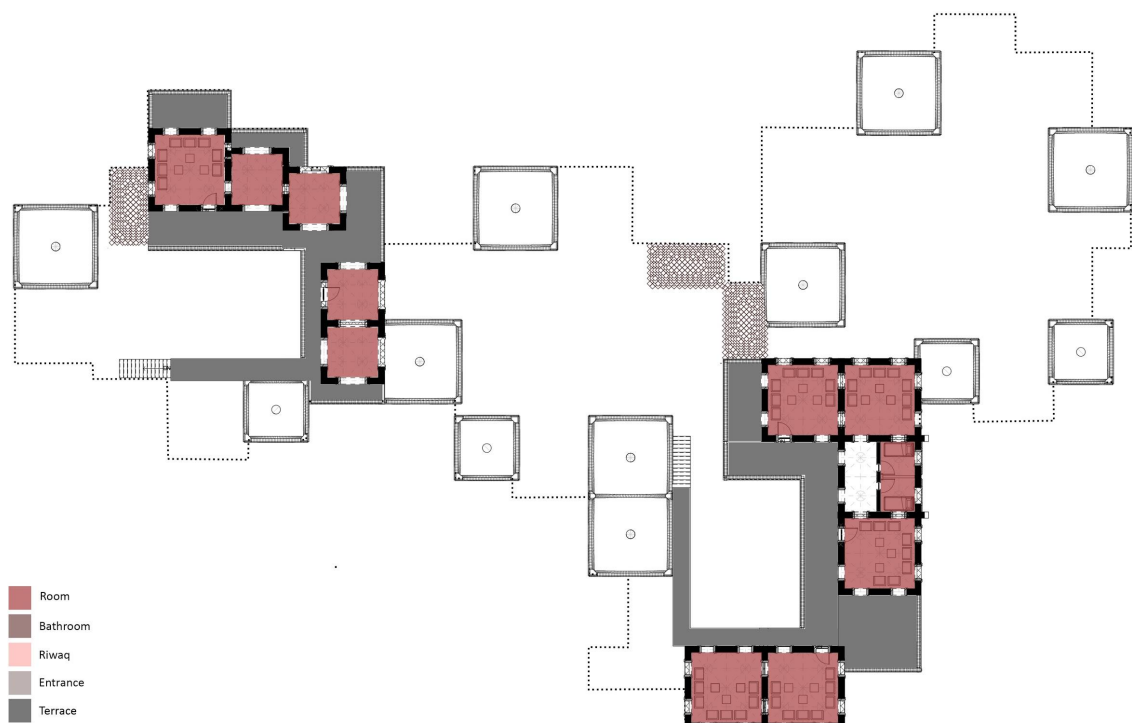


Figure 2.17: Floor plan level 1 (source: own work)

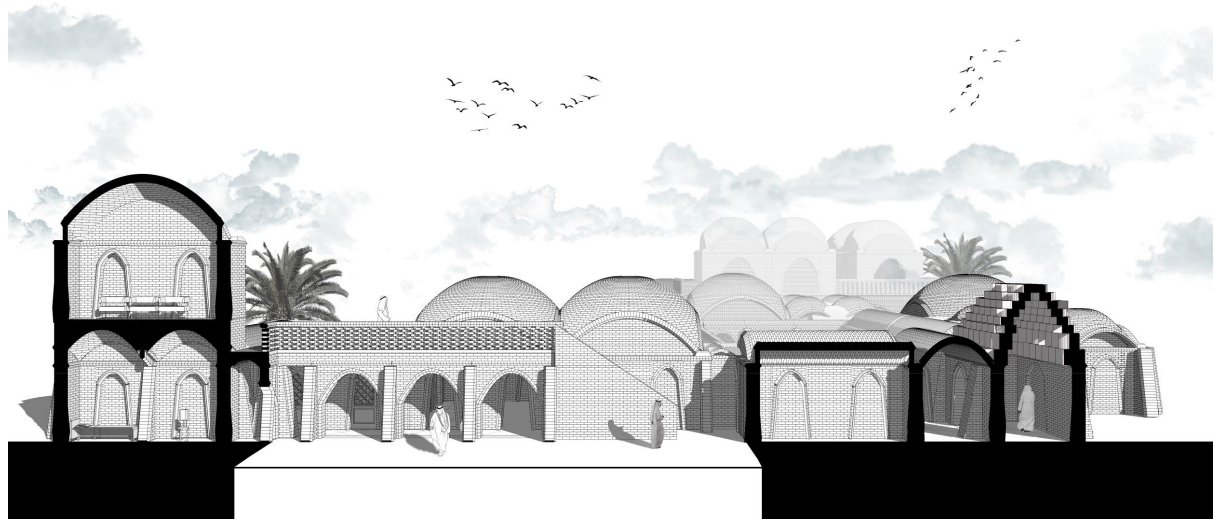


Figure 2.18: Section 1 (source: own work)

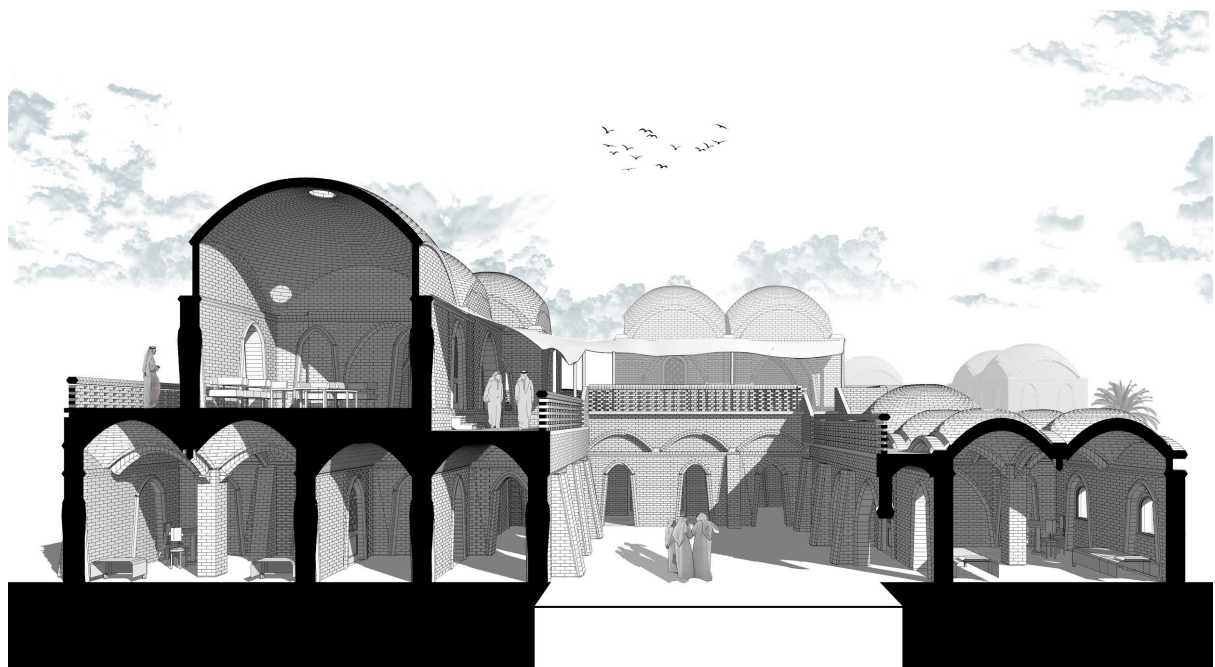


Figure 2.19: Section 2 (source: own work)



Figure 2.20: Section 3 (source: own work)

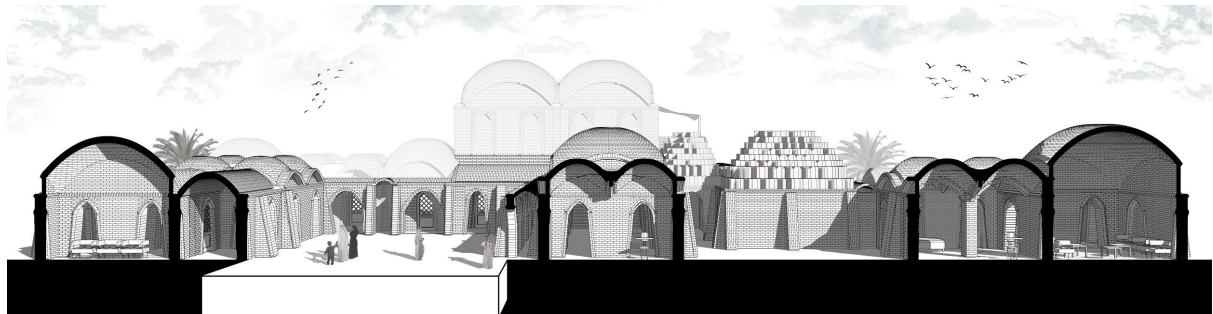
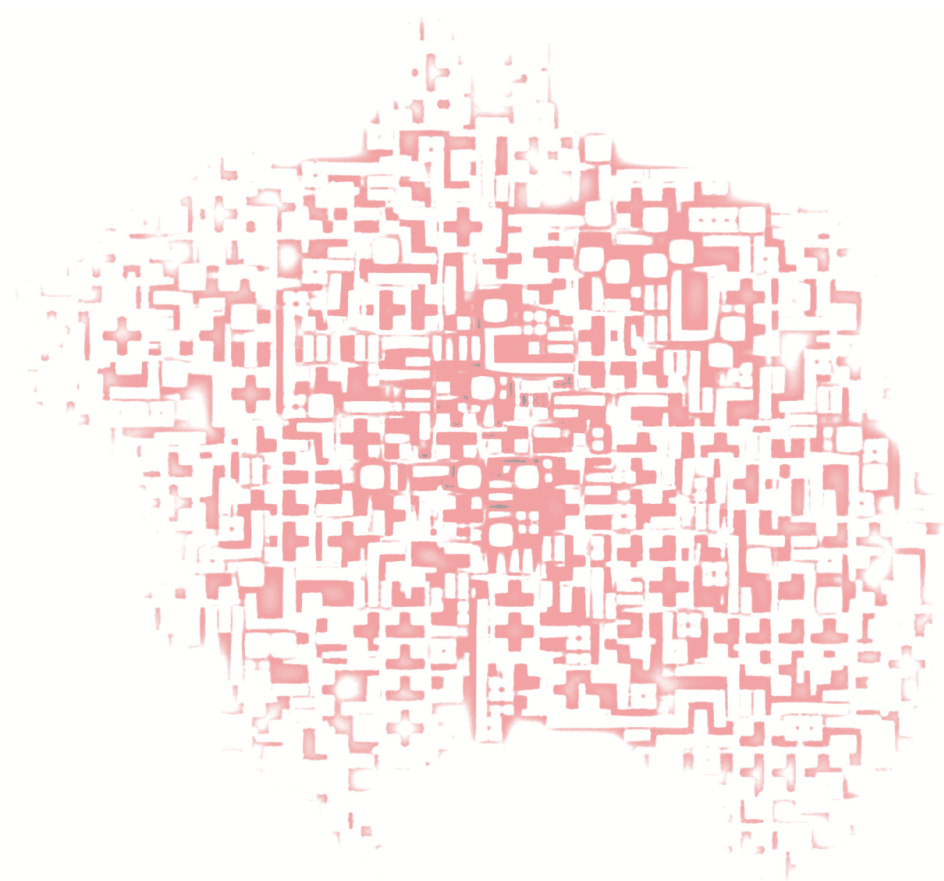


Figure 2.21: Section 4 (source: own work)

2.10 Computational Urban Growth

*Translation
from the **Rules**
to the **Computational Language***



2.10.1. Introduction

Following the configuring phase, the aim of the project was to observe the gaming system on a larger scale than the cluster; the urban scale.

In order to reach a large urban development, the manual approach was instantly disregarded as it is time-consuming, see weeks of work, and very predictable. Therefore, an automated method for the growth is favored.

The concept behind this project is based on a ruling system of connections between different modules that were encoded and connected by the brain logic.

Hence, this section of the report will elaborate on the translation of the human-based rules of the game system into a computational language and logic.

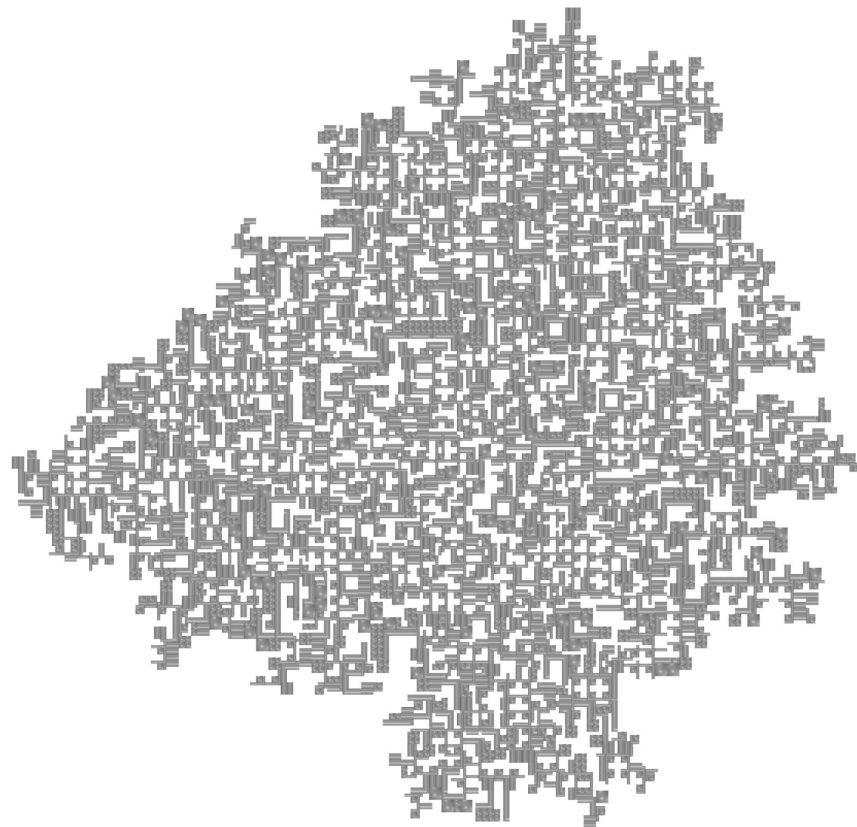


Figure 2.22 : Top View of one Aggregation Version (source: Own work)

2.10.2 Goals

The main goal of the computational design phase is to generate an automated and organic growth of the game, based on the rules' system of the "Modul-AB-ity".

The outcome will allow to visualize an infinite possibilities of configurations for the urban development which are completely unpredictable and random.

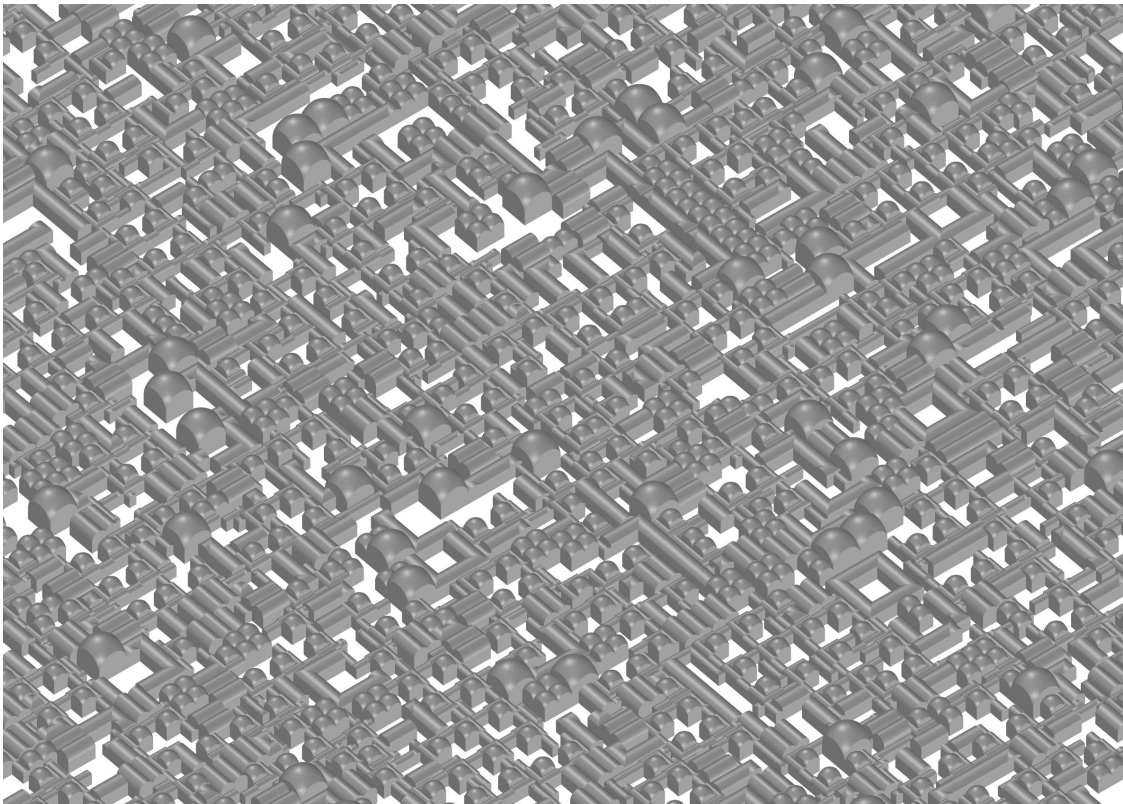


Figure 2.23 : 3D view of a Part of an Aggregation (source: Own work)

2.10.3 Plug-in “WASP” and Software (Tools)

2.10.3.1 Tools and Platform

The platform and tools used for the computed game rules are the plug-in “WASP” integrated within Grasshopper, in addition to Rhinoceros v.6.

2.10.3.2 Role of each Tools in the Aggregation

Wasp is the main tool for inscribing the connections, geometries, rules, colliders and number of modules. As for Grasshopper, it is a median of translation of data between the set of Wasp components and Rhinoceros v.6 working space. Rhinoceros v6 was used for generating all the geometries of the modules, the allocation of the points, the axis of orientation and the collider geometry, which will be explained in another section of this report. All the aggregations were represented in the Rhino working space.

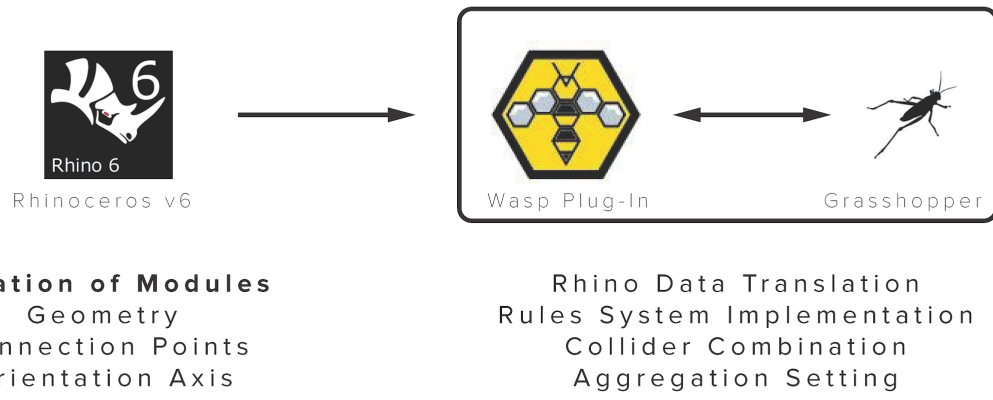


Figure 2.24 : Diagram of the Scheme of Work (source: Own work)

2.10.3.3 About Wasp

Wasp is a plug-in for Grasshopper, developed in Python, that allows to generate an aggregation based on a set of rules as connections between geometries. Each initial part contains several required inputs necessary for the aggregation process; the geometry, the connection points and the orientation axis.

The set of rules is based on the desired connection between parts, and the position of one to another. The outcome represents the possibilities of aggregation from the combination of different modules, as represented in *Figure 2.25*.

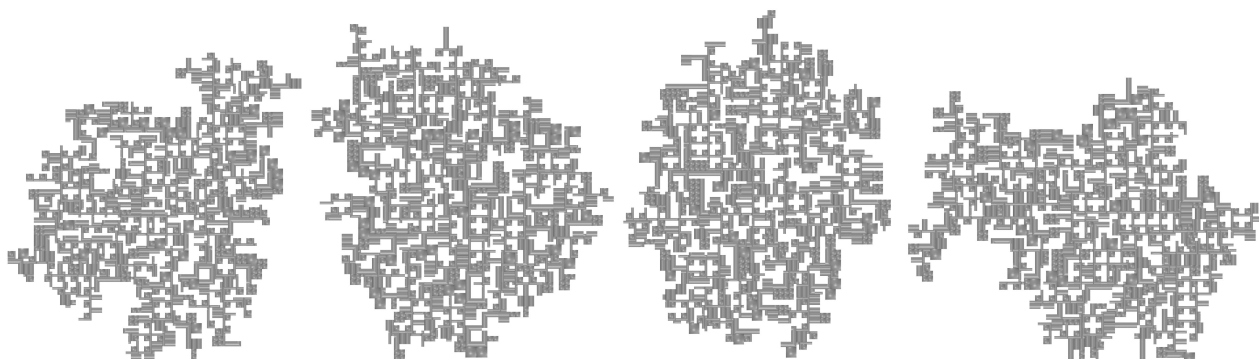


Figure 2.25 : Alternative Random Generated Aggregation (source: Own work)

2.10.4 Methodology of Work

2.10.4.1 Preparation of the Wasp setting in Grasshopper

The script for the formation of the aggregation is divided into 5 main categories represented in *Figure 2.26*. The parts preparation, the ruling system, the merging of data, the aggregation data combination and the last part for the visualization.

Each of this step will be explained in the following section individually.

Note that most of the components used for this script are a combination of Wasp components and basic Grasshopper tools. It is important to get the latest version of the Wasp plug-in for the availability of all the up-to-date components.

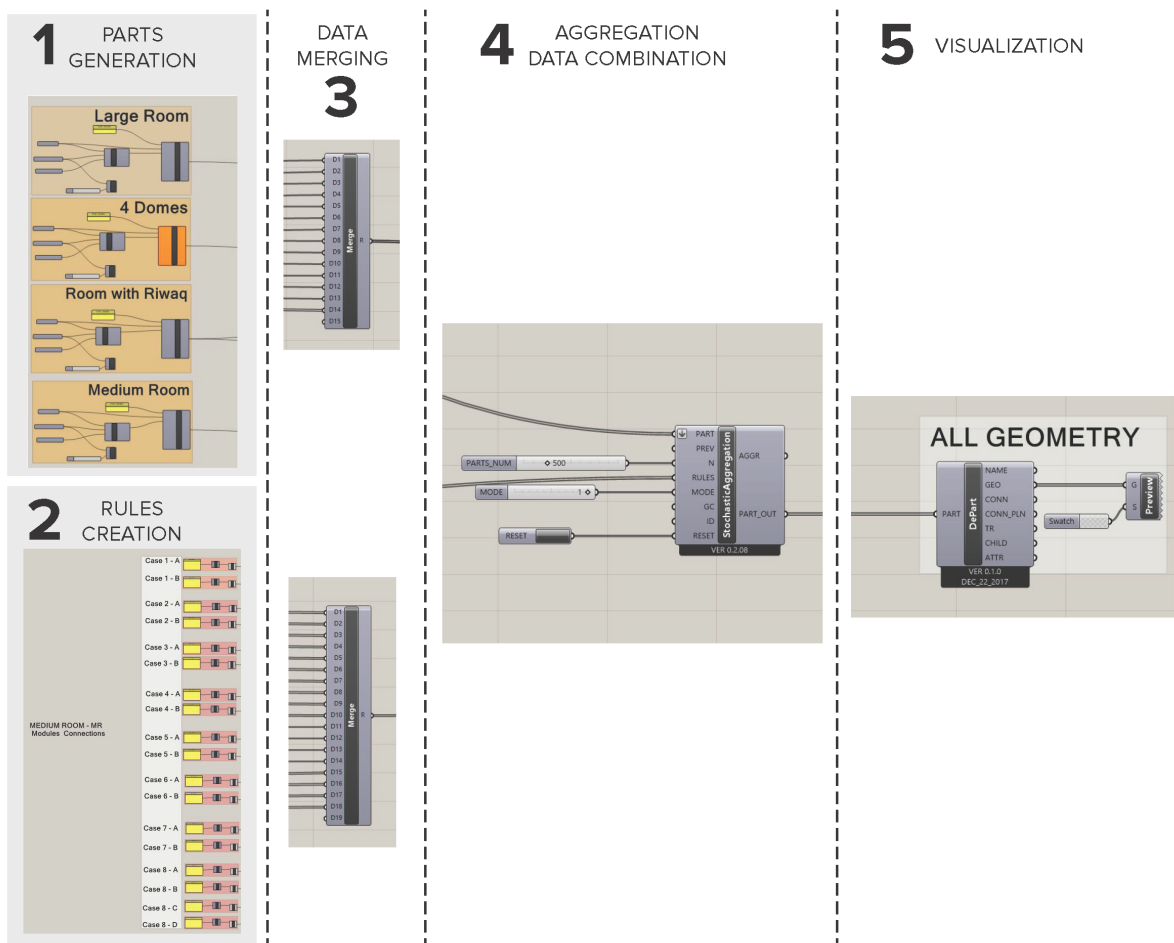


Figure 2.26 : Diagram of the Scheme of the Aggregation Script Formation (source: Own work)

Script Part 1: Components used for parts

The first part of the script is the creation of all the parts representing each one a module of the design game created. The geometry, the connection points and the axis of orientation are all combined in the “ConnDir” *Wasp_Connection from Direction* component, as shown in *Figure 2.27*. The output

represents all the connection data that are the input of the “AdvPart” *Wasp_Advanced Part* component in which the name abbreviation is included to form a completed “Part”. This procedure is applied on all the modules of the game.

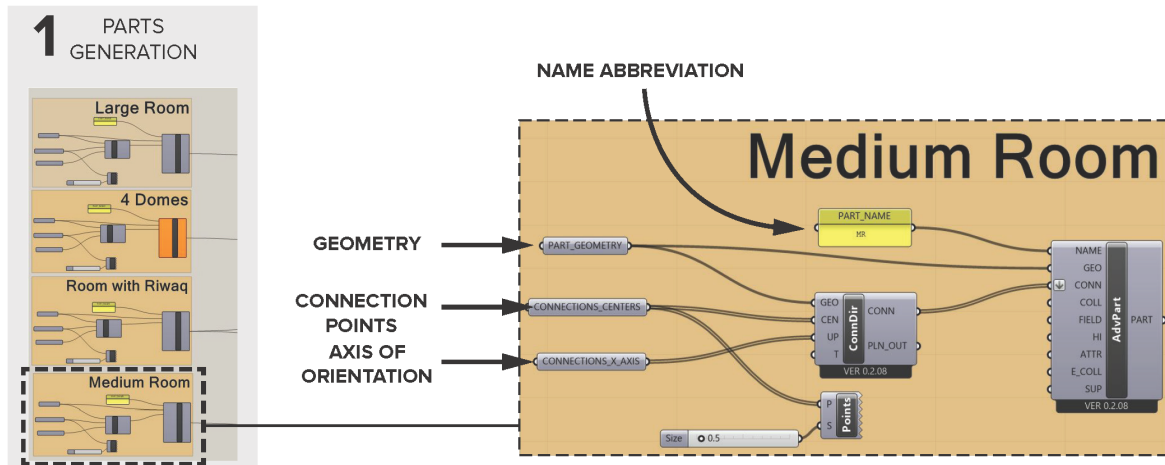


Figure 2.27 : Diagram of the Script for the Creation of the Parts (source: Own work)

Script Part 2: Rules Creation Components (2 Types)

The second phase consists of setting up all the rules of the game. In this section, the basic setting of how to write the rules script is presented.

There are 2 ways of defining the rules with Wasp. The 2 versions are through Wasp components:

- *Version 1* with “Wasp_Rule From Text”
- *Version 2* with “Wasp_Rule”

In Version 1, the component “Wasp_Rule From Text” is used to translate a coding system for the rule written in a panel. This type of code is specific to the language of Wasp.

The format is

“Part1|Conn1_Part2|Conn2”

which translates into

the connection “Conn1” of the part renamed “Part1”
is linked to the connection “Conn2” of the part “Part2”.

As you state that “Part1|Conn1_Part2|Conn2”, the opposite is not true, unless it is added. Therefore, the next part of the text will be “Part2|Conn2_Part1|Conn1”.

It is important to highlight that if you do not include the reverse text, there is a lower probability for the connection between the two parts to occur as the script will not search to connect the Part 2 to Part 1, but will mostly connect Part 1 to Part 2.

For coherence, the name of “Part1” and “Part2” are replaced with the abbreviation given previously to all modules. For example, as observed in *Figure 2.28*, HV and HCL are respectively the abbreviations of “Half-Vault” and “Half Corner Left” parts.

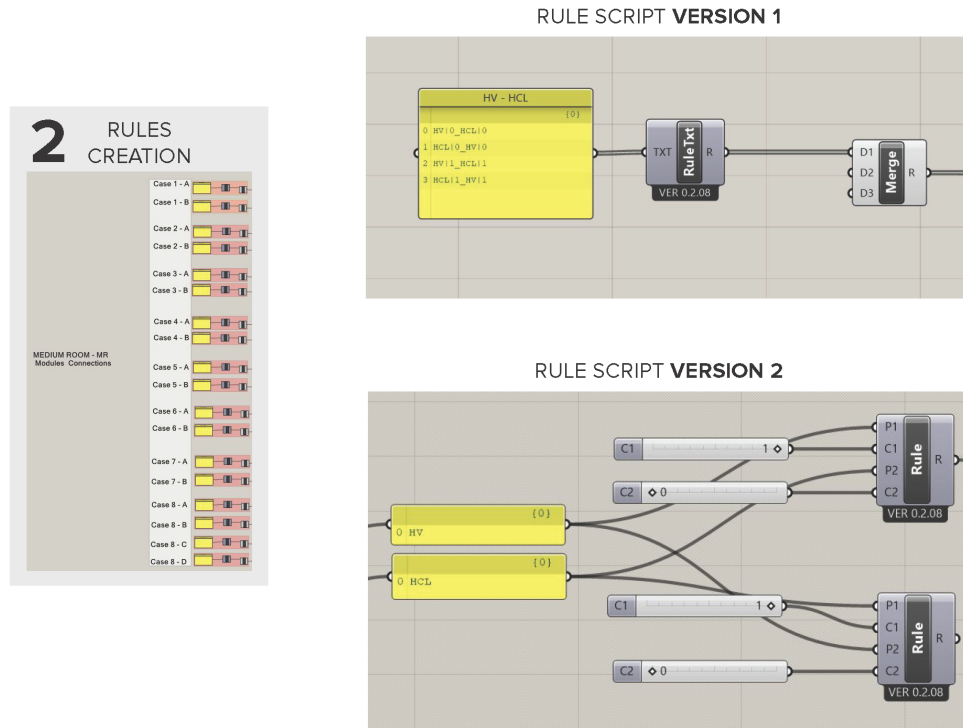
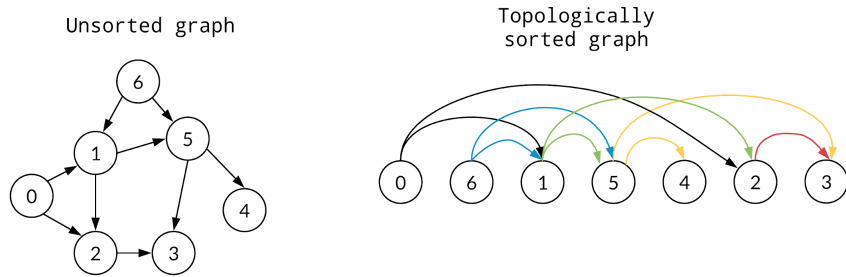


Figure 2.28 : Diagram of the Script for the Creation of the Rules illustrating both Version 1 and Version 2 (source: Own work)

In Version 2, the component “Wasp_Rule” is used to connect two parts with a slider indicating with connection number is taken into consideration. Both the input P1, for Part1, and the input P2, for the Part2, are to be connected to the exact abbreviation or name given to the part. Also, there is the second version of this rule stating the contrary to ensure that the rule is working in two ways.

For simplicity, the version 1 was used in this script as it is easier to read all the rules and detect errors.

The set of connections define the topological graph of the part, which will translate into all the possibilities of aggregation with other parts. The ruling system can be translated in a later stage into a *topological graph*, *Figure 2.29*, for each part (module) created to follow up visually what the connections on the screen signify.



*Figure 2.29 : Example of Topological Graph Representation (Guides.codepath.com, 2019)
(source: <https://guides.codepath.com/compsci/Topological-Sort>)*

Script Part 3: Merging of All Parts & Rules

After the creation of all the parts and the rules, each set should be merged before linking into the inputs of the aggregation. The resulting advanced parts are all merged, as well as the set of rules are merged together through Grasshopper.

Script Part 4: Aggregation and Data Combination + Number of Parts

The fourth part of the script consists of combining all the data needed for the aggregation. The previously merged parts and rules are inserted as inputs in the component “Wasp_Stochastic Aggregation”, as observed in *Figure 2.30*. The additional information needed is the number of parts to be used in the resulting aggregation where a number slider is added.

In addition, the “Reset” button has the role of generating a different configuration with the same number of parts. This is how several aggregation configurations can be explored, which are infinite.

The core of the framework relies on a set of aggregation procedures, allowing the generation of specific structures from the combination of different modules. Each of these procedures is composed of strategies for the selection of basic aggregation rules, described as an instruction to orient one module over a selected connection of another module.

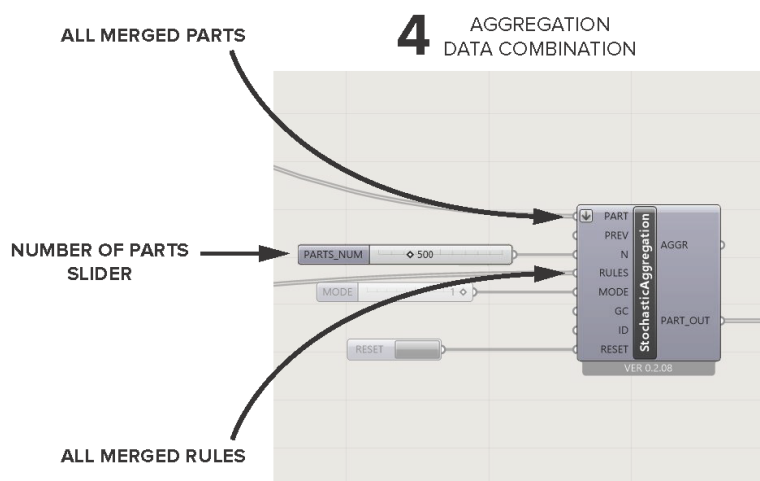


Figure 2.30 : Diagram of the Script for the Aggregation Formation (source: Own work)

Script Part 5: Visualization + Coloring of Geometry

The last part of the script is the visualization of the aggregation. The component “Wasp_Deconstruct Part” is used to allocate all the different modules that has been used. The output of the geometry is then connected to a combination of preview and color palette.

For further visual performance, refer to the section 8 Visualization.

5 VISUALIZATION

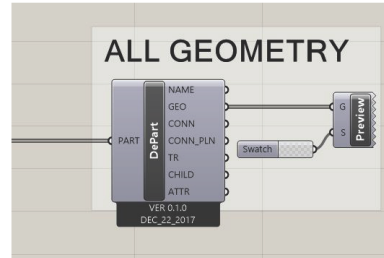


Figure 2.31 : Diagram of the Script for the Visualization of the Aggregation (source: Own work)

2.10.4.2. Modeling Phase of Geometries

For the modeling phase of the modules, there are 3 important inputs to consider:

The Geometry, the Connection Points and the Orientation.

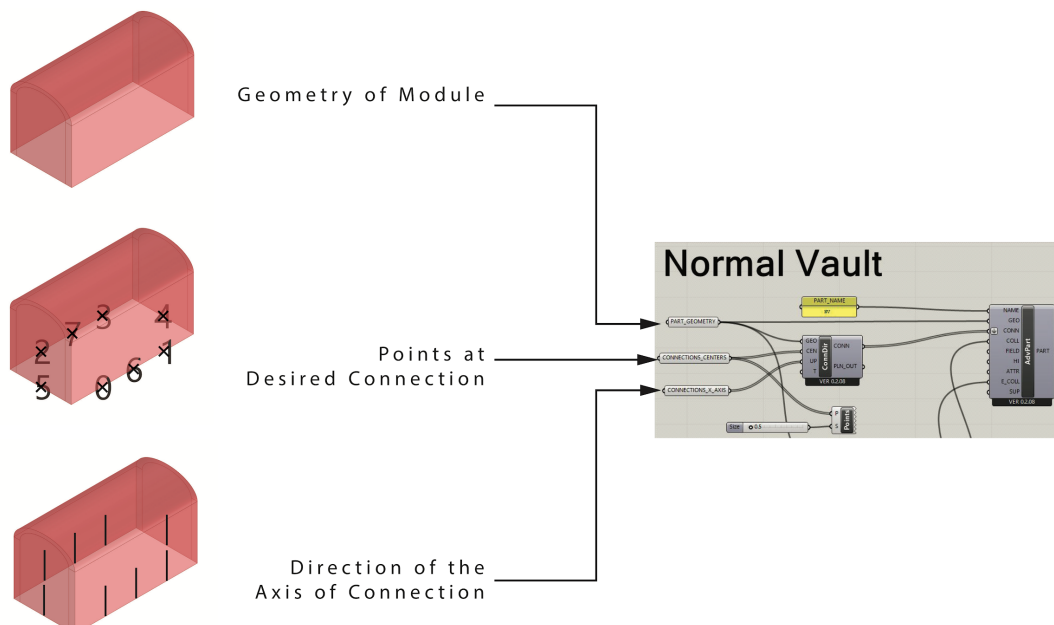


Figure 2.32 : Diagram of the Script for the Creation of a Part (source: Own work)

In total, there are 13 modules in the designed game. Refer to *Figure 2.13*, for the list of Modules. For the first input, each of these modules is modeled in a 3D geometry in Rhino v6. The more simplified is the geometry shape, the faster the calculation time and the visualization. Therefore, all of the opening, details, ornaments or brick pattern are disregarded for this step, as explained in *Figure 2.33*.

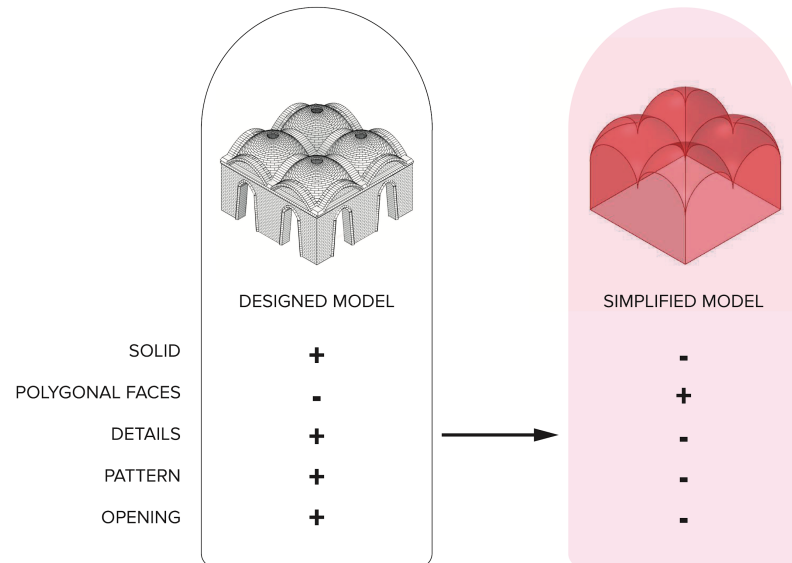


Figure 2.33 : Geometry Comparison between the Original Geometry and the Simplified Model
(source: Own work)

Note that in a later stage, it is possible to replace all the existing module with a final representation for visualization concerns. For the steps of the geometry replacement refer to section 8 Visualization.

The second input needed is the connection location on the geometry. Those points can be placed in Rhino or Grasshopper, on the exact location of the connection needed. There can be as many connection points as needed, as long as they are needed in order to avoid complexity.

Not only is the geometry simplified to improve performance, but also it should be free from openings and holes. In fact, allocating the points requires the presence of a face behind it. If a point is located in the middle of a face, therefore the corresponding face should be completed enclosed behind in order for the plug-in to link them.

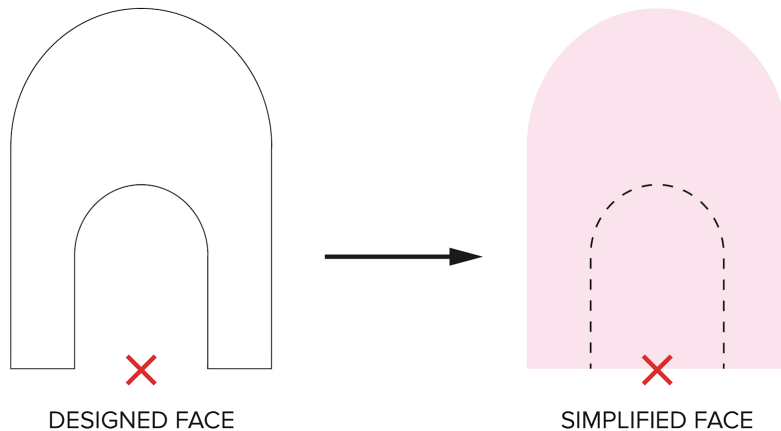


Figure 2.34 : Diagram Explaining the Face in regards to the Connection Point (source: Own work)

The third input of the modeling preparation is the direction of the axis, which represents the orientation of connection. Each point previously created needs an axis to lead the direction in which it is going to be connected to the next modules.

In addition to the inputs, it is required to give a name to the created part. The name can either be a long version text or a shortened abbreviation. For the easiness of the ruling system in the next phase, it is advised to always give abbreviated name. For example, the module in our design labeled “Medium Room” will be identified for the script as “MR”, as “Normal Vault” is renamed “NV”. As advice, it is a good solution to write down on paper all the abbreviation that are given to the parts to be able to follow up the work track.

2.10.5 Inputs Adaptation

At first, the 13 modules that were designed were translated from Rhino geometry to Wasp. Those initial modules created were observed in the resulting aggregation to understand where modifications are needed. In fact, many errors started to appear while running the result.

After observing how the aggregation is growing and in which sequence were the modules placed, additional parts were added to allow the script to work properly and in a similar way to the human-brain logic.

2.10.5.1. Association of Functions to Connection Points

Once the parts are created and the connection points’ numbers are generated, the numbering sequence is associated with labels of “Open Connection” for the legend label A in the module’s plan or “Closed Connection” for the legend label C, shown in *Figure 2.35 to Figure 2.39*.

The “Open Connection” signifies that the door or passage to the next module is positioned at this point. On the other hand, the “Closed Connection” indicates that the point is on a face that has no opening and can be placed adjacent to another module in a “wall to wall” situation.

Although there are “Open Connection” and “Closed Connection”, in addition to the “Courtyard Connection” representing the label COURT explained in the section 7 Collider as Non-Built Spaces, the only essential connection to be used in the rules are the “Open Connection” because it will reduce the probability for the script to create random “Wall to Wall” aggregation that are meaningless for the aim of this project.

Therefore, all “Closed Connection” have been disregarded in this report. For future development, it can be a solution to have some modules connected by closed walls, as long as it follows the logic of the design. Refer to section 10 Future Development for more details on this topic.

The function associations are human decision making, in a way to correspond to the design configurations of the modules. In the *Figure 2.35 to Figure 2.39*, the connections points association to their functions are indicated for each module.

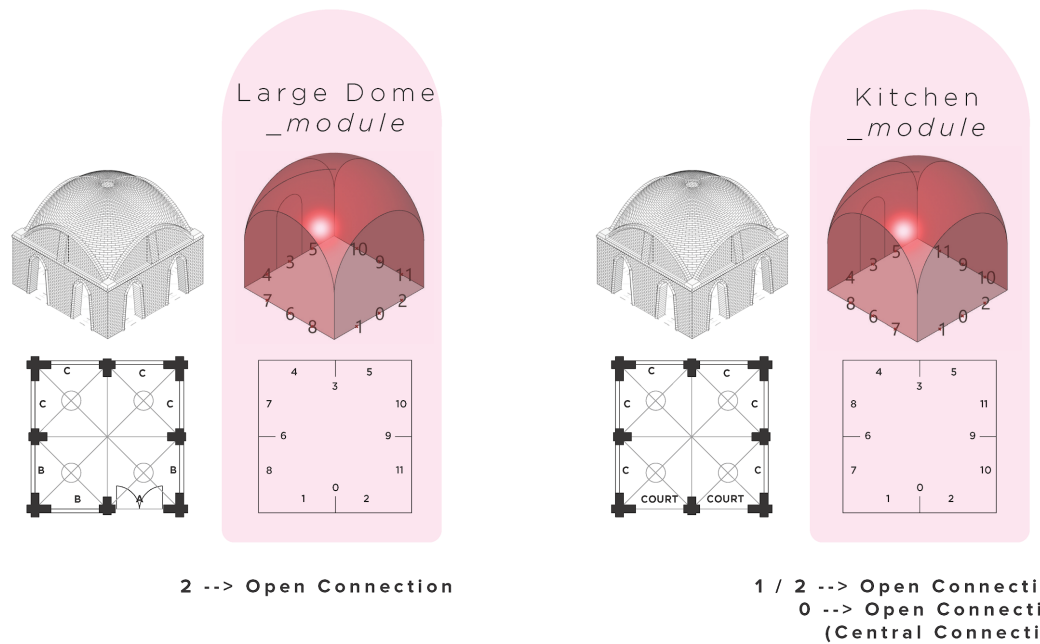
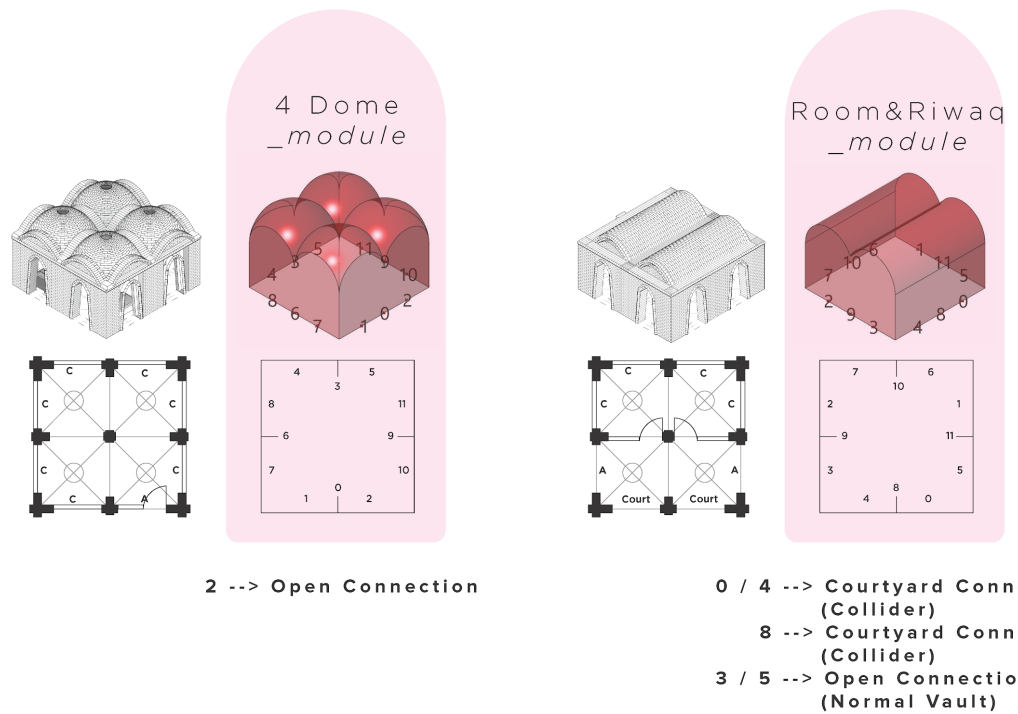
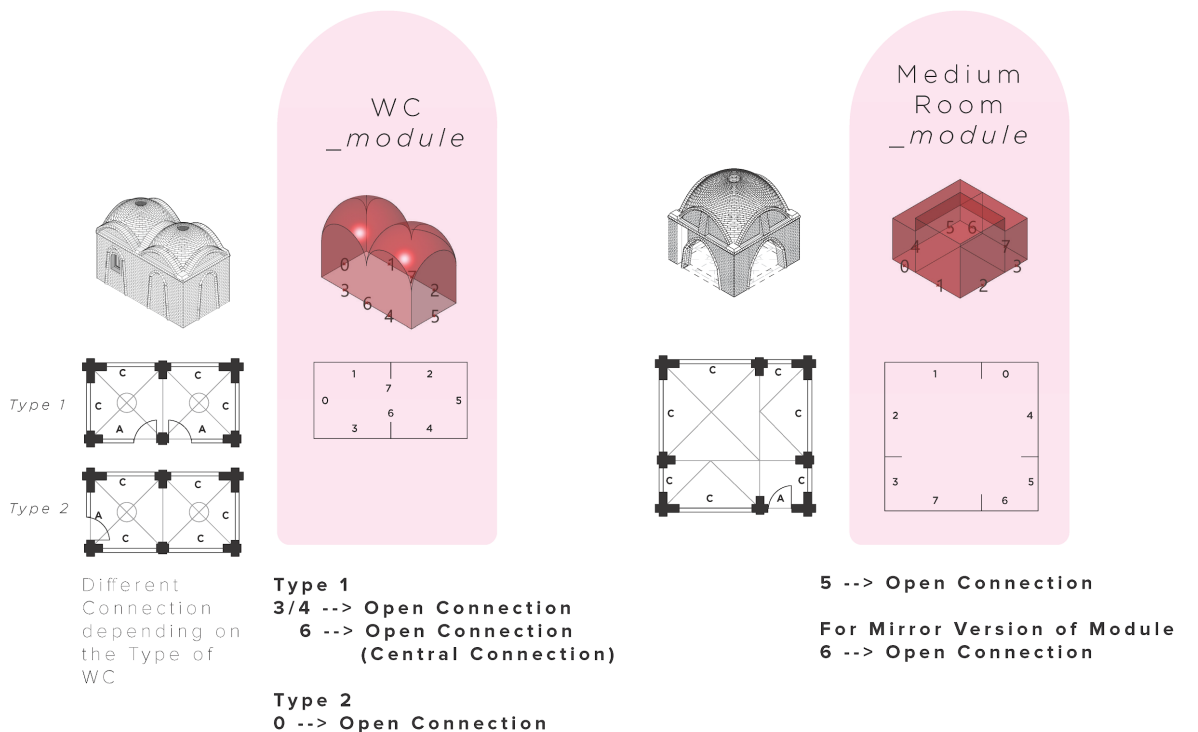


Figure 2.35 : Diagram Representing the Translation of the Module and Connection Points
(source: Own work)



*Figure 2.36 : Diagram Representing the Translation of the Module and Connection Points
(source: Own work)*



*Figure 2.37 : Diagram Representing the Translation of the Module and Connection Points
(source: Own work)*

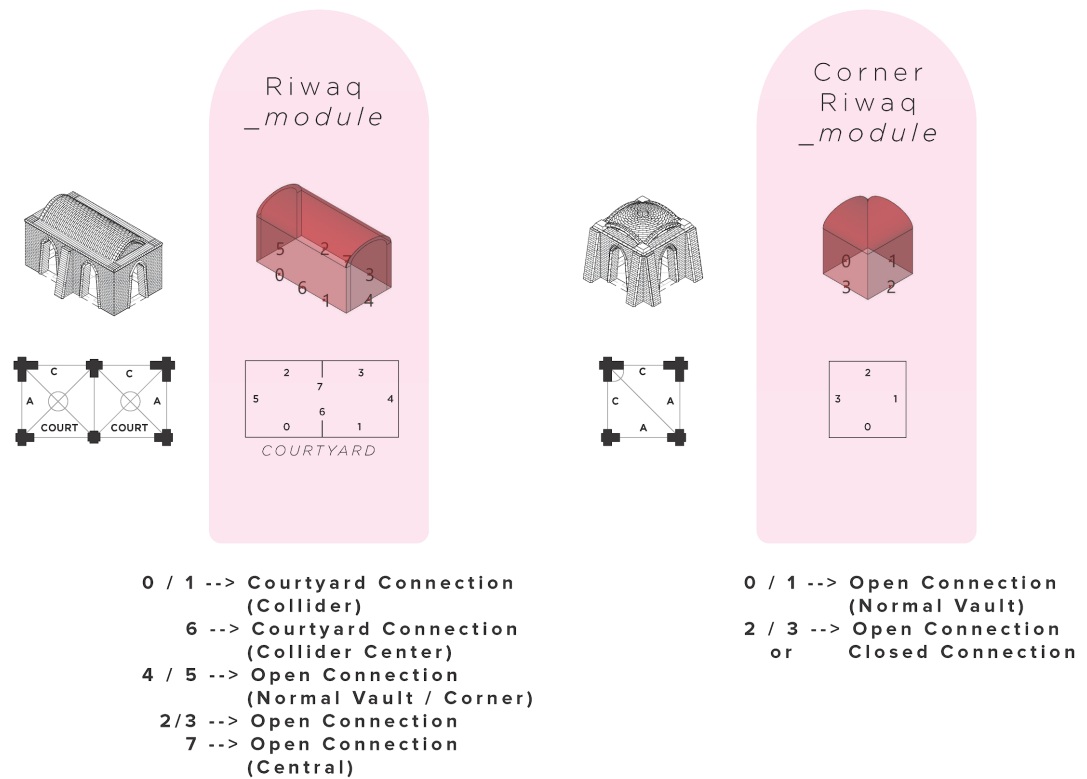


Figure 2.38 : Diagram Representing the Translation of the Module and Connection Points
(source: Own work)

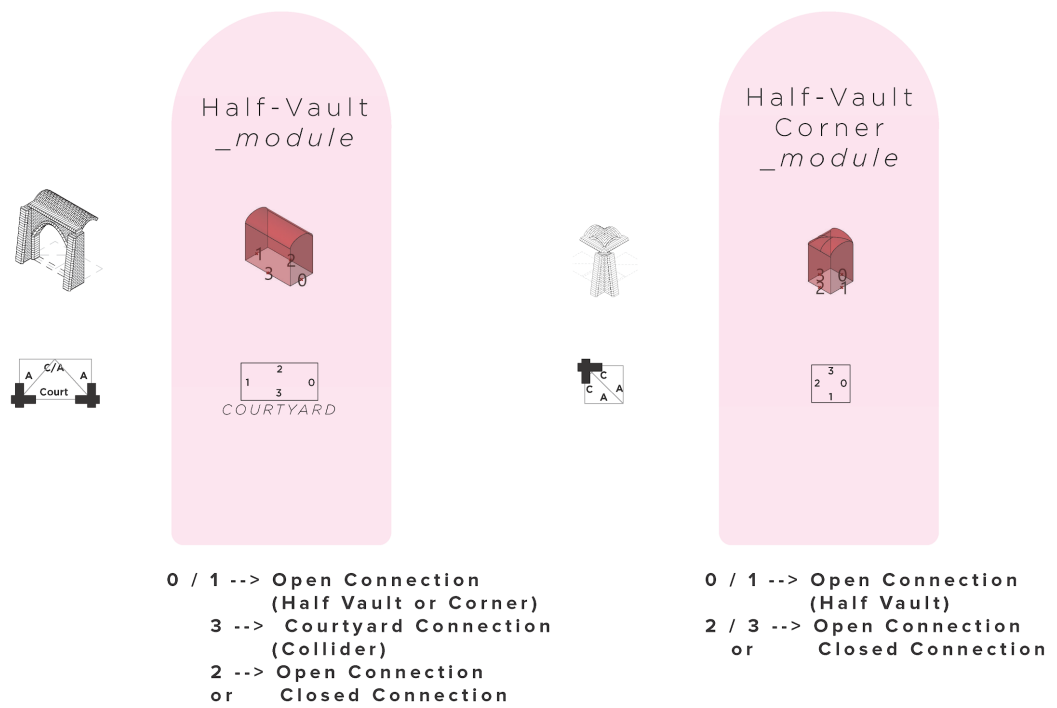


Figure 2.39 : Diagram Representing the Translation of the Module and Connection Points
(source: Own work)

2.10.5.2. Connection Points Location

In the designed domino game, the connections are all located along the edges of the modules, in a unitized ratio, as observed in *Figure 2.40*.

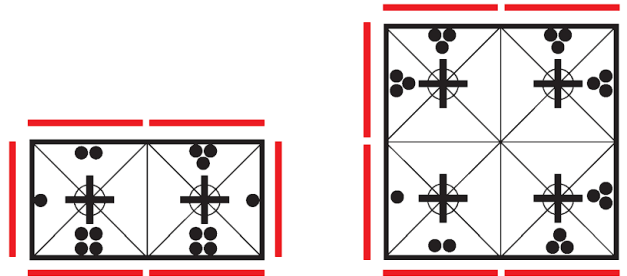


Figure 2.40 : Diagram of the Modules representing the Connections along the Edges
(source: Own work)

When translating the domino game from the human logic to the computational language, it was essential to do some modification in the way the modules will be connecting. Therefore, a middle connection points was needed for linking geometries by center-to-center of their edges, in addition to the unit edges connections. This is due to the fact that, in Wasp when deciding how 2 modules are related to each other, the connection will depend on one single stated rule, and not more.

For example, as shown in *Figure 2.41*, in the domino rules, the 2 modules are connected based on the rule of the first edge “4DOTS → 4DOTS” AND the second edge “4DOTS → 4DOTS”. On the other hand, in the script rules of the computational language, the only needed rule is simplified by one single connection points which will be ruled by “6 → 6”.

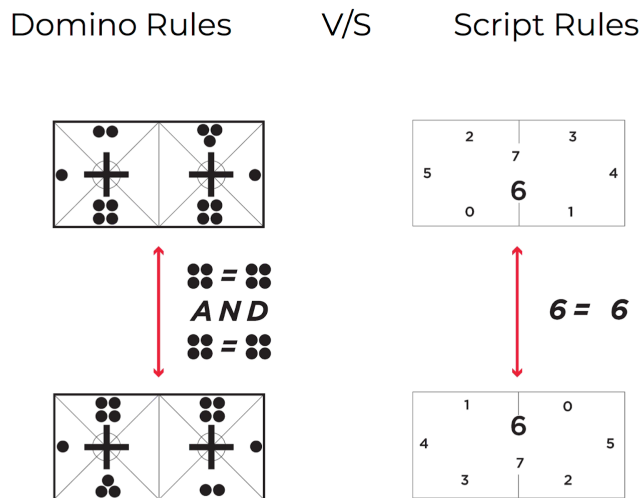


Figure 2.41 : Comparison of the Domino Rules v/s the Script Rules (source: Own work)

The axis of orientation placed on all the connection points are all directed in the Z direction. In fact, the aggregation is a representation of the first floor of the design, located on the ground level. As the

modules are coplanar, the similar axis direction prevents the module from being rotated, flipped or upside down.

To proceed further in this research, the next step would be to add the second floor level, which is explained in detail in the section 10 Future Development.

Along the progress, it is essential to take note manually and write down on paper all the connections points number on the geometry, and their association to opening, closed wall, courtyard or other criteria in the design of the project. For an overview of the paperwork for this script refer to Appendix A “Computational PaperWork”.

2.10.6 Adaptation of Corner Modules

The cluster designed for this project is based on the presence of vault modules surrounding the open courtyard. Those vault modules are the “Normal Vault” and the “Half Vault”. These geometries are the only one in the design that are used for circulation or passage, but as well as the transitional space between all the function room and the courtyard.

The corner modules needs to have 2 versions: one version for the turning on the right and one corner for turning on the left. The two versions can be observed in *Figure 2.42*. It is the exact same geometry that was duplicated but number and labeled in different ways.

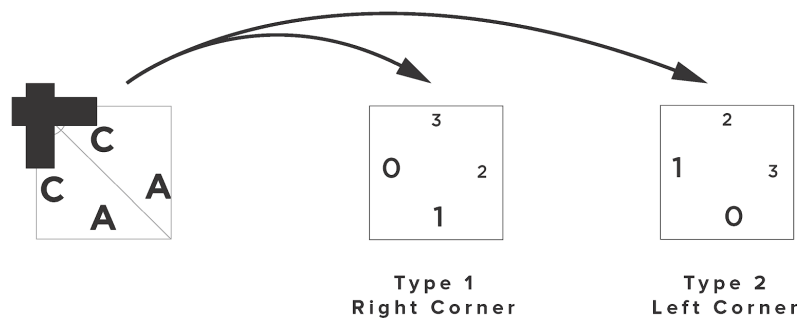


Figure 2.42 : Translation of the Corner Module into 2 Different Versions (source: Own work)

This is due to the connection point numbers that should allow the sequence to be continuous without interruption. It can be observed in *Figure 2.43*, that there are 2 different number sequence happening. In the type 1, the sequence is “5=1, 4=0, 5=1...” whereas in the type 2 it is “5=0, 4=1, 5=0...”. Therefore, it is not possible to merge the 2 sequences with a single corner modules as it will result in unwanted scenario, and not complete any enclosed space.

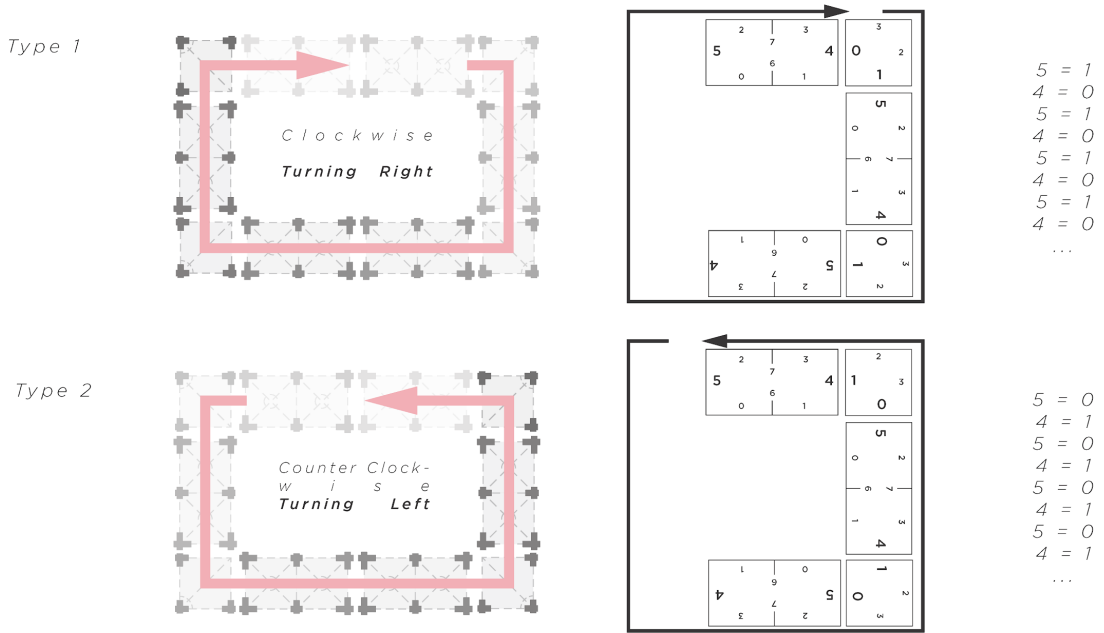


Figure 2.43 : Diagram of the Two Corner Versions Functioning in the Plan Sequence
(source: Own work)

2.10.7 Collider as Non-Built Spaces

In the design configuration of the cluster, there are built spaces representing all the modules connected to each other, as well as void spaces representing open spaces such as courtyards.

Those “Courtyard Connection” are justified as “No Connection to Any Modules” which means a void will take place instead of a module.

The voids can be generated by the lack of presence of a part (module) in the area desired. As observed in the design, those non-built courtyards are always placed on the same edges of all the “Normal Vault” and “Half Vault” modules.

It is possible through a specific Wasp component “Wasp_Collider” to prevent the allocation of another module along the defined edges of both “Normal Vault” and “Half Vault” parts.

The functioning behind the collider component is the presence of a “Non-existing” or “Invisible” geometry that blocks other modules from being placed, as if the space is already occupied.

The collider is first created as a separate geometry in Rhino v6. For this project, all the colliders were shaped as a box placed on the edge of the mentioned modules. This geometry is then connected to the resulting Part created previously, in the inputs “E_Coll” of the component “Wasp_Advanced Part”. After several trials and errors, it has been observed that the collider was not efficiently working when connected directly to the “Wasp_Advanced Part”.

Therefore, another step was added. Within Grasshopper, the module’s geometry data was merged to the collider geometry data by the means of a “Merge” component, and the resulting outcome was linked to the “Coll” input of the the “Wasp_Advanced Part”.

Normal Vault

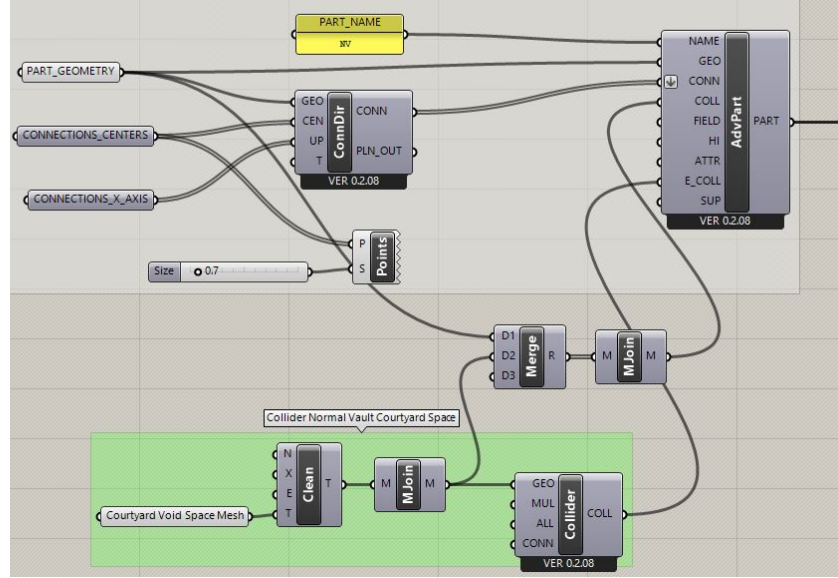


Figure 2.44 : Screenshot of the Script representing the Addition of the Collider to the Module Part
(source: Own work)

In order to reach the best collider dimension, size and scale, to get the result of the courtyard desired, some error and trials has been done by modifying the position and geometry through Rhino and checking the resulting aggregation formation.

This is possible by not “Internalizing” the data of the geometry when translated into Grasshopper in order to be able to control adjustments that are made in Rhino instantly.

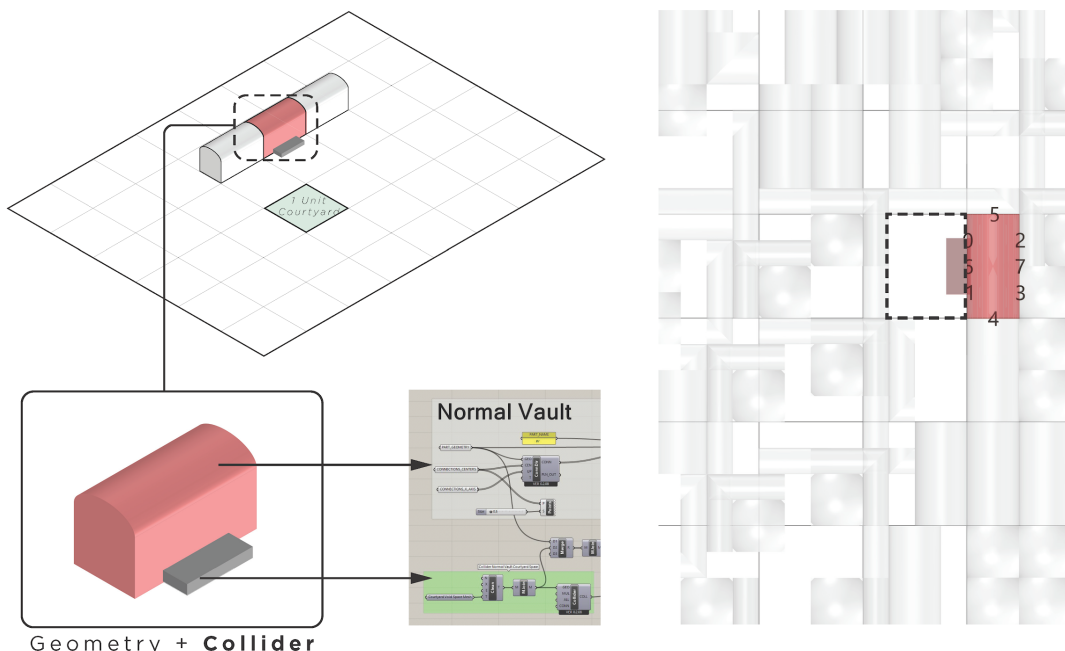


Figure 2.45 : Diagram of the Collider in the Scheme of Work (source: Own work)

For the end result, when many colliders accumulates in a similar zone and close to each other, a courtyard is created in the aggregation.

There are still some limitations to the use of the collider components and its improvement which are explained in the section 9 Limitations.

2.10.8 Visualization

2.10.8.1. Geometry Alteration

The geometry used for all the modules was shown as a simplified version to improve the performance of the computer calculation time. In order to reach the desired visualization of the final aggregation model, it is possible to replace the parts by categories.

For example, all the module of the “Medium Room”, abbreviated “MR”, have been modeled in a very cubical geometry, even lacking the domed roof. For the final outcome, this category of part of “MR” are all replaced with the designed geometry.

2.10.8.2. Color Coding

It is possible to color geometries in the aggregation to facilitate the recognition of which modules has been used or not, or to discern a part from another when their geometry are similar but their non-apparent data, such as connection points, are different.

2.10.9 Limitations

2.10.9.1. Control of Ratio Parts

Although the number of parts is predefined for the aggregation, there is a lack of control over the amount of each type of modules. The process of formation of the aggregation is completely random. As the generated design is given an input of the “Total Number of Modules” to be used, there can be unwanted scenarios such as an undesired larger ratio of “WC” modules to “Large Rooms”. It is not possible to specify that less “WC” modules will be needed compared to those “Large Rooms”, as it does not follow any logic.

In order to get more control over the uneven ratios, the more connection the modules has to other modules, the higher the probability for this module to appear in the end-result. In fact, if the module is connected to all the other modules with a several connection, there is a high probability for it to appear instantly as the number of modules is growing.

Although this is a solution for controlling the unpredictable scenario, it is not the most accurate solution.

2.10.9.2. Scattered Collider

One of the limitations of the collider component is the lack of control over its position in the aggregation. In fact, it is in our favor to gather many colliders adjacent to each other to create “Courtyard” like voids. The result of the collider provided for some of the geometries are either too scattered over the final aggregation or not enough numerous to produce the desired design.

2.10.9.3. Corner System

As observed previously, there are 2 versions for each “Corner” type modules. The issue for allowing the aggregation to grow while turning left and right has solved only a part of the script problem. In fact, as observed in *Figure 2.46*, there are at least 4, if not 5, types of modules needed to recreate an uneven pattern of enclosed space. The grid in this example is a 5x5 unit, representing an uneven pattern. As our modules are 2 units long, but the corners are 1 unit long, the computer will not understand how to fit the parts in order to complete the enclosure of the plan. This is why, the “Type 1” module shown in the example, is a combination of a corner and a pathway to allow the connection to both sides and complete the missing unit of the grid. (This example is just for illustrating the thinking behind the logic of this script and represents one of the solutions was observed. Those modules are not used in this paper, but were under analysis for problem solving.)

Also, the “Type 4” modules might have the exact same pattern and design as “Type 2” but its connection points are different in this case, so it results in another module type. It would have been possible to replace this “Type 4” module and the adjacent modules by a “Type 1” to solve the corner issue.

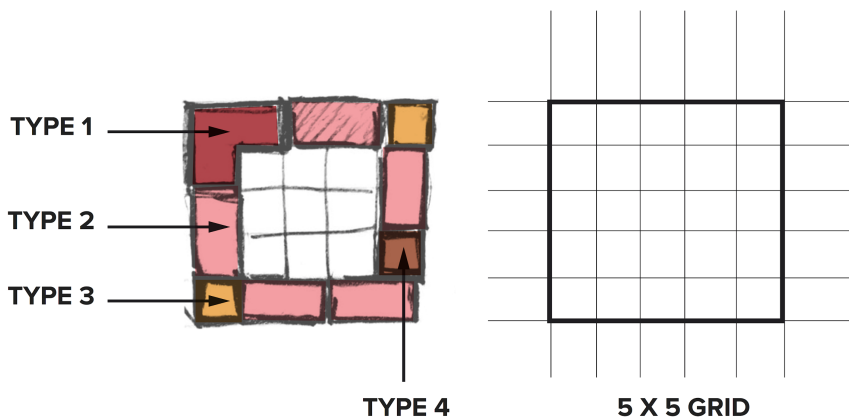


Figure 2.46 : Diagram illustrating the Grid System effect on Modularity (source: Own work)

2.10.10 Future Developments

2.10.10.1. Second Storey Level

The aggregation created has been designed for only a ground level floor plan. In the original design, there are some second storey modules. For further work of this research, the next step is to add another module for the second level. This is possible by adjusting some data in the first phase of the script. When creating the module's geometry, the "Axis of Orientation" are all placed on the vertical faces of the model and directed in the Z direction.

To move the aggregation growth on the second floor, a new additional modules should be created with "Axis of Orientation" on the Top/Bottom faces and directed in the XY plane. The resulting position of the parts will be as observed in *Figure 2.47*.

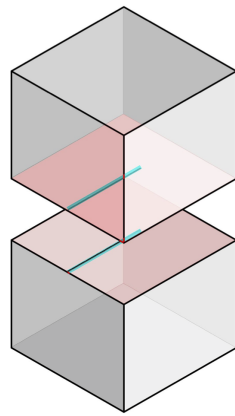


Figure 2.47 : Diagram of Concept for the Second Floor Module Position (source: Own work)

2.10.10.2. Dominant Rule

The way the rules are set or written may affect the domination to another rule. For example, if a rule does not imply its contrary, it might have a lower probability of appearing or not at all. Other possibilities of scenarios are still under studies and can be observed in the script of the *grasshopper file .gh* submitted.

Also, another research is still done on the domination status.

As seen in *Figure 2.48*, if the connection of $0 \rightarrow 1$ and $1 \rightarrow 0$, as well as the center-to-center $6 \rightarrow 6$ is added, there might be a possibility that the $6 \rightarrow 6$ is more probable to appear as it is the shortest way to reach rather than checking 2 rules $0 \rightarrow 1$ and $1 \rightarrow 0$ to assert the connectivity of the 2 modules.

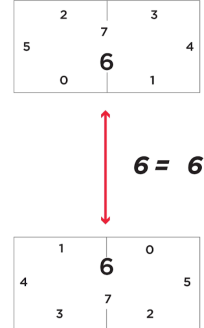


Figure 2.48 : Diagram of Center-to-Center Module Connection (source: Own work)

2.10.10.3. Closed Connection Possibilities

The type of connections that have been presented previously are the “Open Connection”, the “Closed Connection” and the “Courtyard Connection”. The open connection were used for setting the rules of the aggregation. The courtyard were all replaced by the Collider to generate voids in the aggregation. As for the “Closed Connection”, they have been disregarded and omitted from the rules because they were not significant.

In the next stage, finding a logical scenario for linking the “Closed” faces of the modules together when a “Wall to Wall” situation is needed can improve the configuration design. Note that “Wall to Wall” positioning are already existing, indirectly, when 2 modules are adjacent without any rule stating it.

2.11 Physical Model

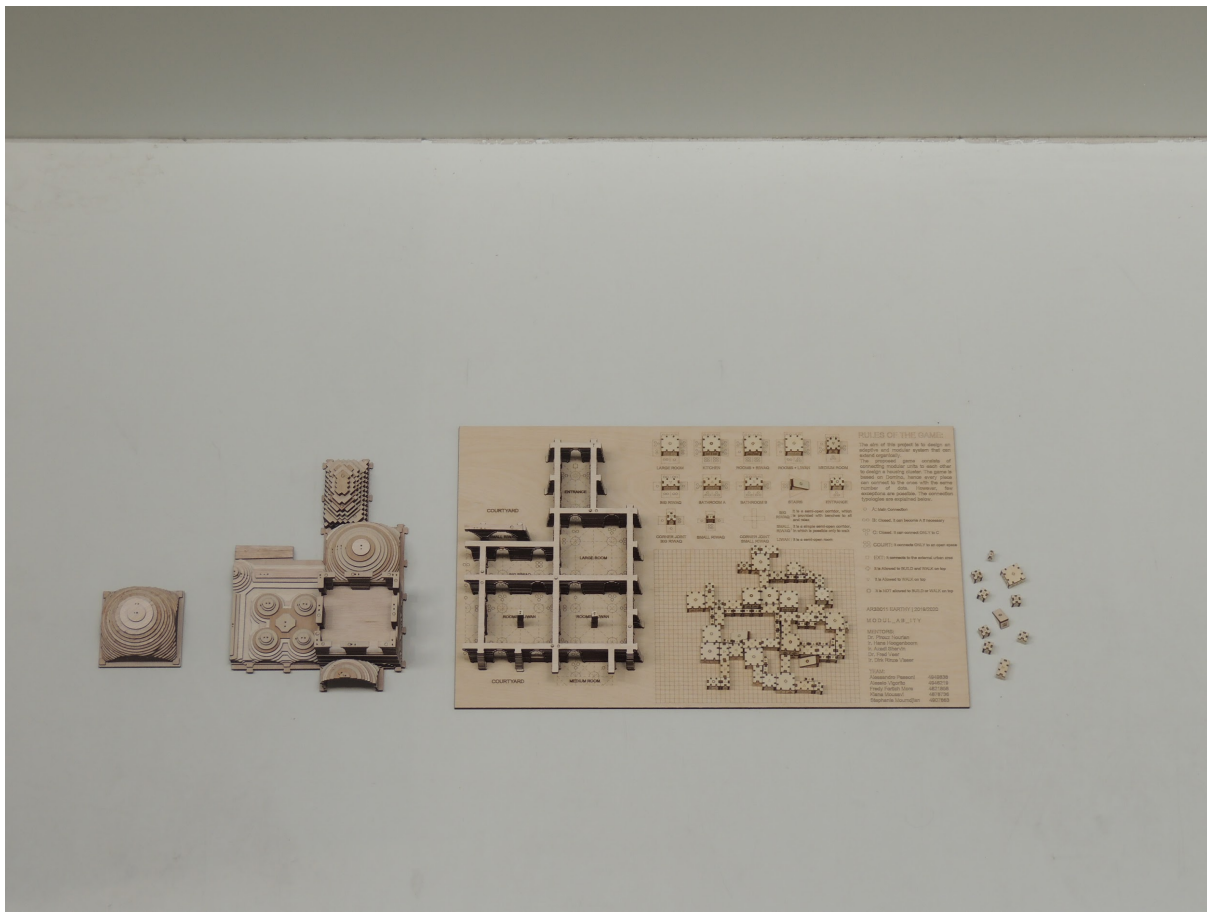


Figure 2.49 : Composition of the physical model (source: Own work)

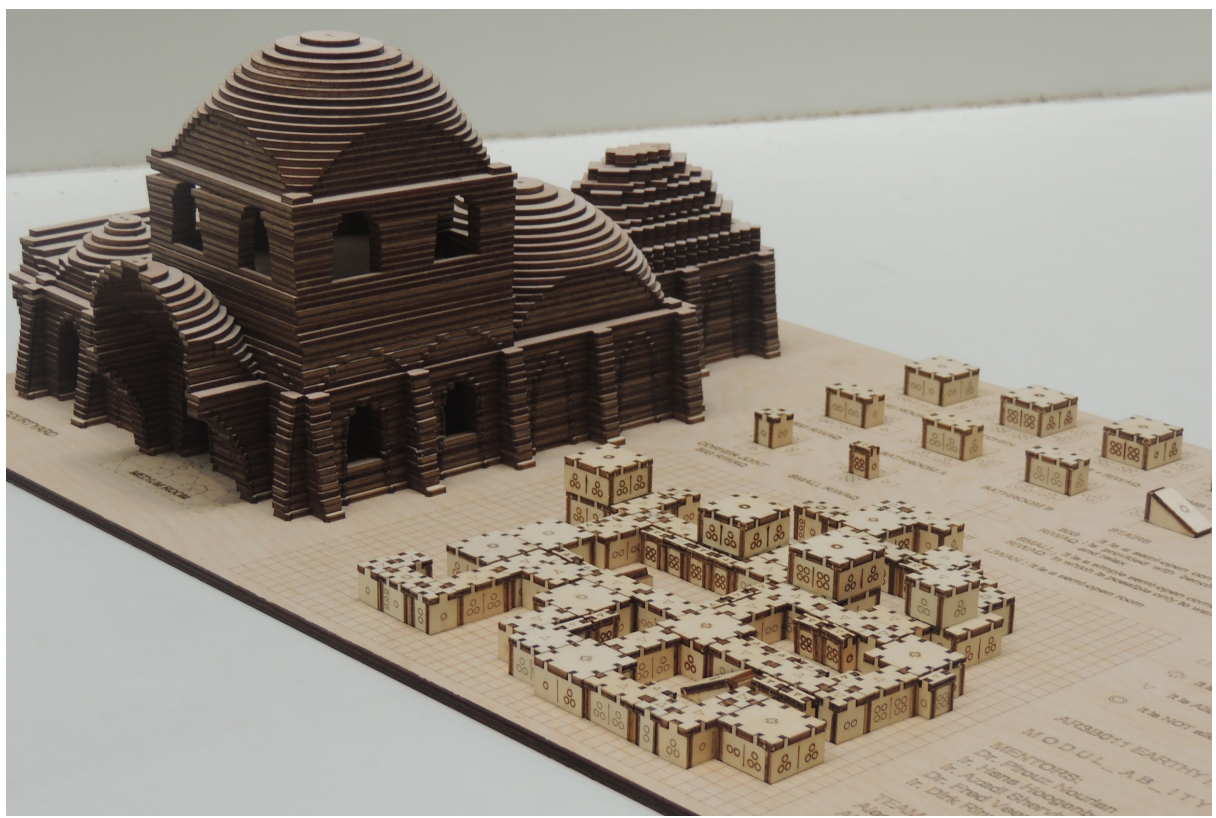


Figure 2.50 : Physical model 1:50 (Left) and domino game 1:200 (right) (source: Own work)

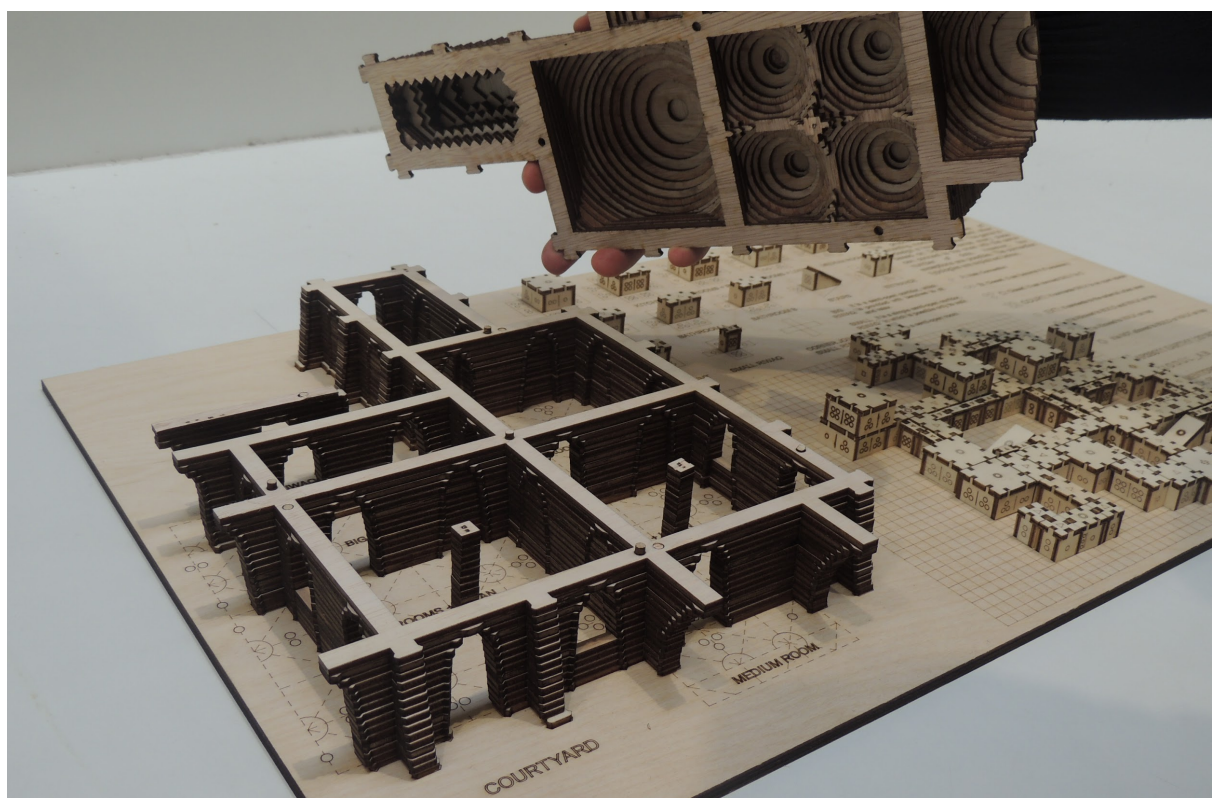
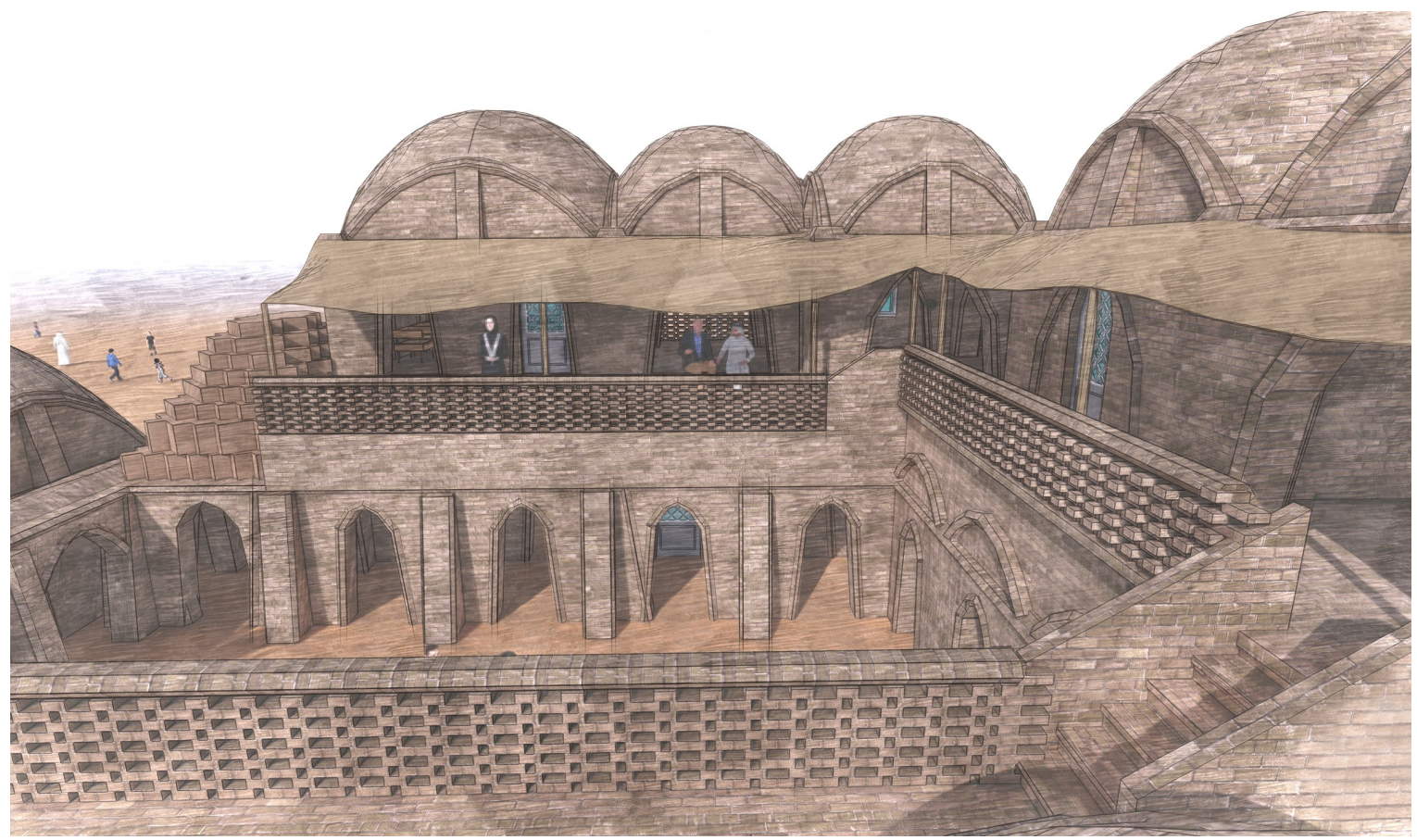


Figure 2.51 : Openable roof of the physical model 1:50 (source: Own work)

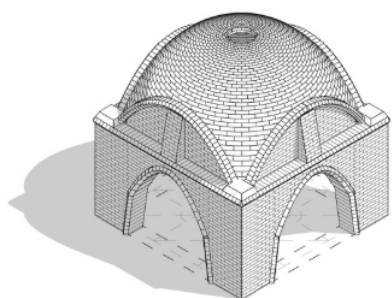


3. Forming

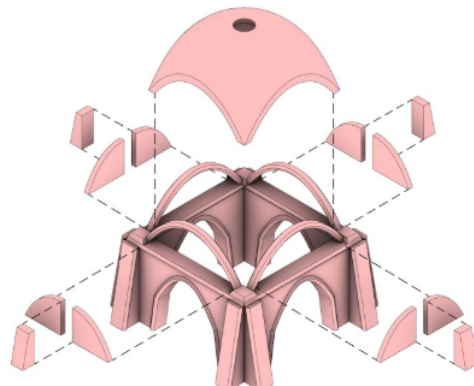
Medium Room Module *Construction Manual*



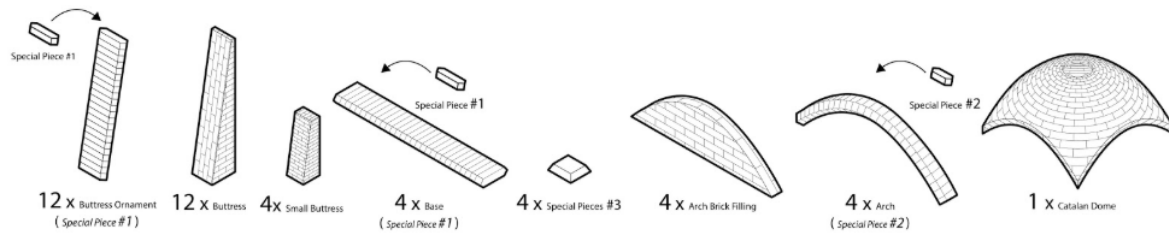
Medium Room
Module in Context



Medium Room
Module Isolation

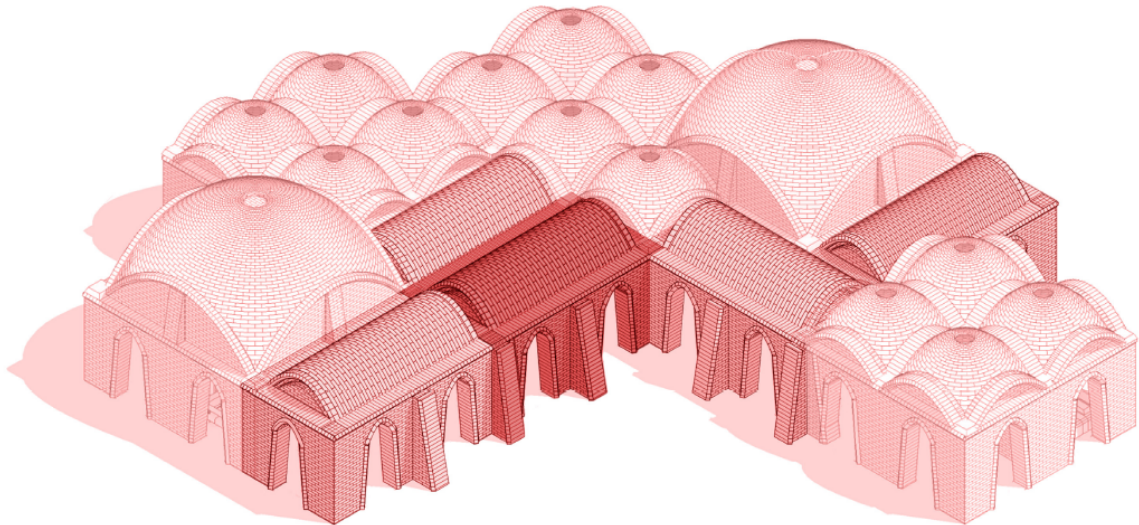


Medium Room
Exploded Axonometric

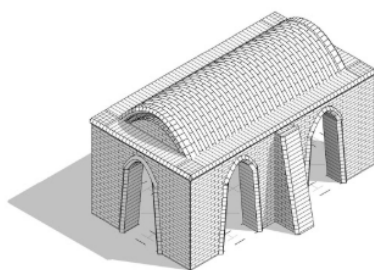


NoramI Vault Module

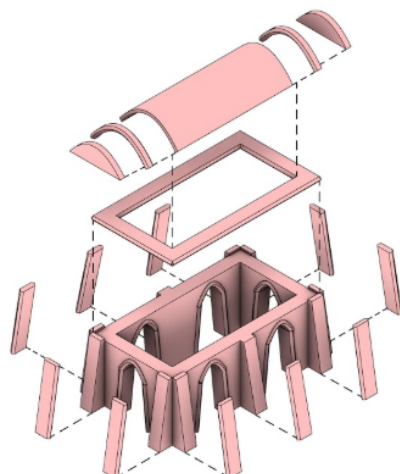
Construction Manual



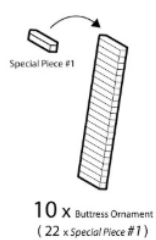
Normal Vault
Module in Context



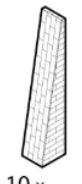
Normal Vault
Module Isolation



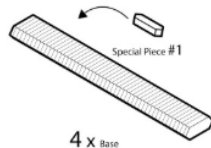
Normal Vault
Exploded Axonometric



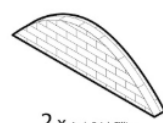
10 x Buttress Ornament
(22 x Special Piece #1)



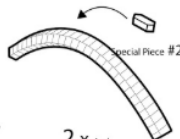
10 x Buttress



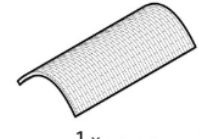
4 x Base
(Special Piece #1)



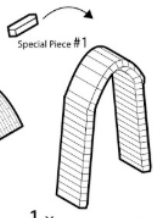
2 x Arch Brick Filling



2 x Arch
(Special Piece #2)



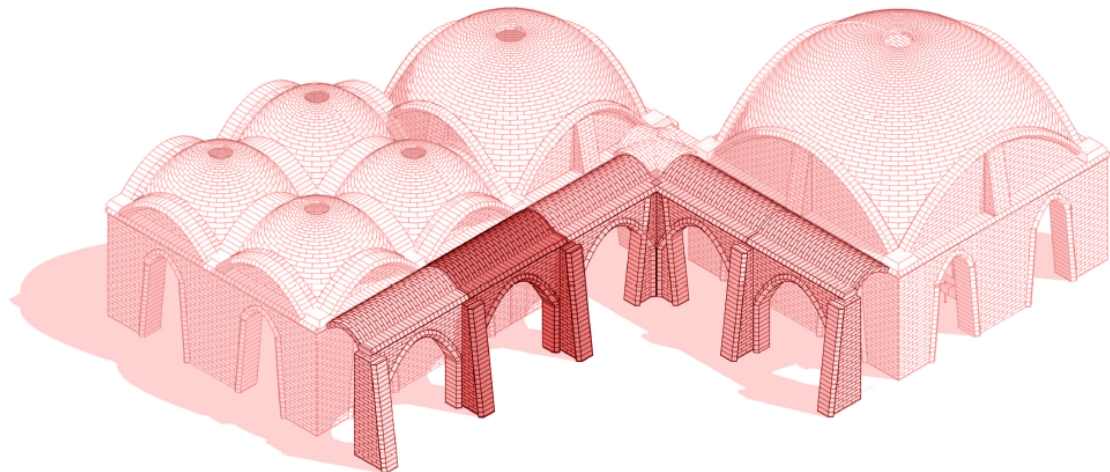
1 x Catalan Vault



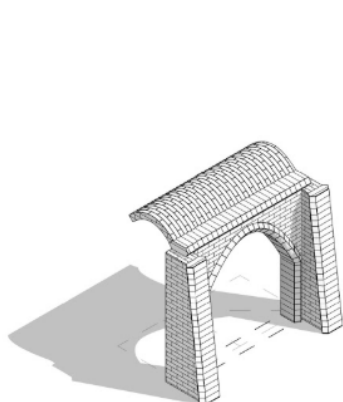
1 x Door Ornament Arch
(Special Piece #1)

Half-Vault Module

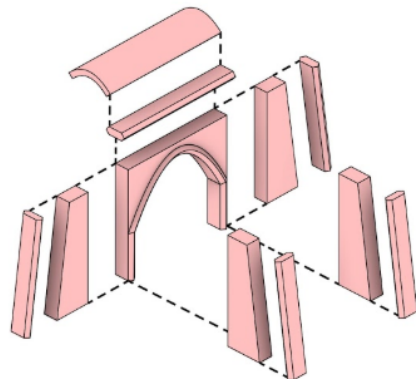
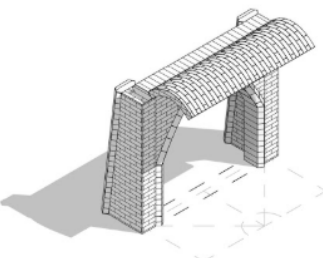
Construction Manual



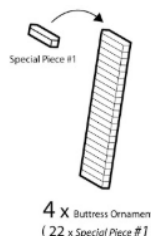
Half-Vault
Module in Context



Half-Vault
Module Isolation



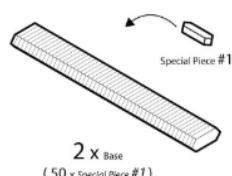
Half-Vault
Exploded Axonometric



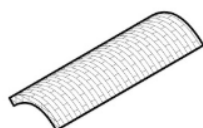
4 x Buttress Ornament
(22 x Special Piece #1)



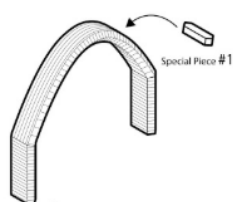
4 x Buttress



2 x Base
(50 x Special Piece #1)



2 x Half Vault

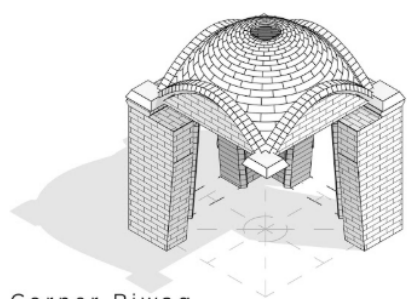


1 x Door Ornament Arch
(Special Piece #1)

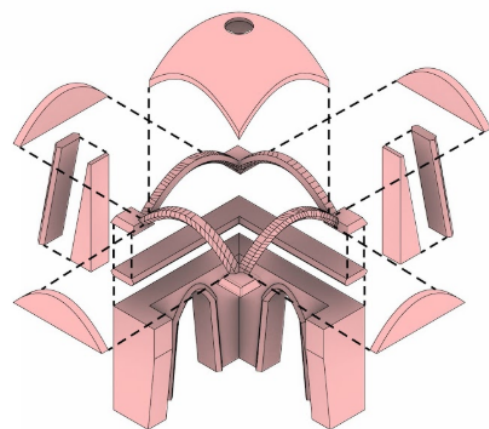
Corner Riwaq Module Construction Manual



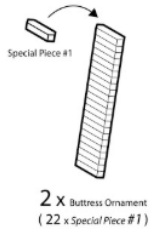
Corner Riwaq
Module in Context



Corner Riwaq
Module Isolation



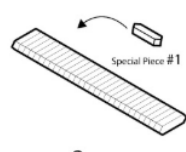
Corner Riwaq
Exploded Axonometric



2 x Buttress Ornament
(22 x Special Piece #1)



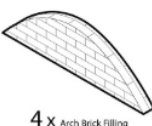
2 x Buttress



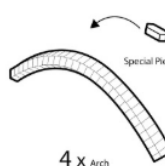
2 x Base
(29 x Special Piece #1)



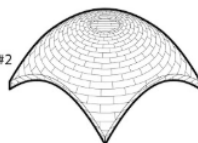
4 x Special Pieces #3



4 x Arch Brick Filling



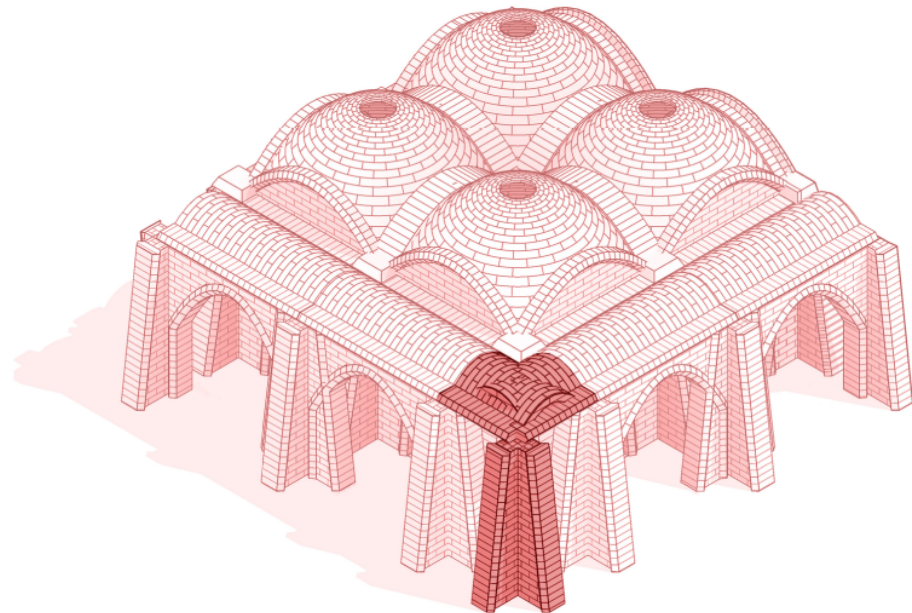
4 x Arch
(28 x Special Piece #2)



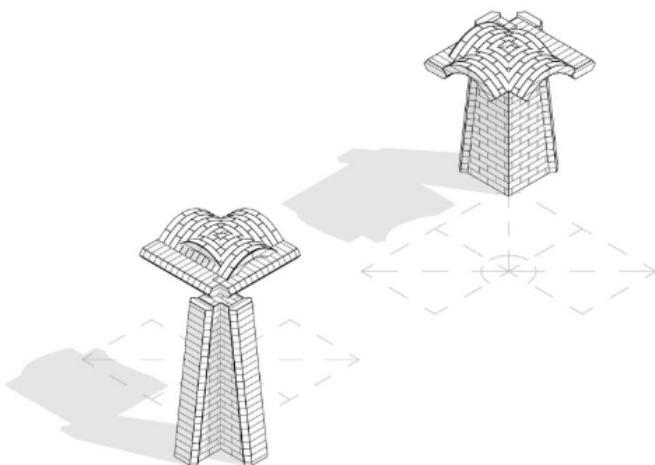
1 x Catalan Dome

Half-Vault Corner Module

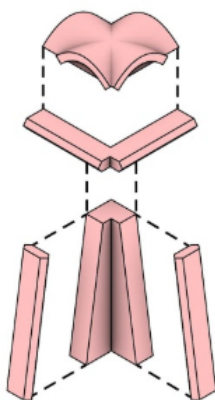
Construction Manual



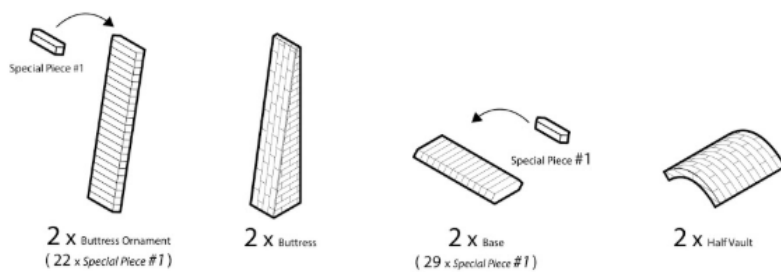
Half-Vault Corner
Module in Context



Half-Vault Corner
Module Isolation



Half-Vault Corner
Exploded Axonometric



Bricklaying & Connections

Multiple exercises were carried out at initial stages to develop practical connections between walls, buttresses and domes/vaults.

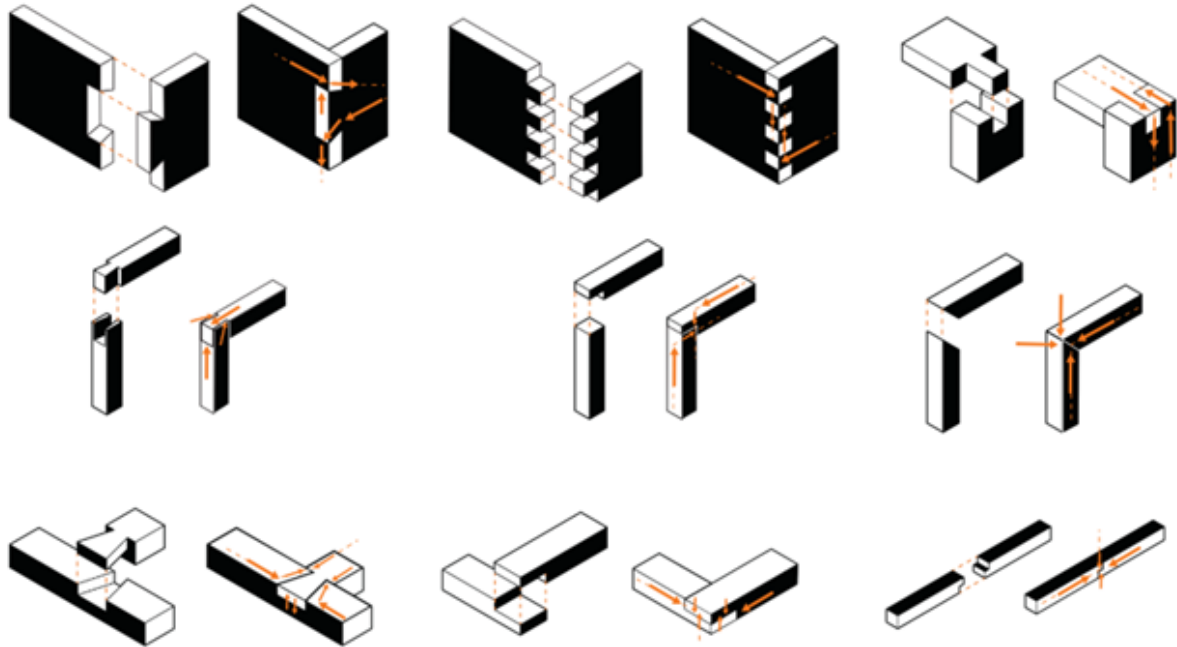


Figure 3.1 – Initial research on Japanese joint connections for possible brick geometry.

Yet another exercise shows our process of trying to come up with a system that would allow for the modules to attach in subsequent phases. This exercise contemplated the bricklaying aspect. (Figure 3.2)

Finally, the chosen system contemplates 4 different brick types (see brick types section) and a traditional interlaced bricklaying pattern. The openings on the walls and buttresses can be finished with the Type 1 brick type. Type 1 brick type also served as the final top level of all the modules; its special tapered geometry is meant for future potential vaults if required. It is important to clarify that the buttresses serve only as temporary lateral support for the modules, once another side module is built, it will counterbalance this lateral force. Due to the temporary nature of the buttresses, the bricklaying with the buttress must not be intertwined or woven with the rest of the wall.

CORNER'S CONNECTORS

اتصال الزوايا

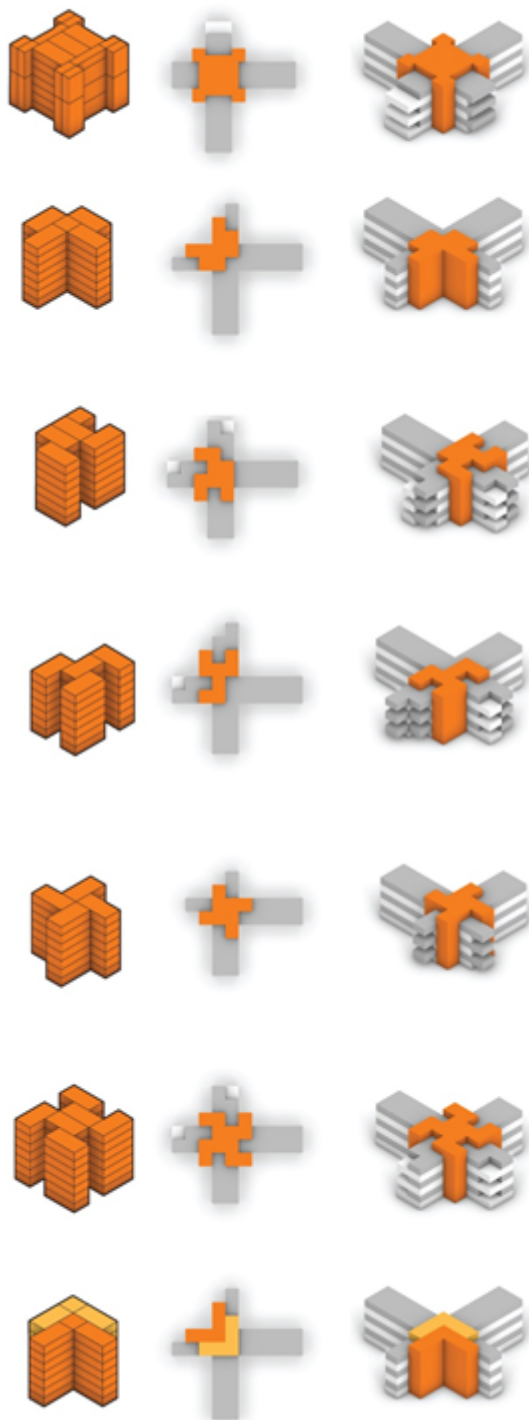


Figure 3.2 -Exercise on joint types to allow for future modules.

Brick types

Initially we looked at many brick types for construction, in the process we came up with a brick that could serve as gutter when the vault did not have a second floor. When a second floor was constructed, this gutter would be filled with another special brick type. Although its geometry made sense for the water collection, this special piece was particularly prone to breaking from the weight of the vault, therefore this detail was eliminated from the final design.

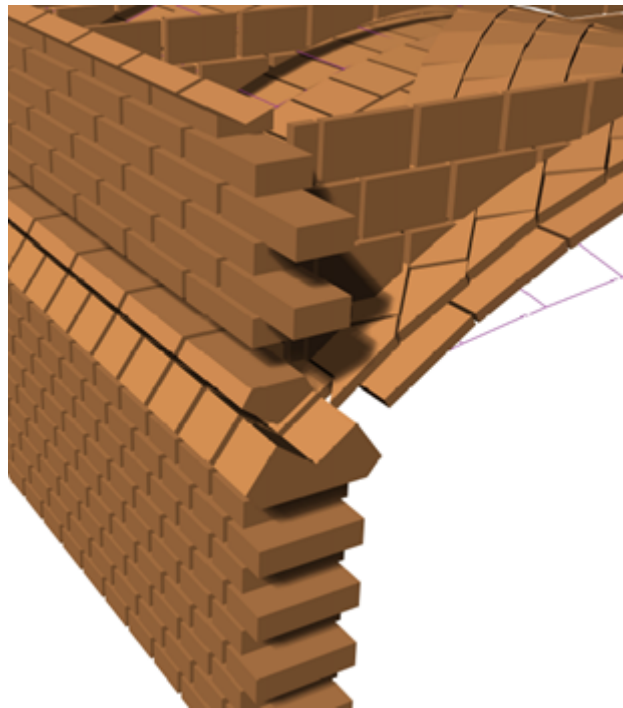


Figure 3.3 – Detailing exploration with different brick types.

In the end, in order to simplify construction, we aimed to have the least amount of brick types possible. These are all the brick types used:

- “Tile” Brick: A lightweight brick used for the Catalan method to close the vaults and domes. (see construction method section)
- Typical Brick: Used for walls and buttresses - 70 x 140 x 280 mm (1x2x4 recommended ratio)
- Type 1 – 440 mm piece for vault connections and buttress/doorway ornamentation
- Type 2 – 220m piece for dome arches. (Half piece to avoid dome overlaps)
- Type 3 - Tapered piece for dome arch bases.

(The different dome sized would affect slightly the angle of this piece, therefore this type would have small, med, large variations – Type 3a, 3b, 3c to avoid cutting on site the “tile” bricks)

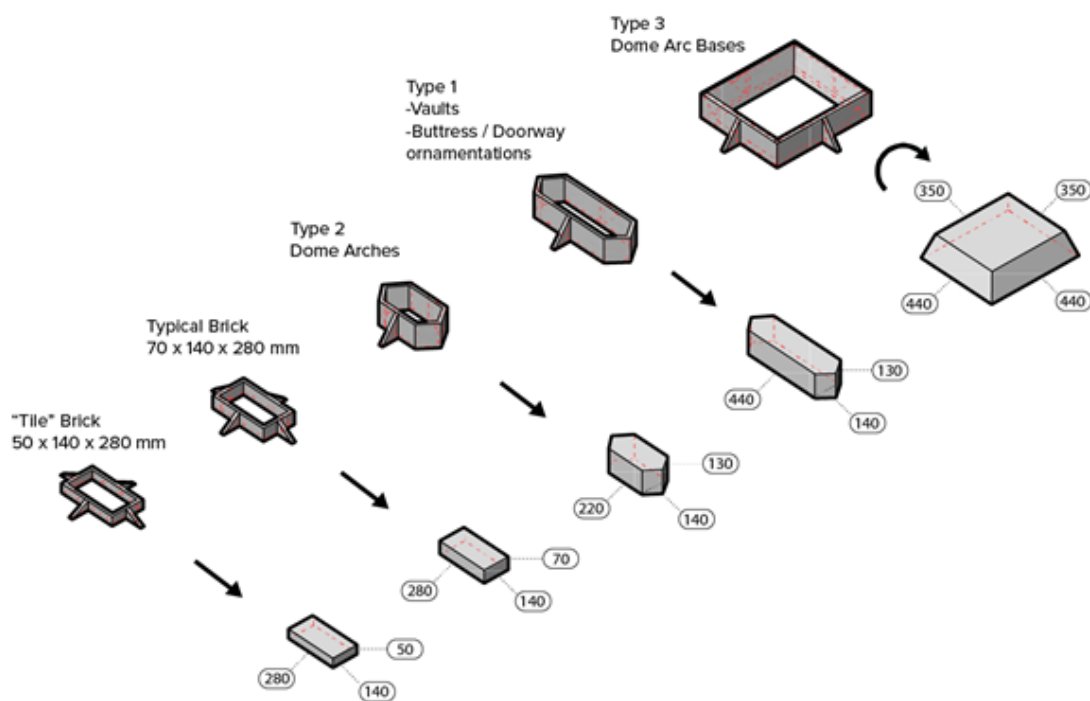


Figure 3.3 Brick Molds & resulting Brick Types

Construction Method

An advantage of the proposed “structural independence” of the modules was that there is an intrinsic stability during the expansion and construction of the camp. The lateral forces from the vaults and domes meant that they required side supports, therefore, when not neighboring another module, buttresses where necessary. These temporary buttresses would therefore need to be present all around the existing perimeter of the cluster. As mentioned previously, if new modules are added, the buttresses would then be demolished.

There are three main methods for creating an arc-based roof: Roman, Nubian, Catalan. The main characteristics of each are:

Fig. 3. Three methods of brick vault construction [7]: a) Northern European vaults require extensive wooden centering; b) pitched brick vaults, built in North Africa and Mexico, eliminate the need for centering; and c) Mediterranean tile vaults may be constructed without centering.

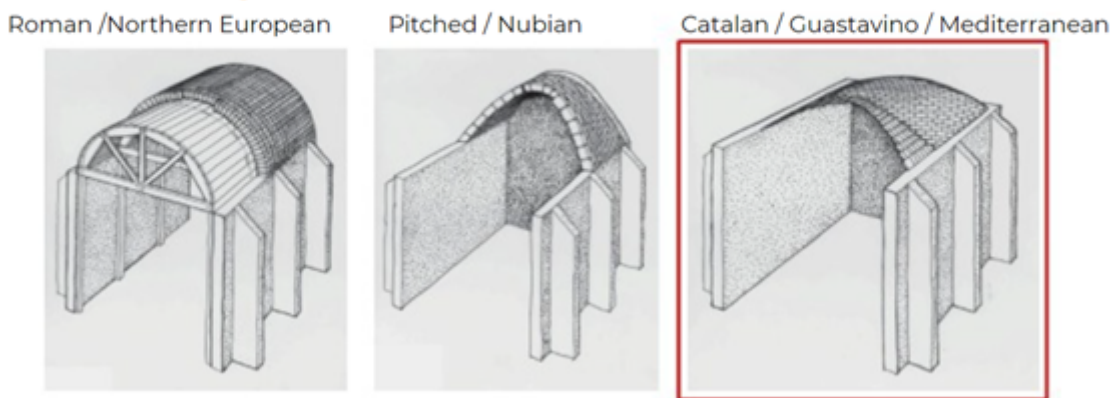


Figure 3.4 – Brick vaults construction options – “Tile vaulted systems for low-cost construction in Africa”, BlockDeJongDavisOchsendorf, 2010

- Roman uses heavy bricks and requires extensive wood centering.
- Nubian uses similarly heavy bricks but is built on an incline, this avoids any centering but requires an initial lateral wall to support the inclined bricks.
- Catalan uses light bricks/tiles bonded together by mortar and subsequent layers.

Since we aimed to use the least amount of resources possible for the construction, we chose the Catalan method because it would not require lateral walls and only wooden or plastic guides would be necessary.

The most important aspect of the Catalan construction was to use thinner bricks (50 mm “tiles” in our case) that could be bonded together by fast setting mortar in a very precise structural curve. This funicular geometry was a critical factor in order to have such a thin construction. Likewise, multiple layers of alternated tiling pattern where necessary to prevent continuous joints and maintain a good structural bond.

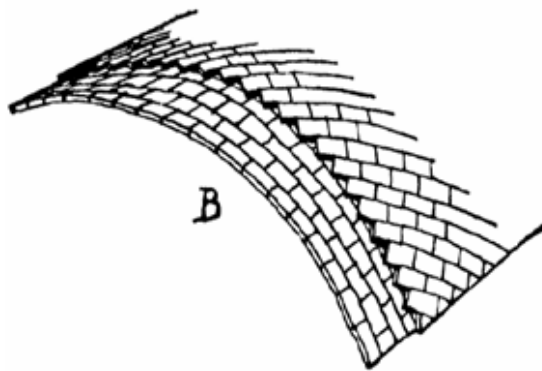


Figure 3.5 – Alternated 3 layered Catalan method.
"Tile vaulted systems for low-cost construction in Africa", BlockDeJongDavisOchsendorf, 2010

Ideally, Portland cement mixed bricks or stone with a high compressive strength would be used, nonetheless our brick analysis resulted in adobe bricks of 159 MPa, thus comparable to the Trachyte stone used for the Mapungubwe project in Africa (150 MPa).

"The proposed vaulting system takes advantage of funicular geometry to limit the amount of material required, and to avoid tensile reinforcements. Stresses are low within the structure, so soil tiles with relatively little material strength can be utilized."

"Tile vaulted systems for low-cost construction in Africa", BlockDeJongDavisOchsendorf, 2010, pg 6

For the mortar, this project used a first layer of fast setting gypsum plaster (Plaster of Paris) and succeeding layers of cementitious mortar. Gypsum is widely available from the Jordan Gypsum Manufacturing Co.

A predecessor of this project is the work of Rafael Guastavino. Guastavino was a Spanish engineer and builder that created extremely thin and shallow vaults and domes with very large spans. He did not invent the layered tile system but did patent it for his constructions in the United states.

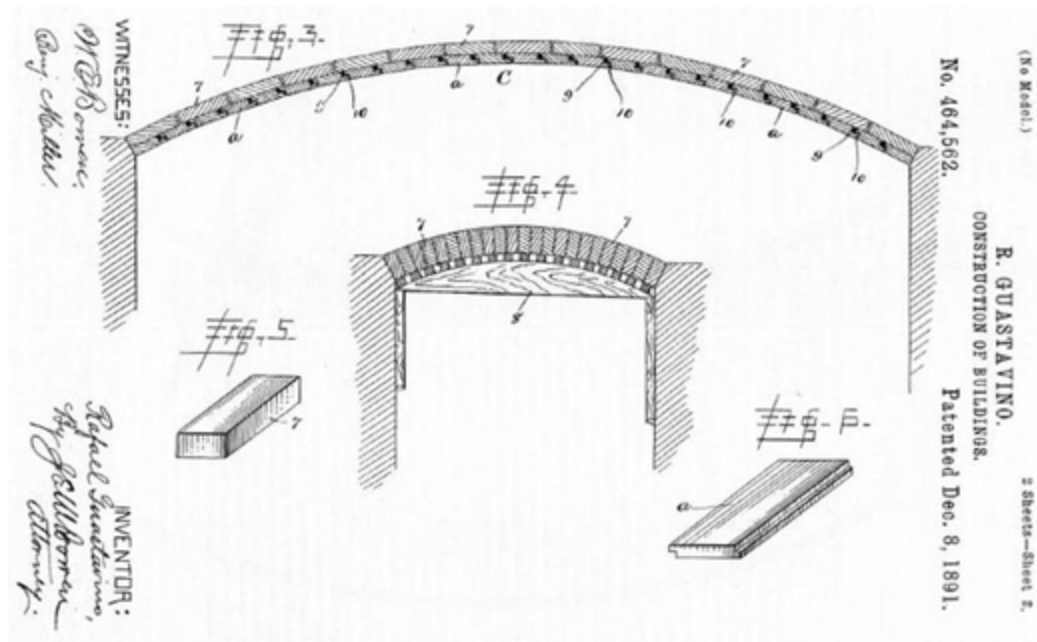


Figure 3.6 – Guastavino Patent (Fig 3) using alternating tiles (Fig 6) compared to traditional arc (Fig 4) using a thicker brick (Fig 5)

A great example of his method is St John the Divine church built in 1892 by Guastavino. This image shows the extremely thin dome compared to other similarly sized domes.

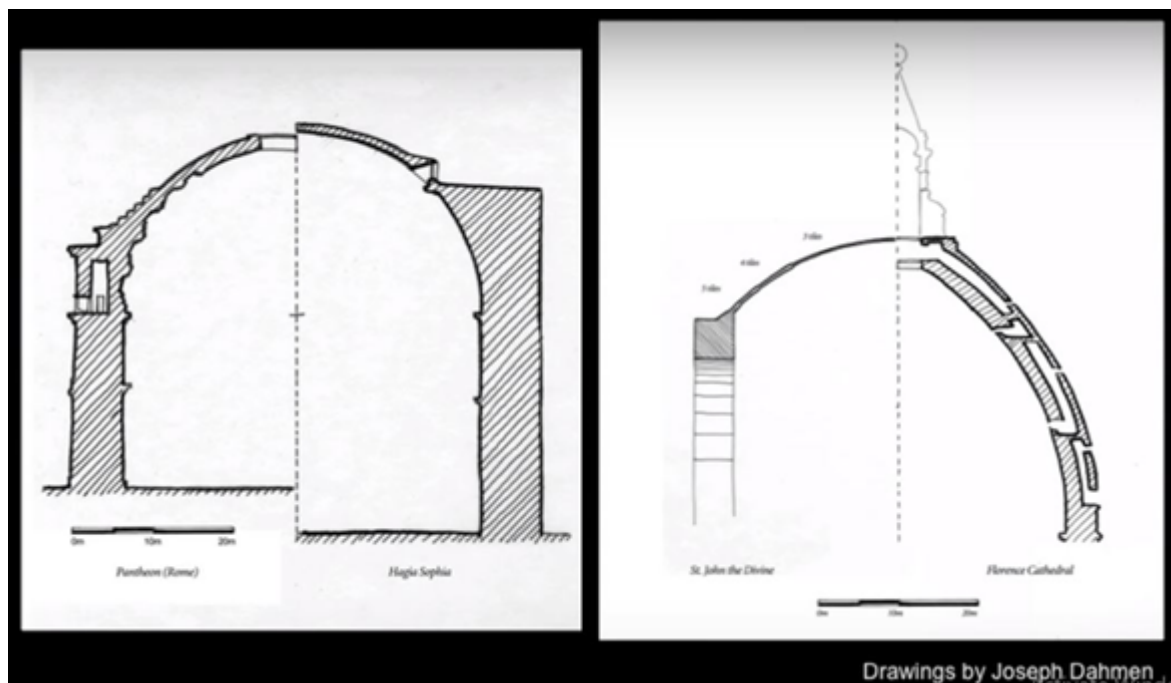


Figure 3.7 St John the Divine Dome (red) Thickness comparison with other similarly sized domes by Joseph Dahmen.

Although these low catenary shapes can hold massive amounts of weight with very little material, they produce very high lateral loads. For our project, there were two possibilities to counter these loads:

1. With the use of massive buttresses
2. With the use of steel rings that would work under tension and tie the domes together.
3. Increase Dome/vault heights.

With our initial low dome proposal, the first option would create buttresses that would follow the thrust line. The resultant forces, where giving a buttress geometry that would create extremely long (up to 2 m) bases of the buttresses.

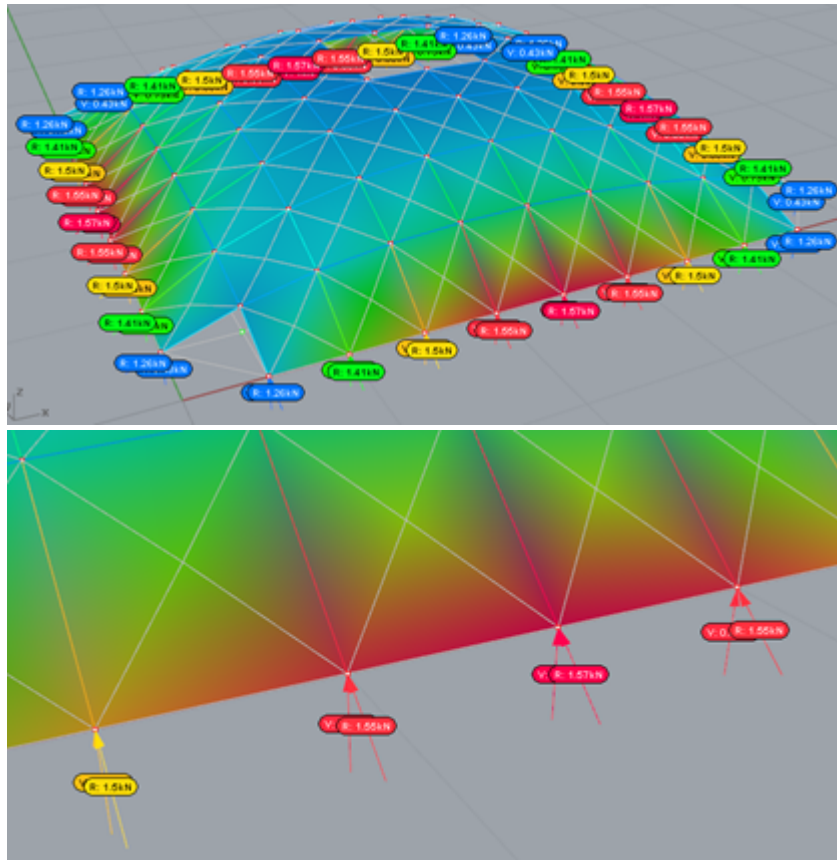


Figure 3.8 - Rhino Vault initial exercise to comprehend forces acting on dome. Resultant forces 1.55 Kn with a dead load of 28.3 Kn.

The second option was to apply a similar approach as used in St John the Divine Church. In this case, steel ties.

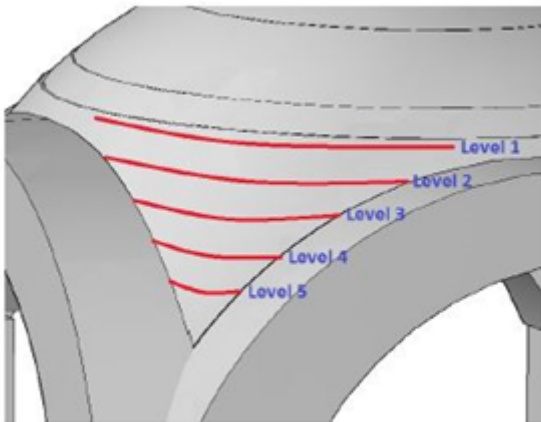


Figure 4.15: Steel ties location at one of the dome corners

Figure 3.9 Structural Assessment of the Guastavino Masonry Dome of the Cathedral of Saint John the Divine, Hussam Dugum, MIT, 2013

This option required an element under tension. We discussed the possibility of using the fencing around the camp and develop a detail with this material that would tie the domes/vaults. This option was discarded due to time limitations to develop the detail and analyze it adequately in our Kangaroo model.

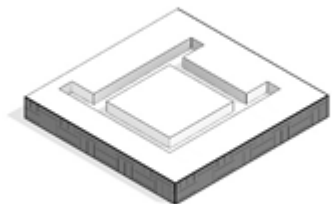
The final chosen option was to increase the height of the domes/vaults and thickening their section. This higher geometry lead to a bigger difference to reach the second floor, but in turn pointed downward the thrust line, thus reducing the buttress base lengths. This higher geometry would also permit an easier construction that wouldn't rely solely on the "stickiness" of the fast setting mortar. Also, the increase of the vertical load meant that we imagined thicker brick "tiles" of 50 mm to achieve the required 200 mm thickness (given by the Kangaroo structural analysis) with only 3 layers of bricks and 5 cm of mortar distributed in between all the binding layers.

For these reasons, we believe that a non-cementitious gypsum mortar could be used to bind the three layers of the vaults, nonetheless, 1:1 construction/performance mock up would be necessary to prove our hypothesis. Due to time limitations, this was not done.

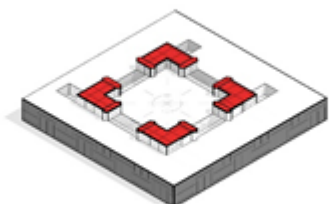
General Construction sequence

As mentioned earlier, a critical point in our proposal was to generate independent modules that can be built in phases as the camp grows progressively, thus the construction sequence was also critical.

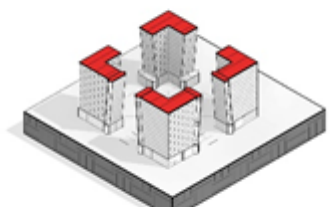
Steps:



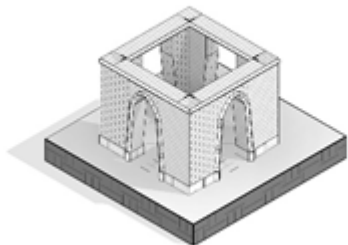
Dig ditches for foundation



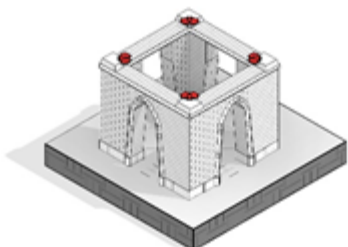
Foundation 20 cm above ground



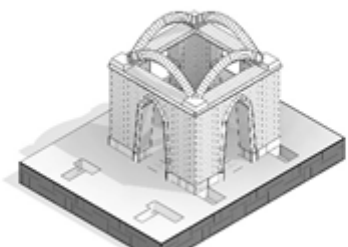
Build Adobe walls to 2.3 m height



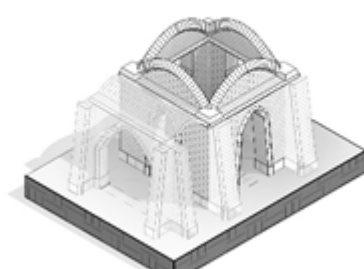
Install perimeter Special piece 1 for future vaults.



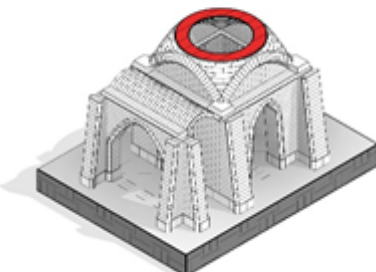
Install corner Special piece 3 for future domes



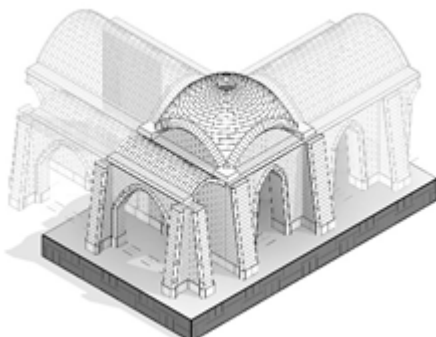
Make arcs from Special piece 2



Close arches off with wall and build buttresses or other modules to balance lateral forces of the dome.



Build dome



Add other modules



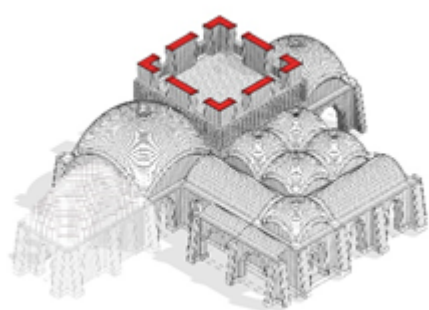
Fill spaces (lightweight) to avoid rainwater accumulation.



Build perimeter walls above 4dome module and vaults to contain lightweight fill.



Fill with lightweight fill – soil or pumice stone and finish floor for second level



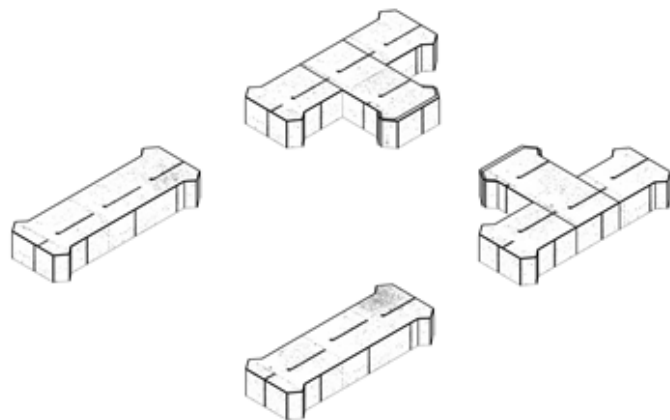
Only build on top of ones that have been calculated for a second floor according to game rules.



Final Modules

Construction Process

Foundation

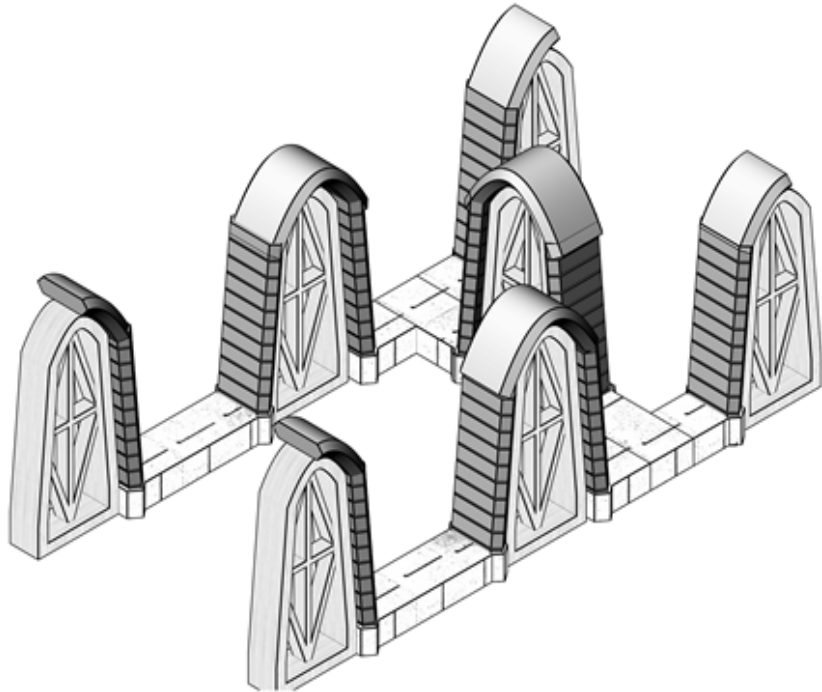


Minimum foundation of 20 cm above ground level to avoid water capillarity permeating into the adobe bricks.

Foundation options:

- Basalt Stone. - (Basalt stone is widely available nearby at Harrat al-Sham – Black Desert) (Ibrahim Bany Yaseen, January 2010)
- Portland cement mixed bricks
- Gravel stones mixed in concrete. (Reference pending)

Door Arches and Finishes



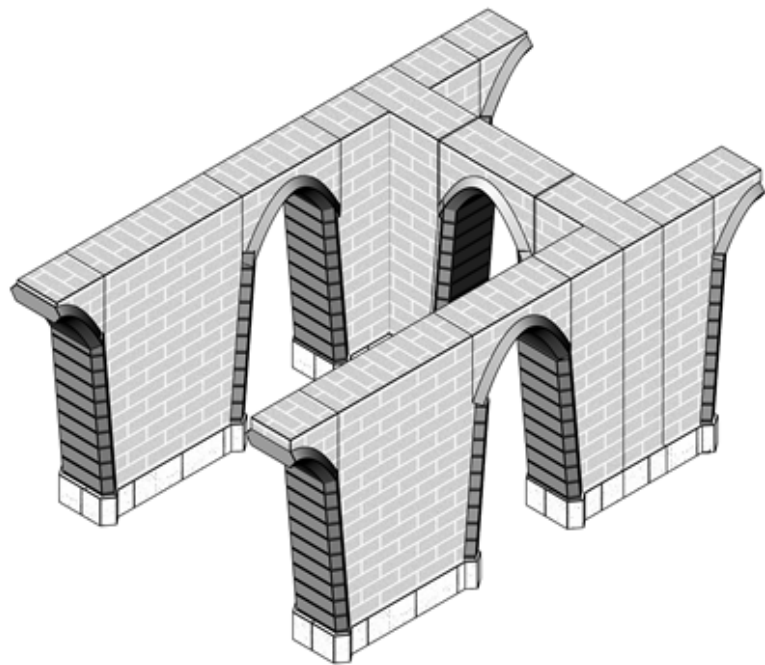
In order to maintain a constant shape throughout the project, two typical door arch frames are made:

- Typical door arch
- Large door arch of small Riwaq module.

These frames can be made of wood, plastic or steel, the latter being preferred because it will last longer as they will be used repetitively.

Type 1 brick type is used for the borders. The top arches can also be deconstructed into sections of Type 1 type (even though this example shows a complete arc).

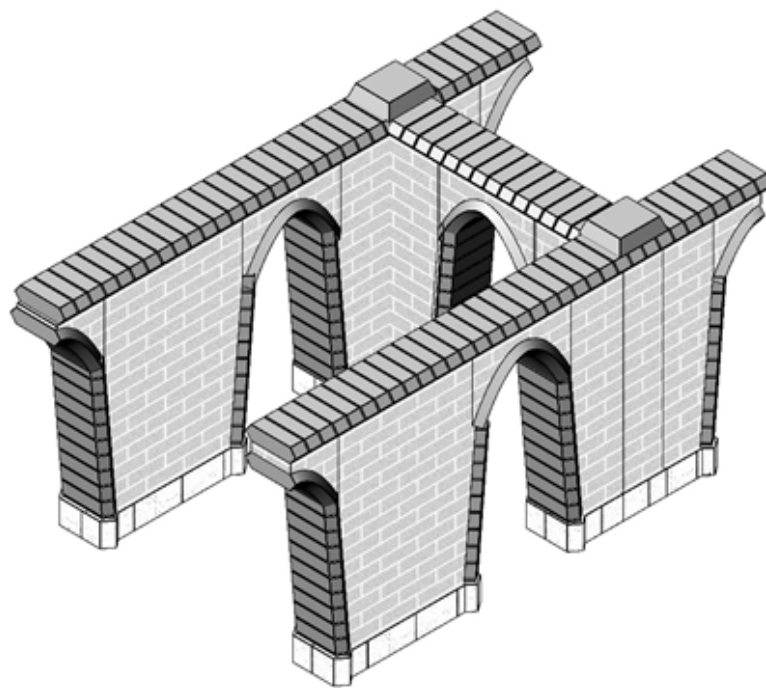
Walls



Walls are constructed with Typical Brick size.

Bricks must be cut when they intersect with previously constructed door arches.

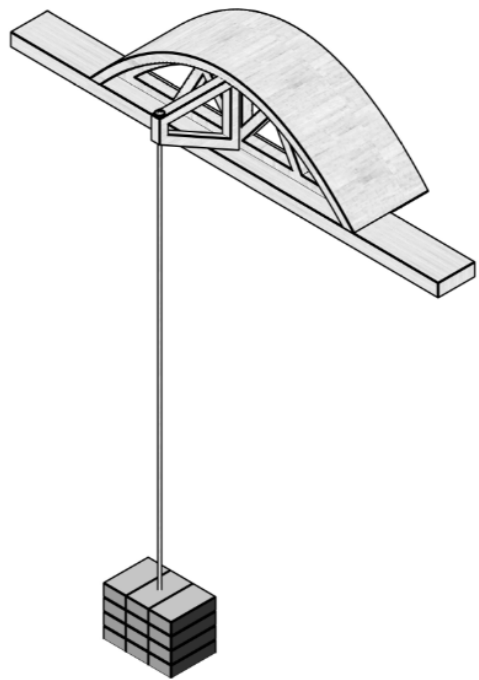
Top Finishes



Bricky Type 1 is used once again to finish the top edge. This will allow for future vaults of other modules.

Brick Type 3 is placed on top of Type 1 in order to allow for future domes.

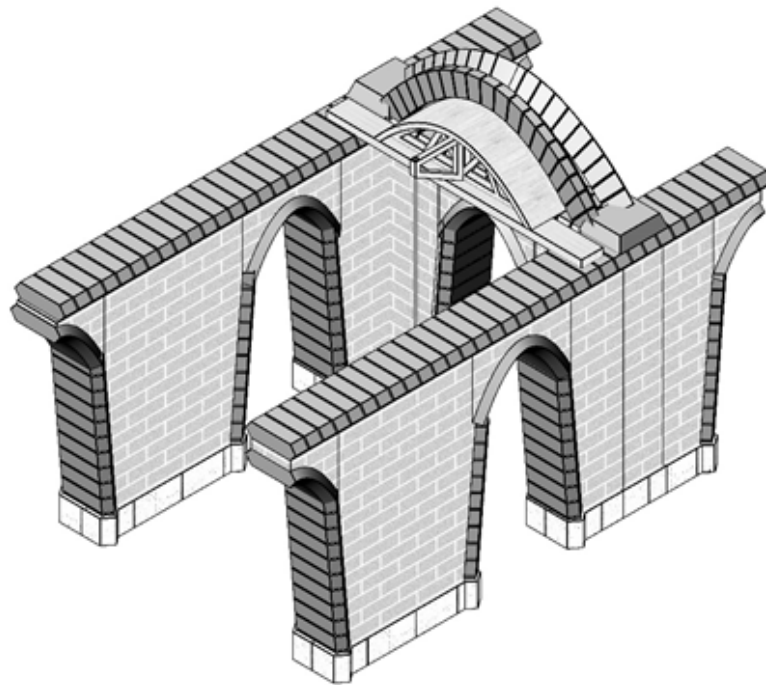
Counterbalanced guide



This tool is used to ensure that the bricks remain in place during the setting of the first layer. Bricks at its base serve as a counterbalance measure and are attached by means of a rope to a cantilever at the opposite side of the curve guide.

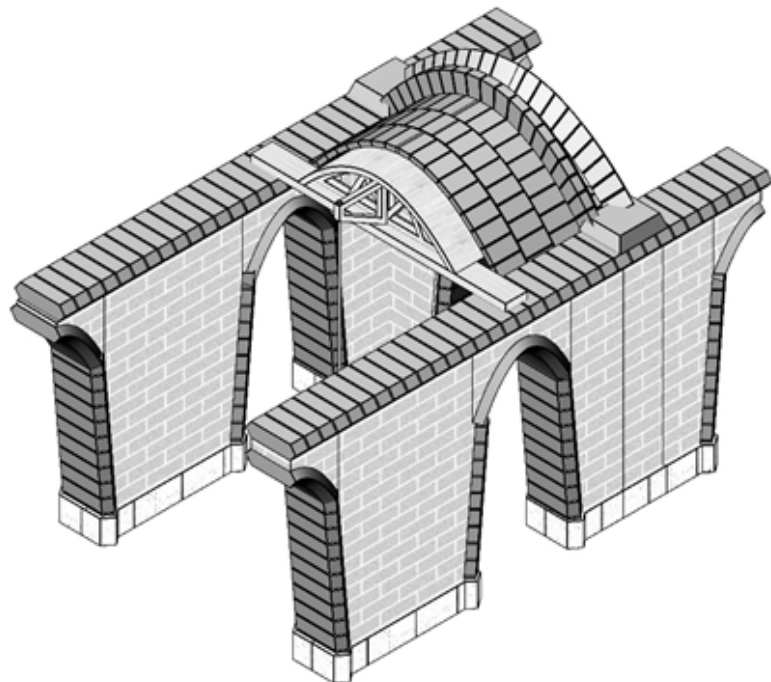
The curvature is given from an upside down chain with the span and height defined in the structural analysis.

Vault and Dome Arches



With the use of the counterbalanced tool, the arches of the domes or vaults are created. Type 2 brick type is used for these arches. They rest on top of Type 3 brick type.

Vault arches

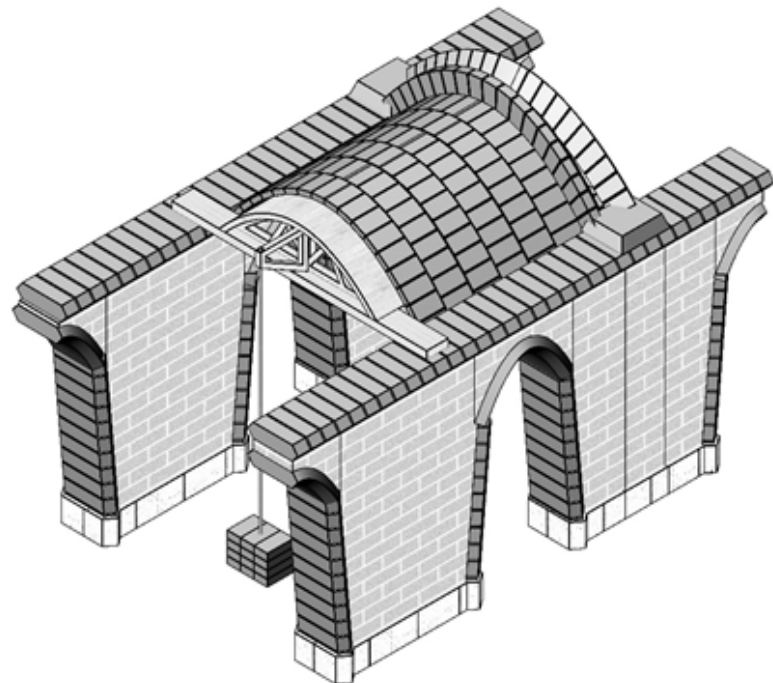


The vault arches are attached one after another.



Activate V

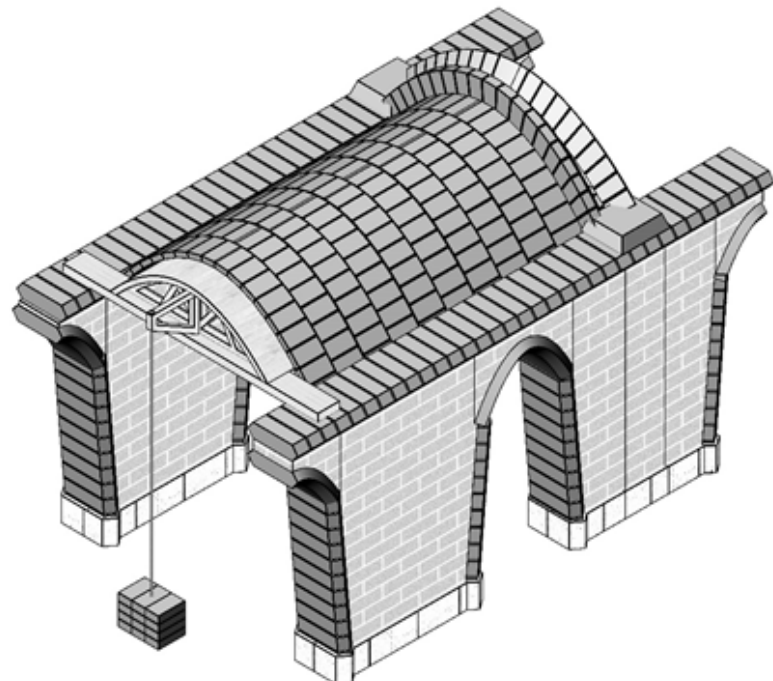
Making of the “Beyond Bending” ceramic tile and earthen vaults. Block Research Group. 2016.
<https://vimeo.com/193874177>



Arc process is repeated.



Making of the “Beyond Bending” ceramic tile and earthen vaults. Block Research Group. 2016.
<https://vimeo.com/193874177>

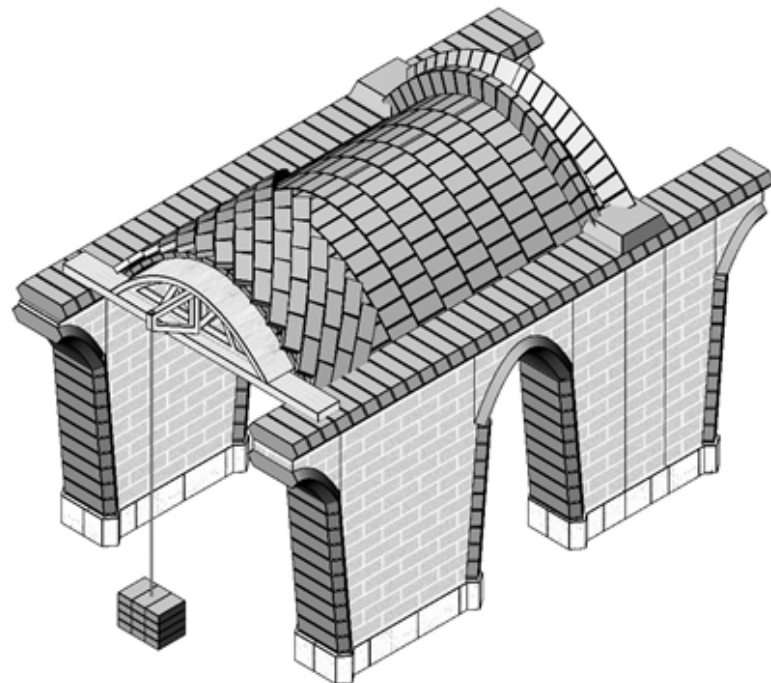


Final layer is finalized.



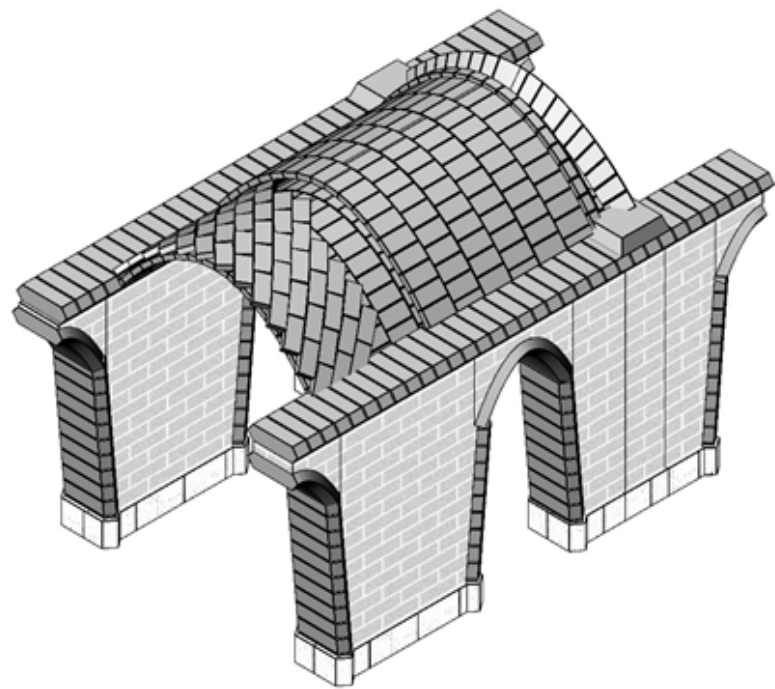
Activate W

Making of the "Beyond Bending" ceramic tile and earthen vaults. Block Research Group. 2016.
<https://vimeo.com/193874177>



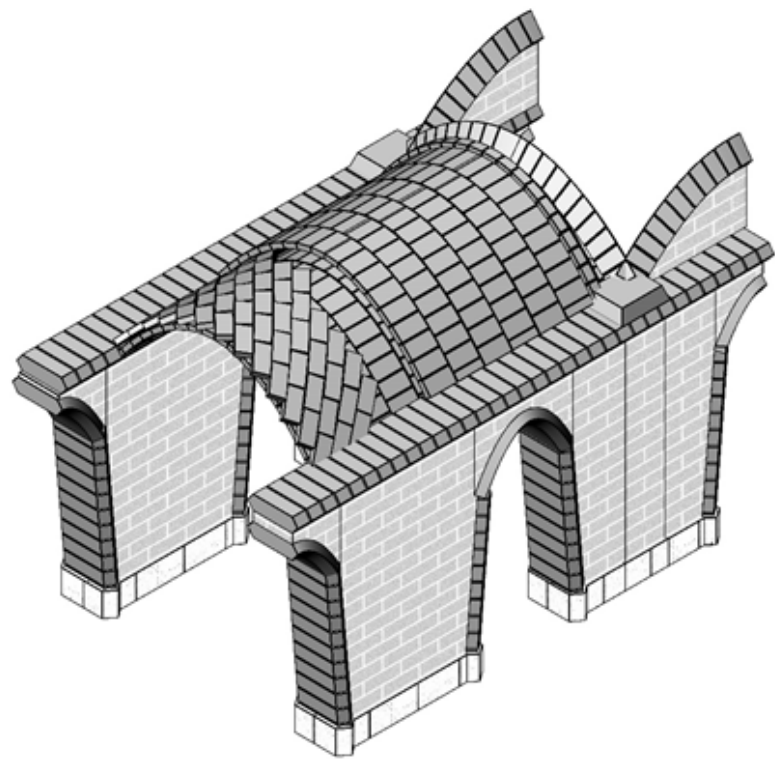
Making of the “Beyond Bending” ceramic tile and earthen vaults. Block Research Group. 2016.
<https://vimeo.com/193874177>

Vault arches



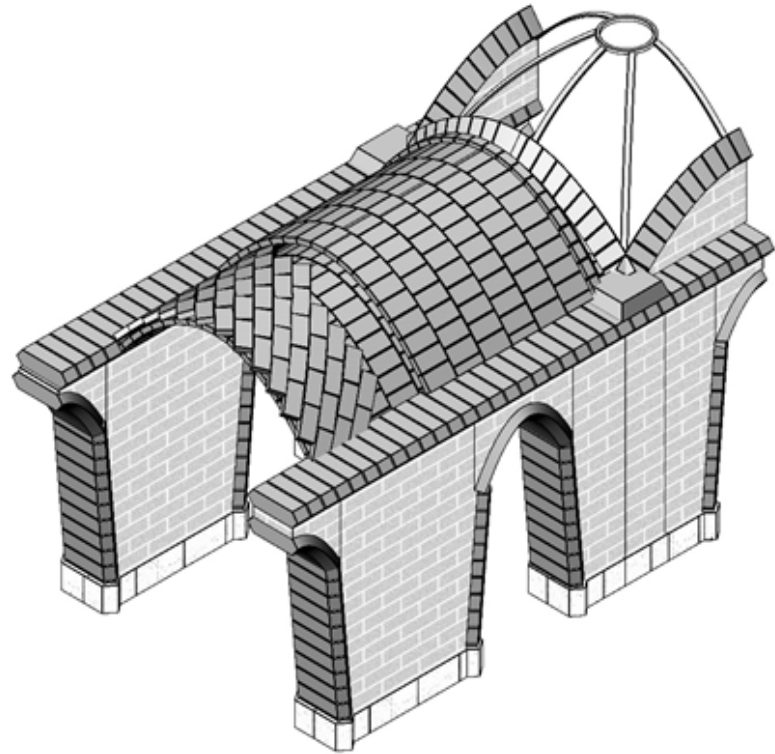
Final layer again perpendicular but with tile joints not aligned.

Dome arches



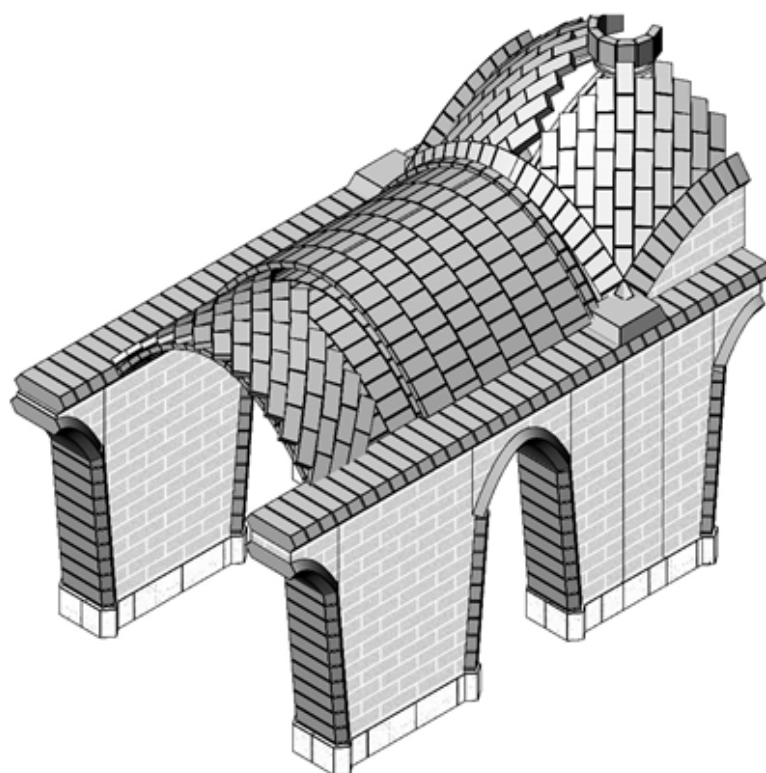
Dome arches are constructed using a similar guide method.

Dome Guides



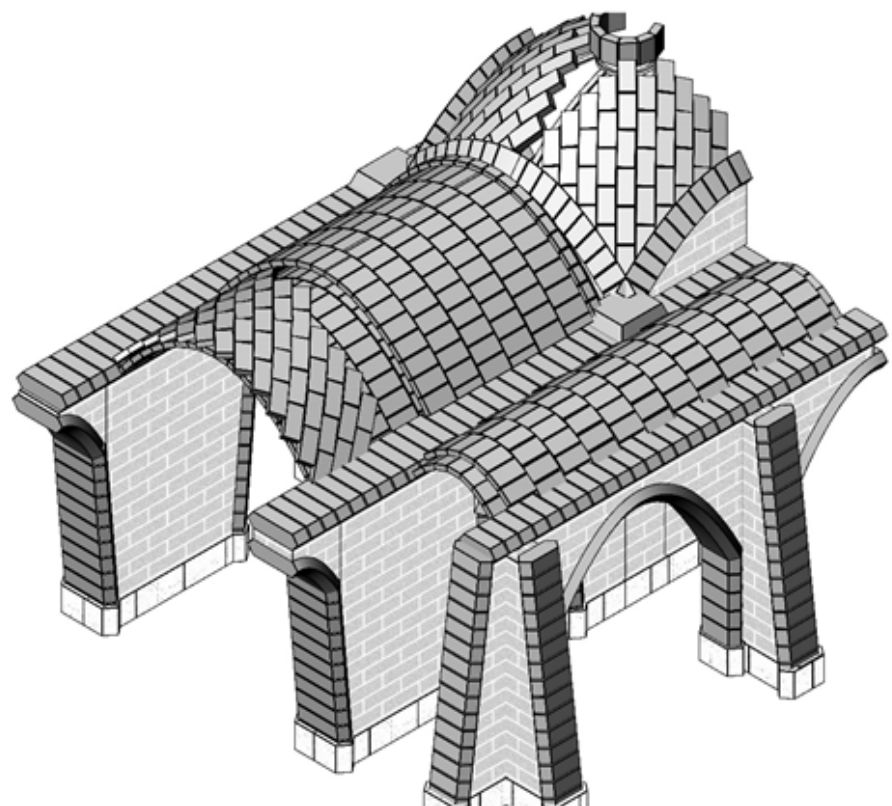
Dome guides are placed to ensure correct geometry, not necessarily to keep the bricks in place.

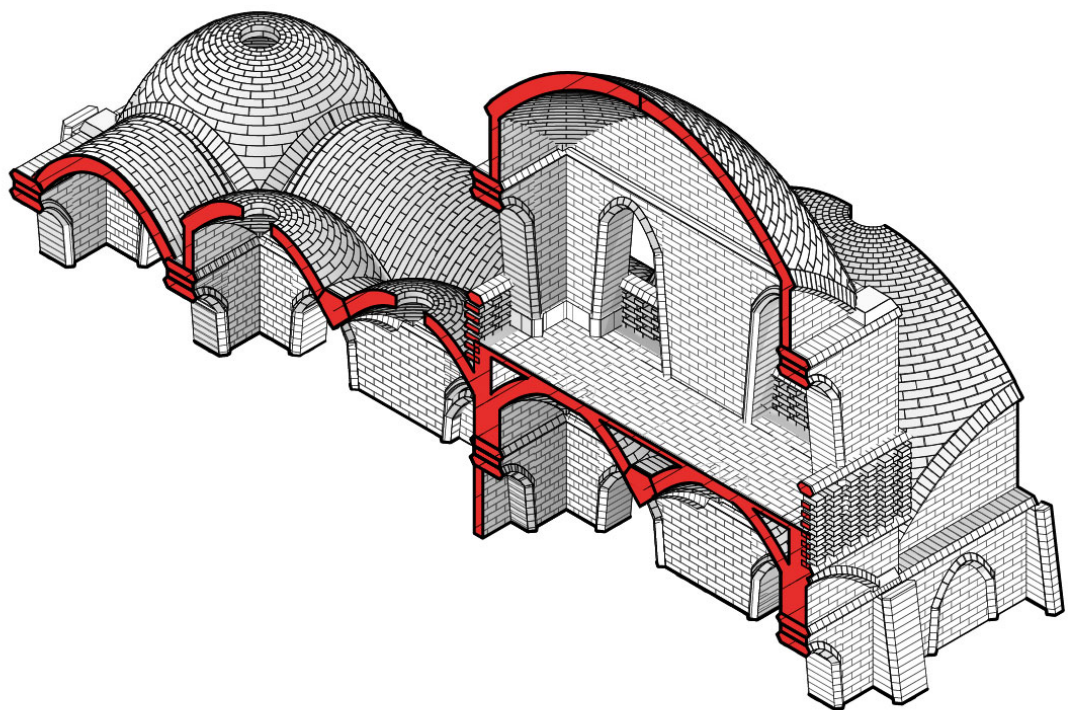
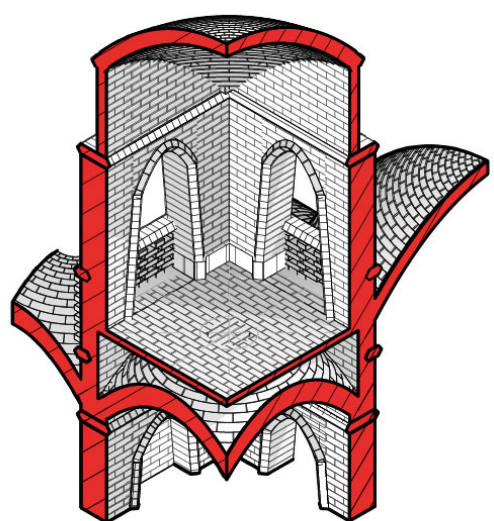
Dome

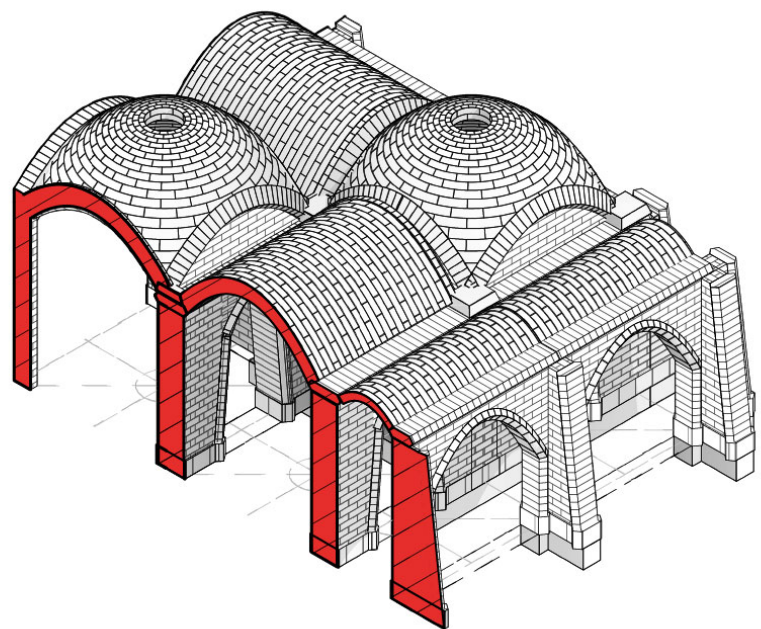


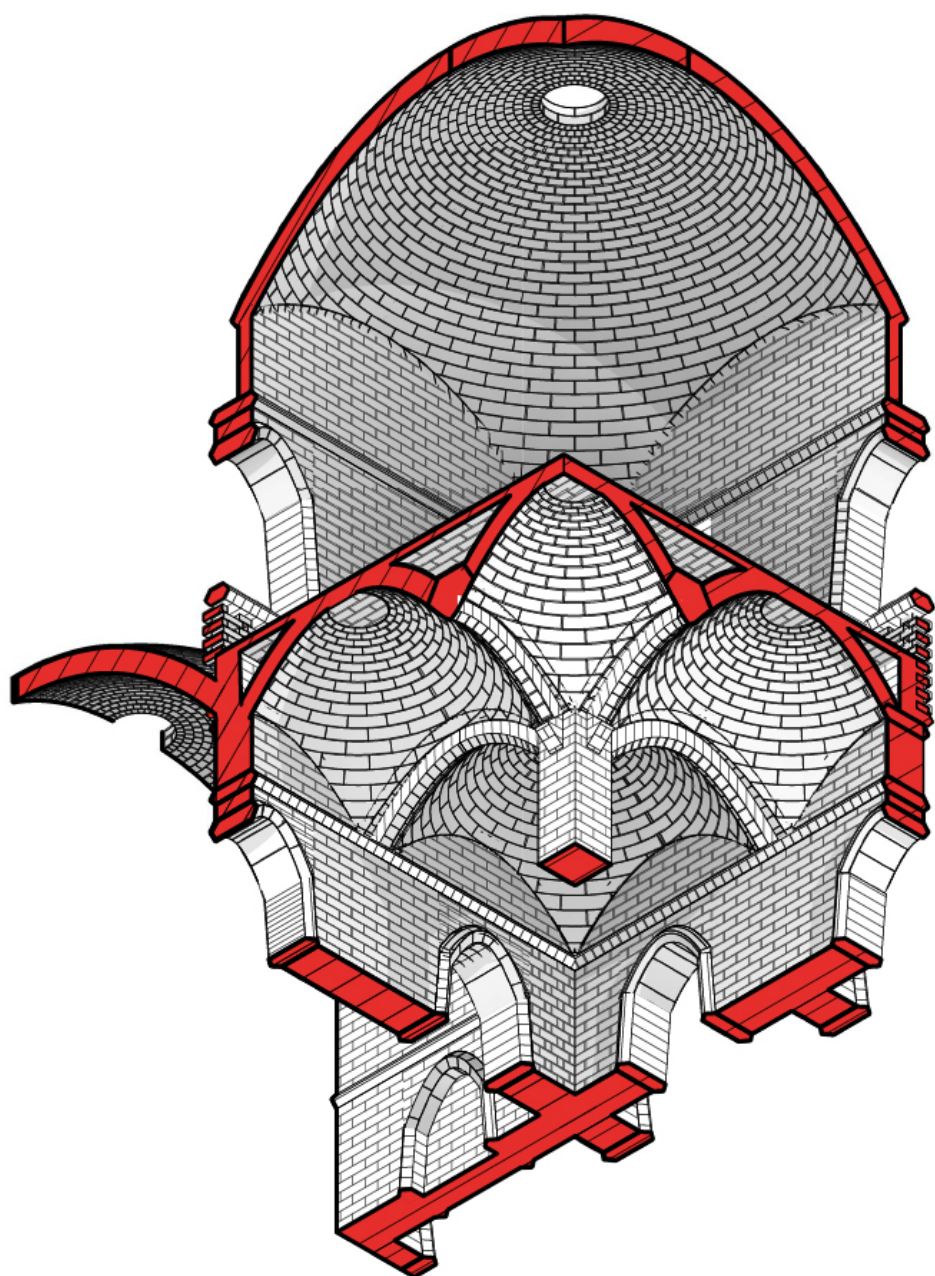
Domes tiles are places using the similar 3 layer vault system. The second layer also needs to be at an angle.

Module with small neighboring riwaq











4 Structuring

4.1 Introduction

This paper describes the analysis ran on the structure of the design realized for the course Earthy at the faculty of architecture and the built environment of TU Delft. The main objective of the project is to reorganize the refugee camp of Al Zaatri in Jordan through the implementation of computational tools in the design process and considering handmade adobe bricks as the main material for the construction.

The main idea behind the chosen design is that every space is defined by a specific unit with its specific geometry and construction method. These units, given the intention to have a system that can be expanded, must necessarily be structurally independent. Initially, the methodology is explained briefly introduce the context and the analysed structures. Furthermore, the tools utilized for the structural analysis are introduced and explained along with the simplification performed on the structures. Finally the results are discussed and the limitations taken into consideration and addressed.

4.2 Methodology

The design and structural analysis processes were carried out in parallel to find the right compromise between desired architectural expression, construction method and optimal shape. First of all the parameters that would have been later used to change the geometry according to the results of the structural analysis were defined. The width of the openings and the height of the arch above, the extension of the reinforcements, the height of the arches on which the domes rest and the extension of the latter were defined as variable parameters while the plan dimensions of the modules, height of the walls and maximum height of the modules having a second floor were set as constraints to respect the architectural intentions.

Once the parameters were set the shape of the arches, vaults and domes were form- found through the use of the Kangaroo plugin for Grasshopper in order to support their self-weight. Subsequently a structural analysis was conducted via Karamba considering all the external loads. A second form-finding phase was then carried out to optimize the shapes according to the new loading conditions, the final geometry was structurally analyzed and the results evaluated according to the limitations of the material taken into consideration. Finally the evolutionary solver Galapagos was used to try different combinations of the variable parameters to optimize even further the structure.

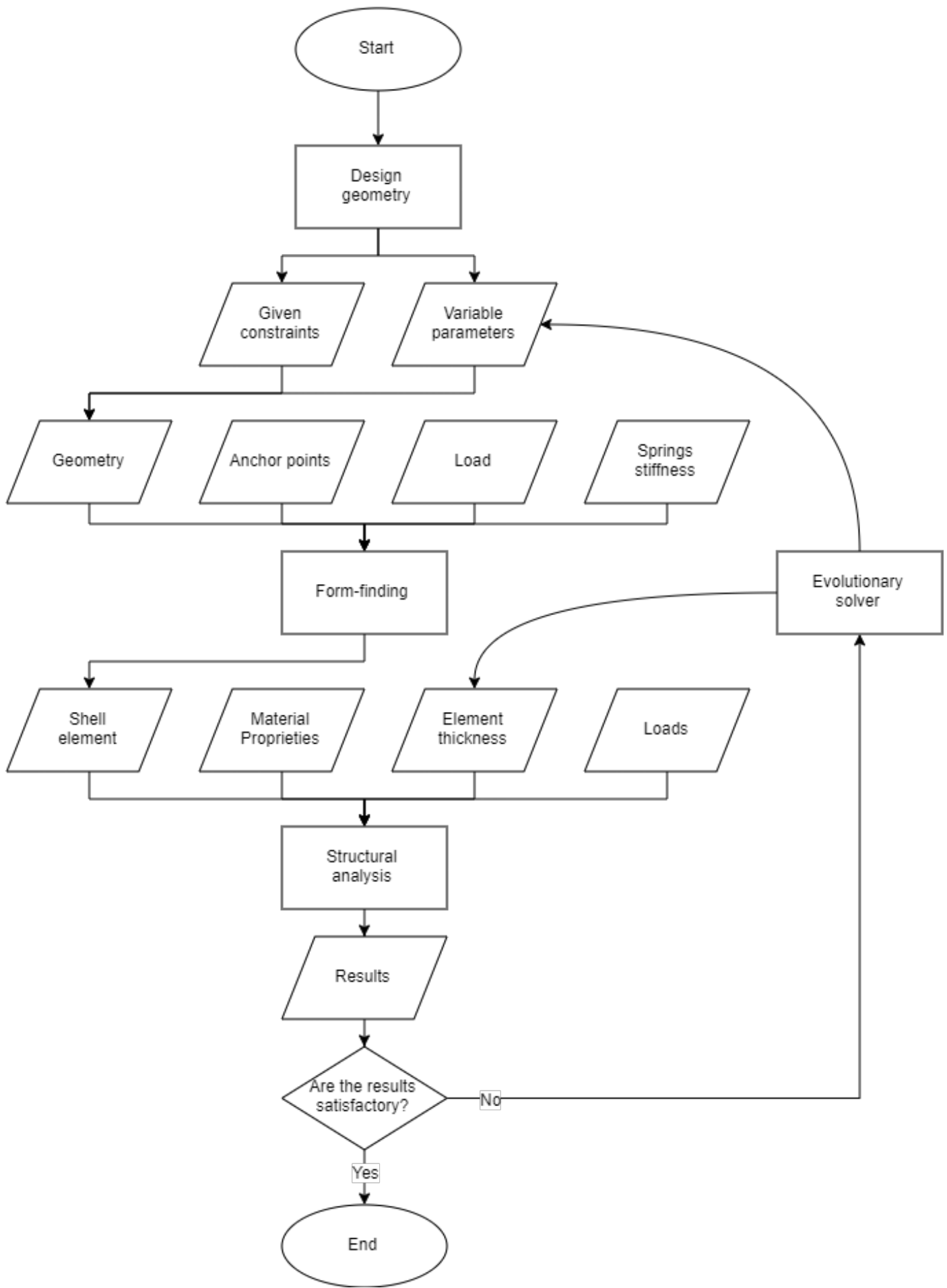


Figure 4.1: Process flowchart

4.2.1 Geometry design and mesh refinement

The geometry of the modules was drawn inside the grasshopper plugin for rhino. The units were initially defined by two-dimensional surfaces with the intention then to apply thicknesses and perform the form finding process for the parts most subject to stress. All the geometries have been designed so as to be easily modifiable according to the needs dictated by the results of the analysis as well as any changes dictated by design choices. The dimensions of the individual parts have been managed within the plugin by numerical sliders, as well as by practical aspects, to be able to assign these sliders as genomes for the solver galapagos (more on the topic in section 4.2.4).

Once the surfaces defining the structure were obtained, they were translated into mesh to be able to perform the form-finding as well as the FEA analysis. The difference between the geometries has led to a refining of the single meshes for each unit. The subdivisions used were of the Catmull-Clark or Loop type depending on the case, having as objective that of having the meshes formed by vertices distant not more than 10cm from each other, in order to have the most reliable results possible. [Fig.4.2 - 4.4] In the case of contact between two different elements (for example between domes and walls) it was important for the FEA analysis through Karamba, to check that they had all the vertices in common in the contact area. Having vertices in the same position is translated by Karamba into a single structural node and forces can then move from one element to another without errors dictated by geometric inconsistencies [Fig.4.5]. Once the geometries with the respective variable parameters have been defined, we have moved on to the form finding phase for the arcs above the openings and for the ceilings.

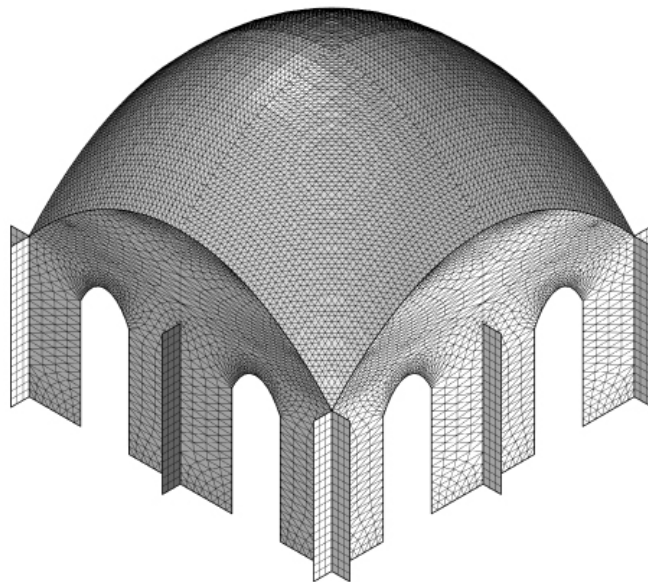


Figure 4.2: Large dome unit mesh refinement

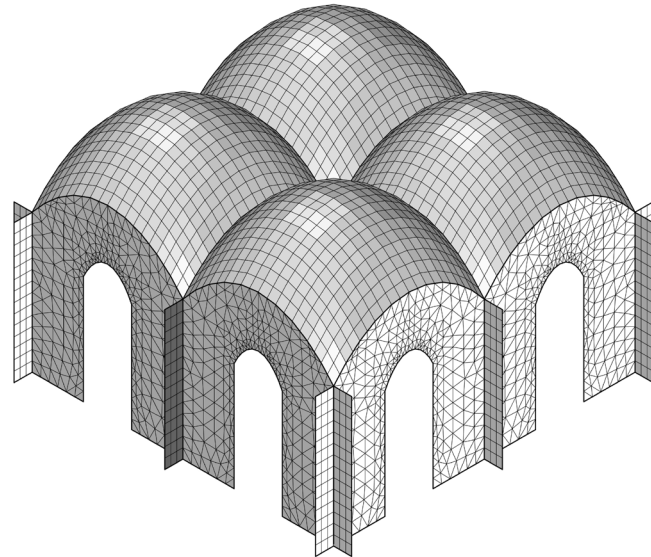


Figure 4.3: Four dome unit mesh refinement

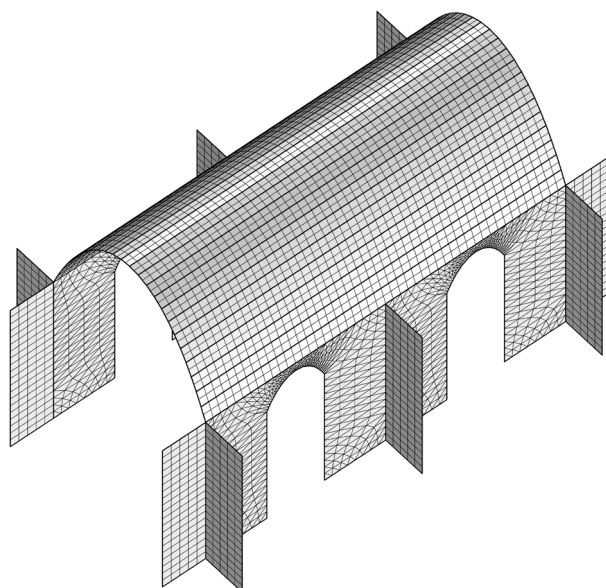
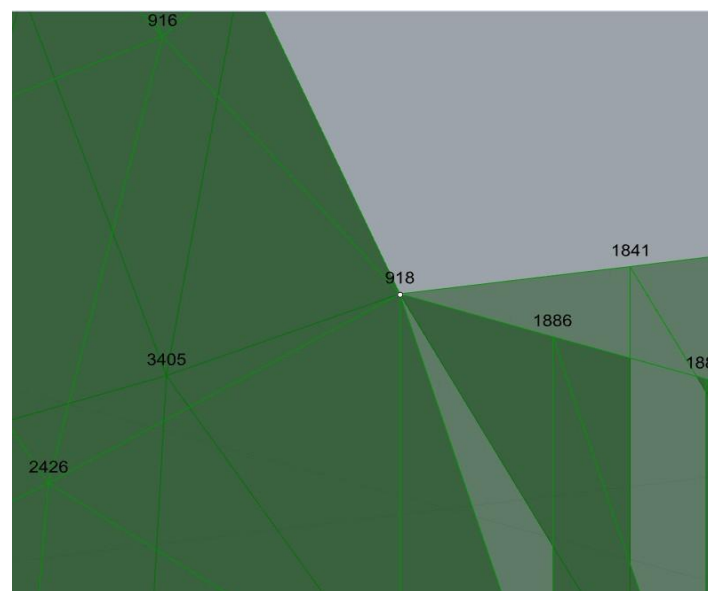


Figure 4.4: Riwaq unit mesh refinement



*Figure 4.5: Single
node between different elements*

4.2.2 Form-finding

This method has been implemented in computational tools such as Grasshopper and Kangaroo to provide a physical engine simulation and form finding process to architects and engineers. Concerning the procedure, the system is composed of particles and springs. The first ones are point mass that behave according to Newton's second law, while the latter are considered weightless and linear elastic with unchanged stiffness. Therefore, the springs are connected only to the particles to create a two or three-dimensional system. Initially, the network is in a static position. However, when the particle accelerates, the spring stretches out creating a force and the movement will continue until an equilibrium state is reached. During the form finding process, vertical upwards forces are applied to the particles to reproduce the loads that bears on the shell structure. Hence, the simulation will show an inflated surface in which the springs are in tension. However, in reality the tension of the elements resembles the compression which the shell structure is subjected.

The form finding process was carried out for the openings and the coverings. Both elements have undergone two formfinding processes. An initial transformation was dictated by the desire to have a structure capable of supporting a uniformly distributed load such as its own weight and sand load, sufficient in the case of the one dome unit, not having an upper floor. Subsequently a second process of finishing the form was carried out for the riwaq and the 4 domes so as to counteract the stress caused by the possibility of having an accessible or buildable plan above them.

The mesh refinement is particularly important in this phase as it will have to adapt to a new geometry without compromising the position of the vertices at the edges. In the following figures [Fig. 4.6-4.7] the result of the dynamic relaxation of the openings arches is shown.

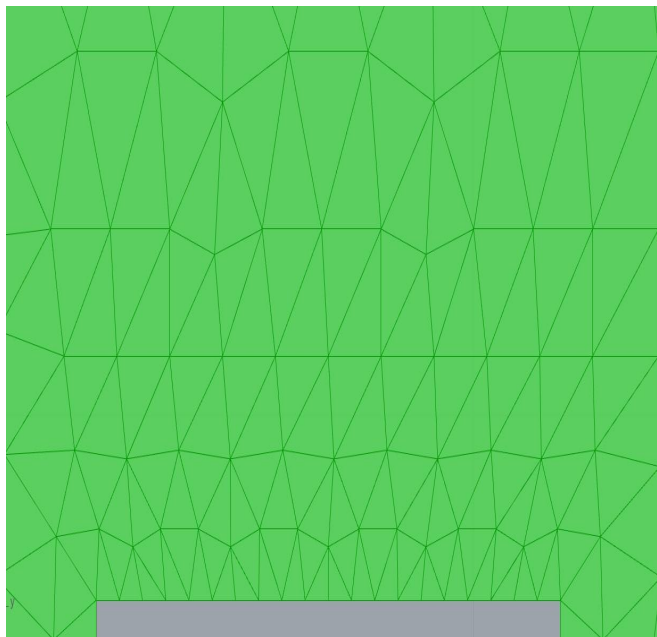


Figure 4.6: Unrelaxed geometry

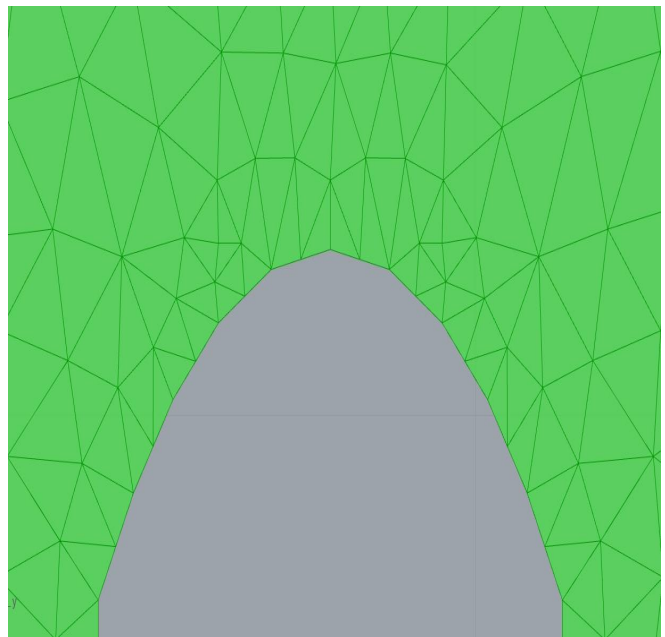


Figure 4.7: Relaxed geometry

4.2.3 Karamba settings

Once the geometric model was completed, the structural analysis was carried out, but not before having carefully set the required settings in karamba, the software chosen to run the FEA. The properties of the material have been set paying attention to the units of measurement required as input in Karamba. the Young's Modulus is for example required in KN /cm² while the density of the material is in KN/m³. Both values are selected from the literature consulted for the brick report (Appendix B) and are respectively of 60 MPa for the Young's Modulus and 1900Kg /m³ for the density, which are then transformed to the right units. This solution is related to the drying period of the tested bricks, which was of 7 days compared to the 28 days suggested by the literature. As explained further in Appendix B, this short period for completing the drying can affect drastically the Young's modulus value and the density (indeed, moisture can still be present and therefore result in a heavier brick). Therefore, it was preferable to utilize the literature values for these properties.

The geometries to be analyzed are identified by Karamba as "elements". In the case analyzed, the elements have been classified as shell elements and each one of them has been assigned its own cross section, having different collaborating elements but with different thicknesses (buttresses, walls, ceilings, arched walls, and eventual arches below domes). The thicknesses of the different cross sections have been set through number sliders, a necessary requirement for the assignment of the same as genomes in the next phase that will see the evolutionary solver analyzing the different possible combinations. The support conditions were then assigned to the vertices of the model having an elevation equal to zero (ie in contact with the ground) blocking both translations and rotations in all directions, simulating a clamped support.

Lastly the various loads acting on the structures have been set (in detail in chapter 4.2.4). Once the inputs required by the system have been set, it has been decided to multiply the outputs by a factor of 10, this due to the fact that by default the displacement is expressed in cm and the stresses in KN/cm² and to avoid errors it was decided to report them respectively in mm and in KN/mm² or MPa. In the following Figure 8 is shown the connection between the components in Karamba.



Figure 4.5. Example of model settings

4.2.4 Loadcases

Before introducing the methodology behind the assignment of the loads acting on the structure, it is worth recalling that the structural analysis were carried out almost in parallel in the three models. The minimum thickness of the walls, for example, was given by the 4 dome unit as it is the most subject to tensile stress and then applied to all the modules to make their construction more clear and effective. However to obtain results from the analysis of the 4 dome it was necessary to have the support reactions of the large dome unit which would then have constituted the agent load of the second floor. The first step was then to assign a satisfactory thickness to the walls of the large dome, used the relative constraint reactions as a load in the 4 dome and assessed whether or not to increase the thickness and repeat the process.

All the loads assigned to the structures fall into one of the following two categories defined within the Karamba software: mesh load or point load.

The first was used for distributed loads acting on the totality of a mesh with a perpendicular direction to the global horizontal reference plane. The loads applied through this system were the live loads. The component called point load was used for the gravity and all those non-uniform loads such as the weight of the earth filling above some modules and its retaining wall, as well as to apply the support reactions of the second floor built on the 4 dome unit as load on the latter.

A description of the methodology behind the definition of the loads follows. Gravitational load: it is automatically calculated by the software with a special component that multiplies the acceleration of gravity specified for the mass which, in turn, is calculated from the density value of the material. Assigned to all units.

Live loads: they have been applied as uniformly distributed loads on the affected units with a value of 1.5 KN for the sand load (applied on large dome unit) and a value of 4KN for occupancy load in the case of practicable covers (riwaw unit), 6KN in the case in which the addition of mobile objects was foreseen such as furnishings (four dome unit) Earth filling load: as this is a non-uniformly distributed load, it was applied as a point load on the vertices of the affected meshes. the value to be applied to the vertices has been approximated by calculating the area of the mesh faces close together and multiplying it by the distance from the plane passing through the highest point of the dome or vault. Obtained the volume of earth above a given vertex then proceeded by multiplying it by the density of the material, obtaining a point load in KN variable according to the amount of the earth [Fig. 4.10]. Load applied to four dome and riwaq units.

Retaining walls: similar to the earth filling, variable point loads were defined multiplying the length of the edges of the mesh by the wall's thickness by the distance from the plane passing through the highest point of the dome or vault. the volume obtained was then multiplied by the density of the material, obtaining point loads in KN. Load applied to four domes and riwaq units.

First floor load: After calculating the support reactions of the large dome unit [Fig. 4.11], these have been applied with an opposite direction on the top of the containment wall on which the first floor rests. The support reactions of the retaining wall were then assigned again, in the reverse direction, to the edge of the 4 dome module [Fig. 4.12].

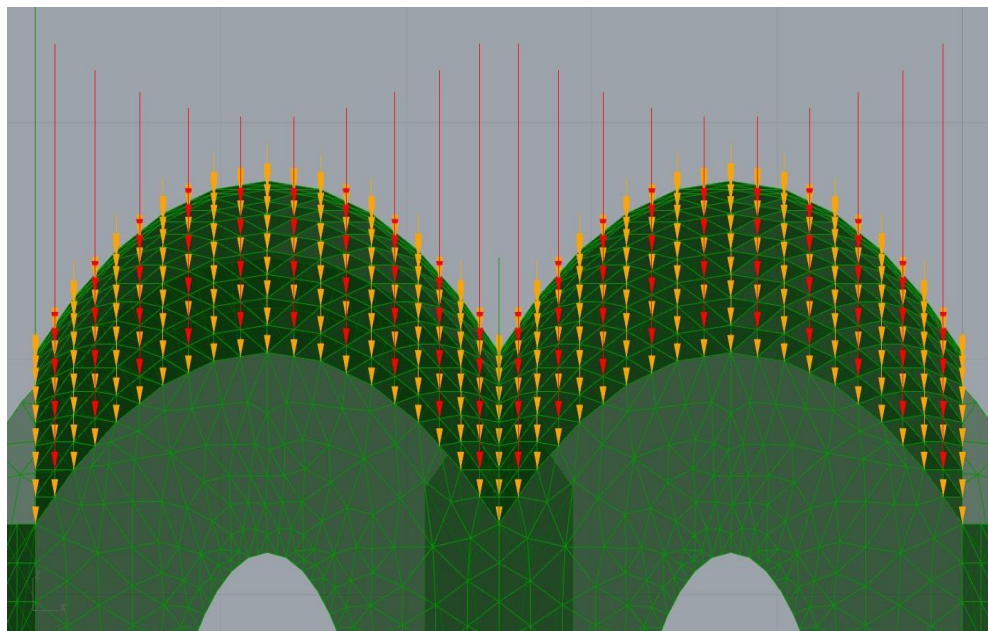


Figure 4.9: Distribution of earth filling load (red) and sand load (yellow)

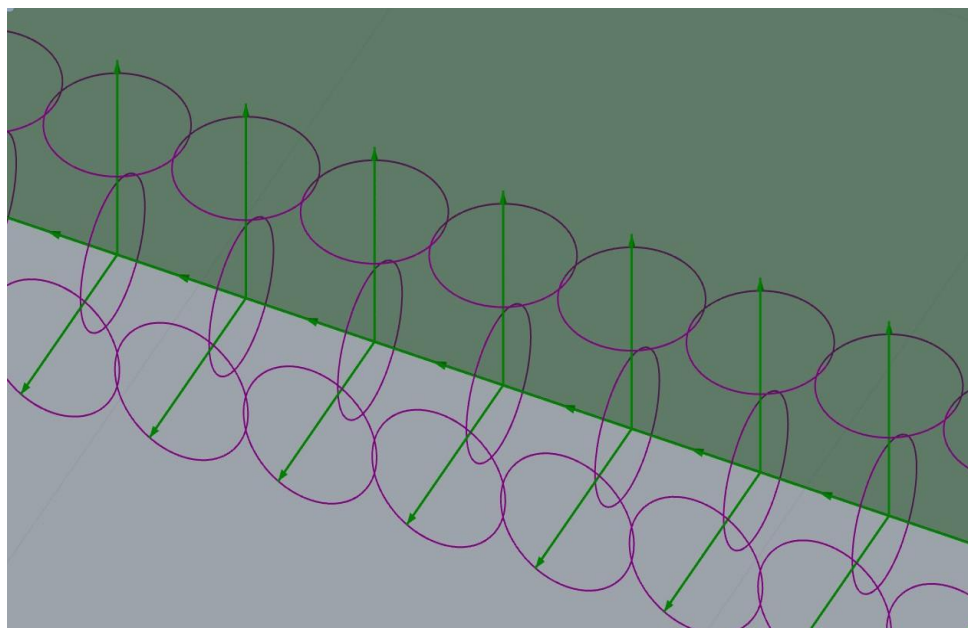


Figure 4.10: Reaction forces of the first floor (green) and reaction moments (purple)

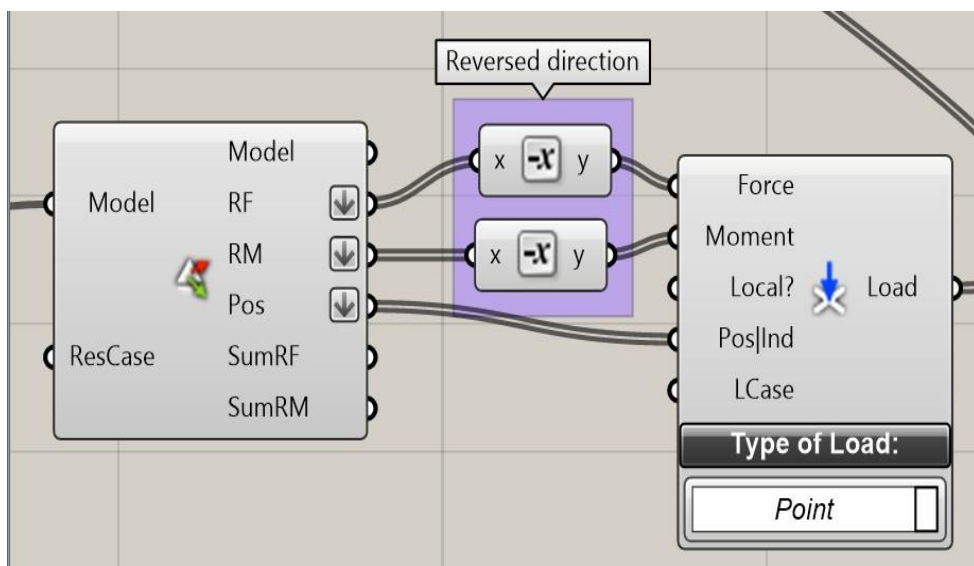


Figure 4.11: The reaction forces and moments are applied as load.

4.2.5 Evolutionary solver

To obtain the best combination of geometry dimensions in order to minimize the stresses and displacement in the structure, an evolutionary solver has been used. The chosen one, for its simplicity in use, was Galapagos, a plug-in for Grasshopper. Galapagos uses the logic behind evolutionary computation in order to optimize a given parameter. In evolutionary computation, a set of candidate solutions called Genomes is iteratively updated. Each iteration produces a new generation obtained by removing less desired solutions, and introducing small random changes (mutations). As a result, the population will gradually evolve to increase in fitness, in this case the chosen fitness function of the algorithm was to minimize the value of displacement and tensile stress.

Obviously if Galapagos was free to optimize geometry and thicknesses at the same time, the result would be a massive structure with a form finding of the ceilings not limited in height. To overcome this problem, a maximum height has been set for some geometries and the thickness combinations have been manually selected to find a compromise between admissible tensile stress and displacement with a limited use of material. The following Figure 4.12 shows the combination of optimal thicknesses according to Galapagos to minimize the displacement. The result follows the initial intuition that the structure can resist better if it is massive and therefore the values found are almost at the maximum limit set. Naturally, by decreasing the thicknesses there will be a greater displacement, the solution chosen manually will therefore have the objective of being in any case below the permitted limit.

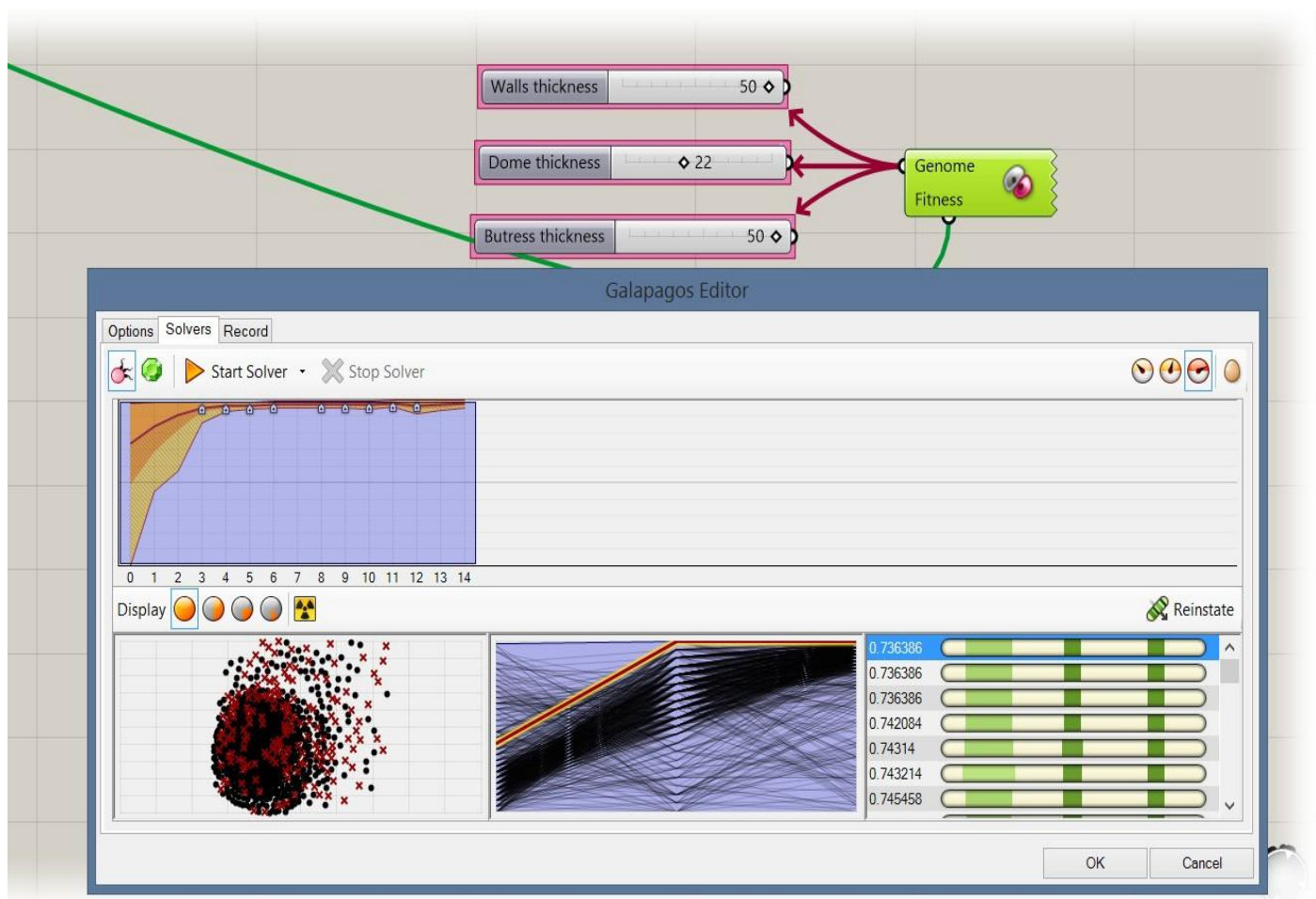


Figure 4.12: Results of the evolutionary solver in Galapagos after 14 generations.

4.3 Evaluation and discussion of results

Before analyzing the results obtained, it is good to remember what were the limits of the material taken into consideration. The maximum allowable displacement was decided analyzing the results obtained from the brick testing, and it was decided not to have a value greater than 15% of the thickness of the element taken into consideration as if this limit was exceeded, the material sees its mechanical properties reduced.

In the cases analyzed, the major displacement has always been identified in the ceilings, which following the structural analysis and the chosen construction method, have been defined according to a thickness of 200mm. consequently the maximum acceptable displacement is 30mm. The compressive strength taken into consideration was

1.5 MPa while the tensile strength was calculated as one tenth of the latter, ie 0.15 MPa. For more details on the calculations made to reach these values, see the brick report. The following chapters show the values of displacement and maximum values regarding for the first and second principal stress. The images shown refer to the inferior layer of the elements, the one most subject to tensile stresses.

4.3.1 Four dome unit

The four dome unit had to withstand the worst combination of loads and it gave us the minimum wall thickness to use on every module to make the construction easier and more clear. The walls thickness was set as 400mm, as well as the buttresses. The domes and the arched wall on which they rest have a thickness of 200mm, half the wall thickness to allow future extensions to share the wall (details in the construction method). The arches below the domes were dimensioned as well according to the load case with a cross section 150mm wide and 500mm high. Apart from the self weight we considered the earth filling on top of it, the containment wall and all the support reactions of the one dome build on top of it with a reverse module. This is the worst recorded case regarding the tensile stress with a maximum value of 0.1 MPa which is still below our limit of 0.15MPa. The displacement is acceptable being of 11.9 mm.

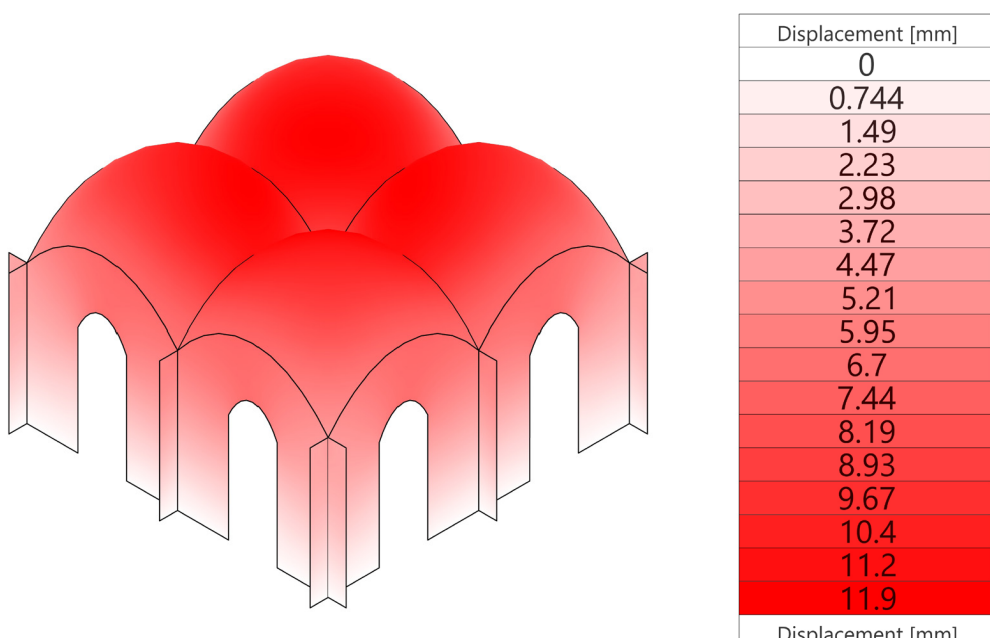


Figure 4.13: Displacement in the four dome unit

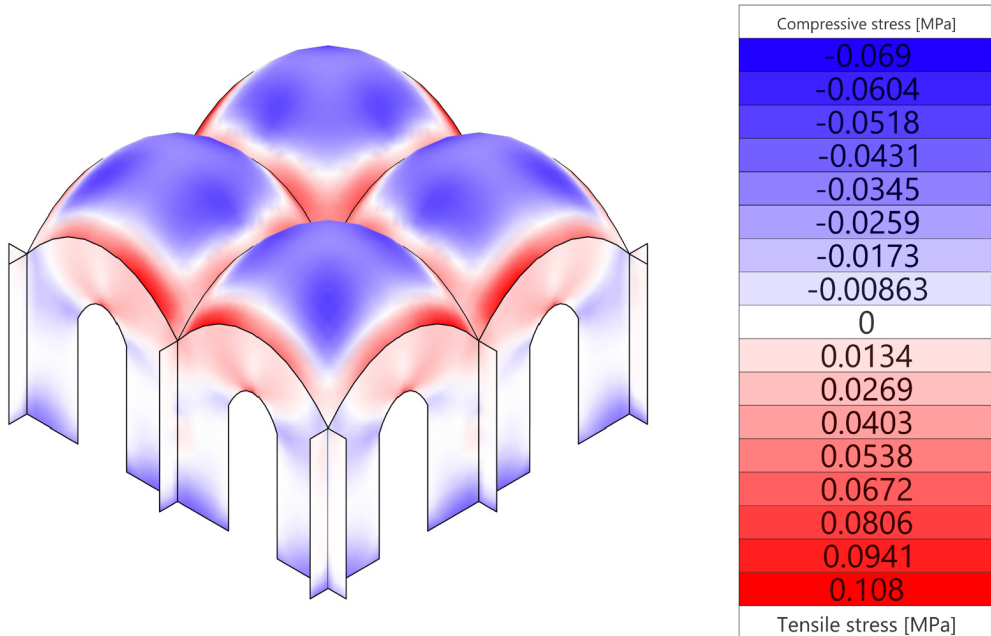


Figure 4.14: First principal stress in the four dome unit

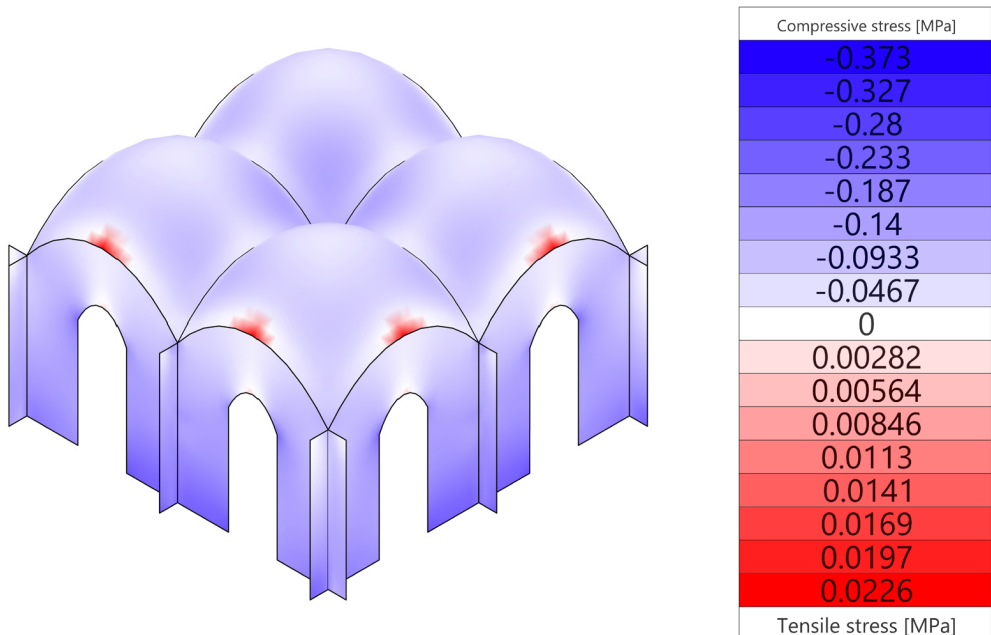


Figure 4.15: Second principal stress in four dome unit

4.3.2 Large dome unit

The large dome unit has the largest span but not having any limitation regarding the height due to the fact that the design rules do not allow a second floor on top of it, it has been managed to have an optimal form finding process that had to counteract just the self weight and the sand load. The thicknesses of the elements are the same as the four dome unit so 400mm for the walls and buttresses and 200mm for the dome and the arched wall on which it rests. The maximum tensile stress found is 0.6 MPa and a displacement of 7mm.

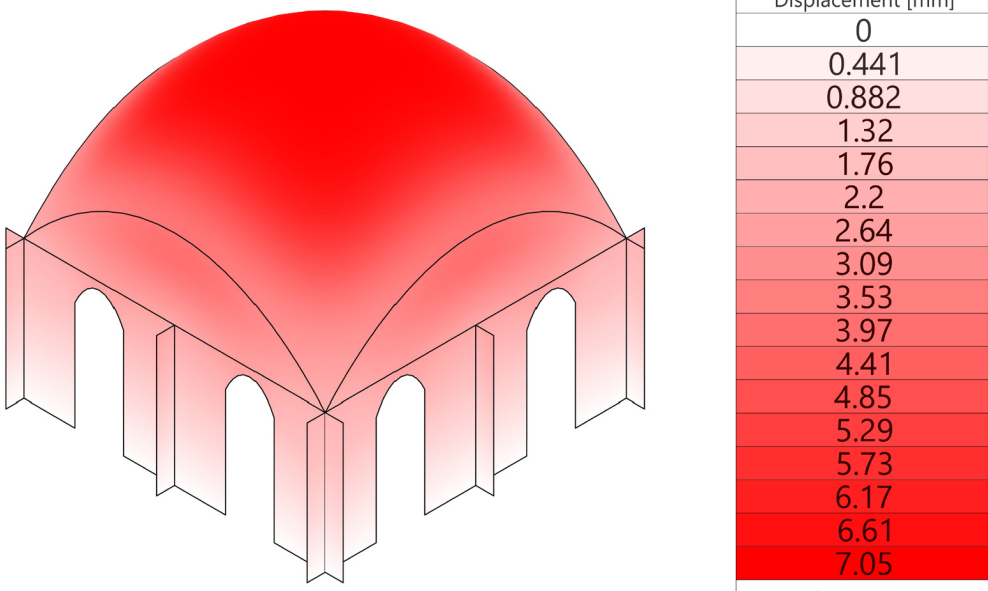


Figure 4.16: Displacement in the large dome unit

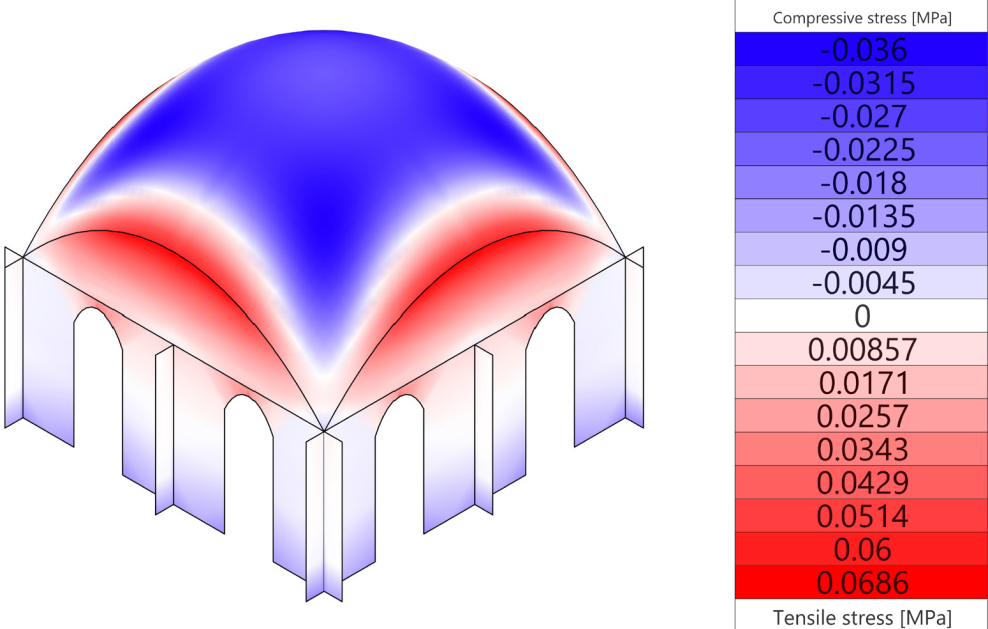


Figure 4.17: First principal stress in the large dome unit

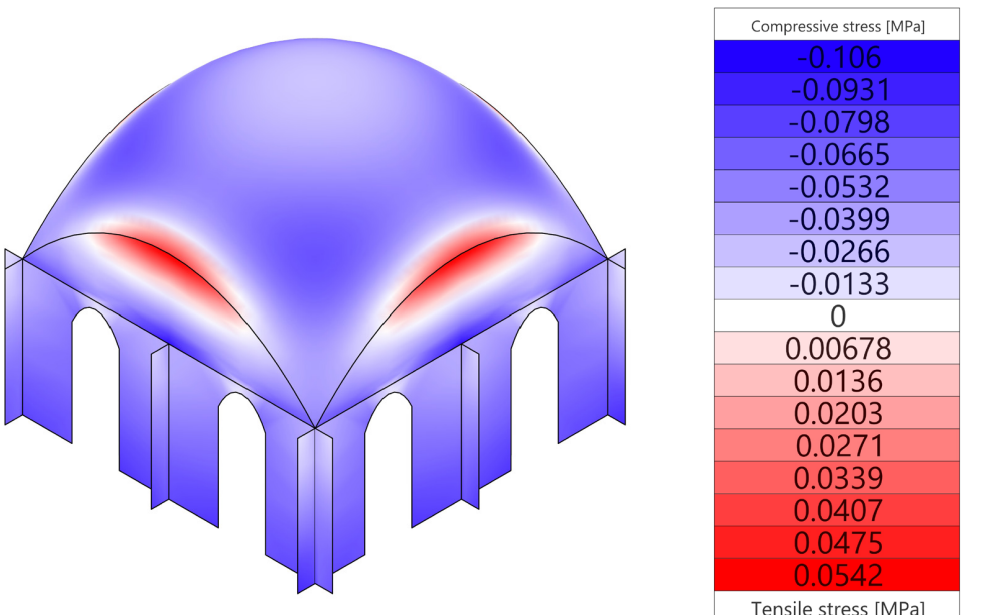


Figure 4.18: Second principal stress in large dome unit

4.3.3 Riwaq unit

The riwaq unit present a vault which was form-founded but due to the necessity of having it of the same height of the four domes unit because of the second floor allowed on top of it, the shape is not the optimal one, although thanks to the fact that the riwaq is always facing the courtyard we could design longer buttresses of 700mm. The dimension of the buttresses helped in part to keep the stresses and displacement below the set limit. The presence of a second floor and the non optimal form-finding process have led to results similar to the ones found in the large dome unit although the span here is inferior. The tensile stress and displacement are still acceptable with values of 0.7 and 11mm respectively.

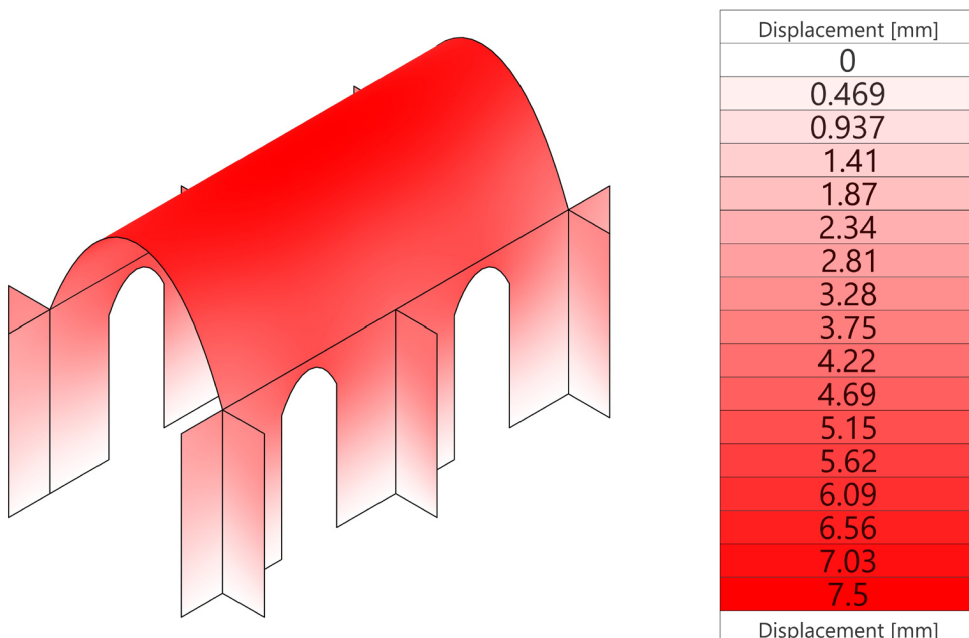


Figure 4.19: Displacement in the Riwaq unit

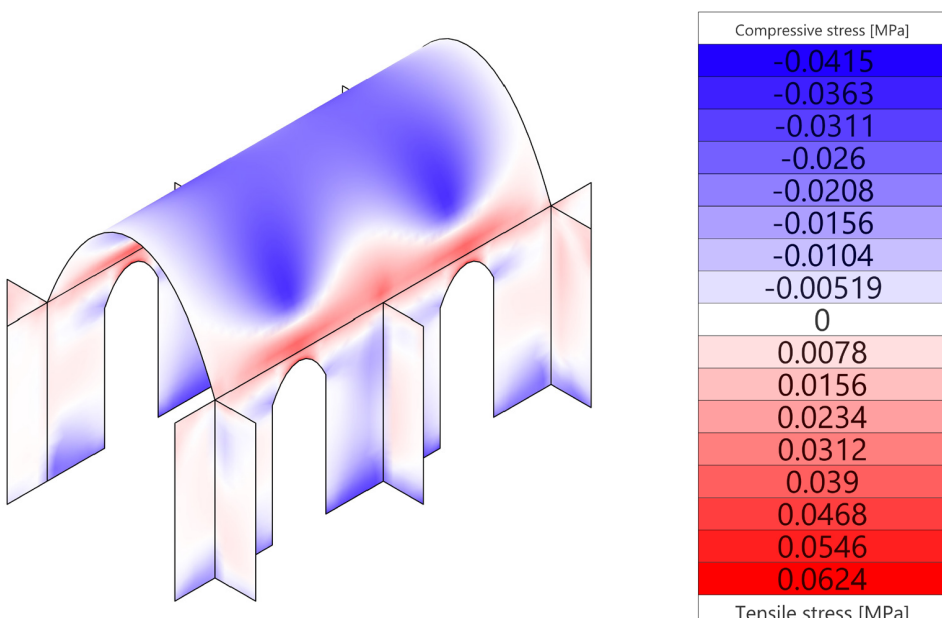


Figure 4.20: First principal stress in the Riwaq unit

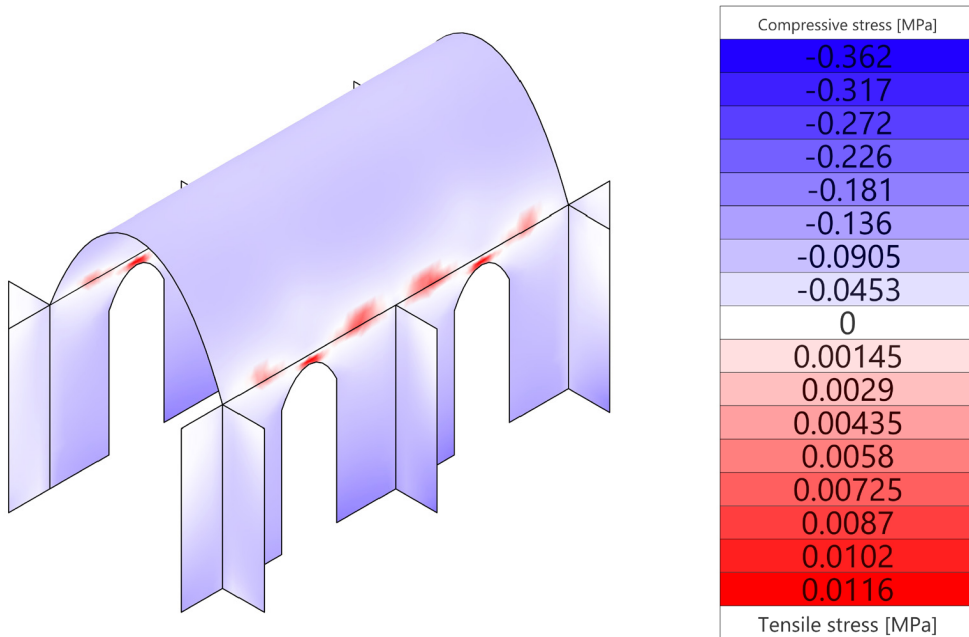


Figure 4.21: Second principal stress in the riwaq unit

4.4 Conclusion and limitations

The results obtained from the structural analysis show how the designed units can withstand the loads to which they would be subjected. This has been possible in large part thanks to the simplicity of the structures designed in the perspective of a constructive method accessible to non-skilled workers and in a context such as that of the refugee camp of Zaatri.

There are however some limitations that should be taken into consideration. The geometric models have been taken into consideration as a single structure composed of several elements identified as shells. No matter how this seems to be the most appropriate solution with regard to the ultimate behavior of the structure, there was no time to verify whether analyzing the elements individually and then applying the various reaction forces and prescribed displacement to the underlying elements there is a discrepancy or not in the results.

Regarding the analyzed geometry, Karamba does not allow to assign a direction to the thickness assigned to the elements. This was a problem in this case as the ceilings rest on half of the wall below and not in its interaxis as analyzed by the software. A solution to this problem can be to create a two-dimensional model by transforming the applied loads into linearly distributed loads.

Another limitation in the structural analysis was given by the impossibility of applying the forces exerted on a given module by the neighboring modules. The problem encountered is that having the mesh refined differently in the modules, the vertices of one unit would not match those of another, and in that case the forces are approximated and brought to the nearest vertices by the calculation software. The results obtained through this system show a decrease in stress within the structure analyzed but were deemed unreliable and therefore were not taken into consideration.

In conclusion, the result of the analysis carried out, considering some unavoidable approximations, was considered satisfactory. The design can however improve with less use of the material in some cases if taken the limitations described here are taken into consideration and overcome.

5 Bibliography

CORPUS Levant. 2004. Traditional Syrian Architecture. CORPUS Levant, France.

Hussam Dugum. “*Structural Assessment of the Guastavino Masonry Dome of the Cathedral of Saint John the Divine*” Massachusetts Institute of Technology. June 2013

Guides.codepath.com. (2019). *Topological Sort / CodePath Android Cliffnotes*. [online] Available at: <https://guides.codepath.com/compsci/Topological-Sort> [Accessed 4 Nov. 2019].

Philippe Block, Matthew DeJong, Lara Davis, John Ochsendorf. “*Tile vaulted systems for low-cost construction in Africa*” ATDF JOURNAL Volume 7, Issue 1/2 2010

Rossi, A. (2019). *Wasp*. [online] Food4Rhino. Available at: <https://www.food4rhino.com/app/wasp> [Accessed Nov. 2019].

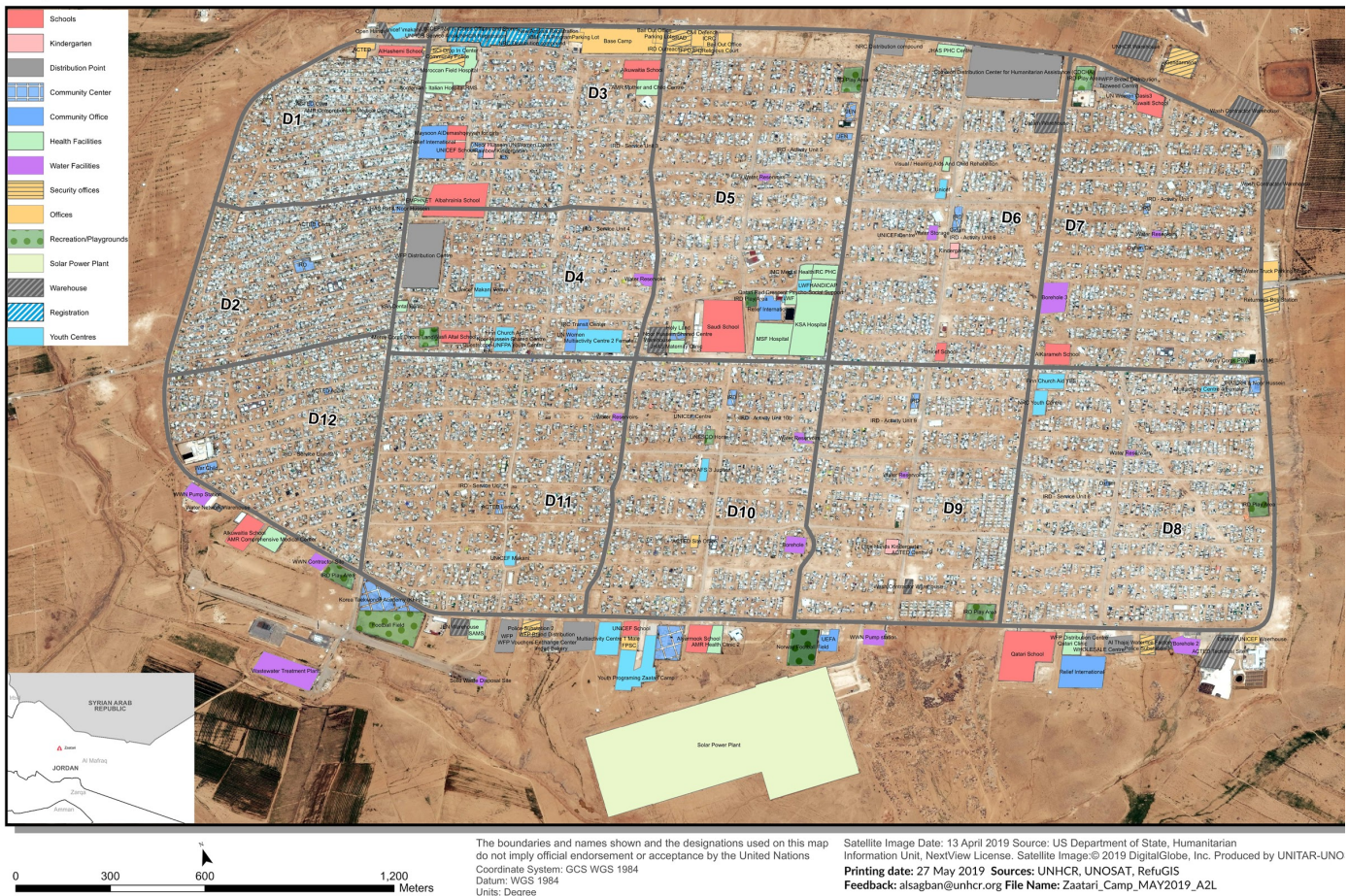
Timár, E. 2016. Developing Zaatari: Urban Planning in a Syrian refugee camp, Jordan. City of Amsterdam and VNG International

Making of the “Beyond Bending” ceramic tile and earthen vaults. Block Research Group. 2016. <https://vimeo.com/193874177> [Accessed Nov. 2019]

Appendix A

Zaatari Refugee Camp - Infrastructure and Facilities

May 2019





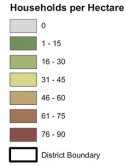
JORDAN - Al Za'tari Refugee Camp Household Density - January 2015

For Humanitarian Purposes Only
Production Date: 28 January 2015

For more information scan to visit the Open Street Map Portal



Household Density
Households per Hectare



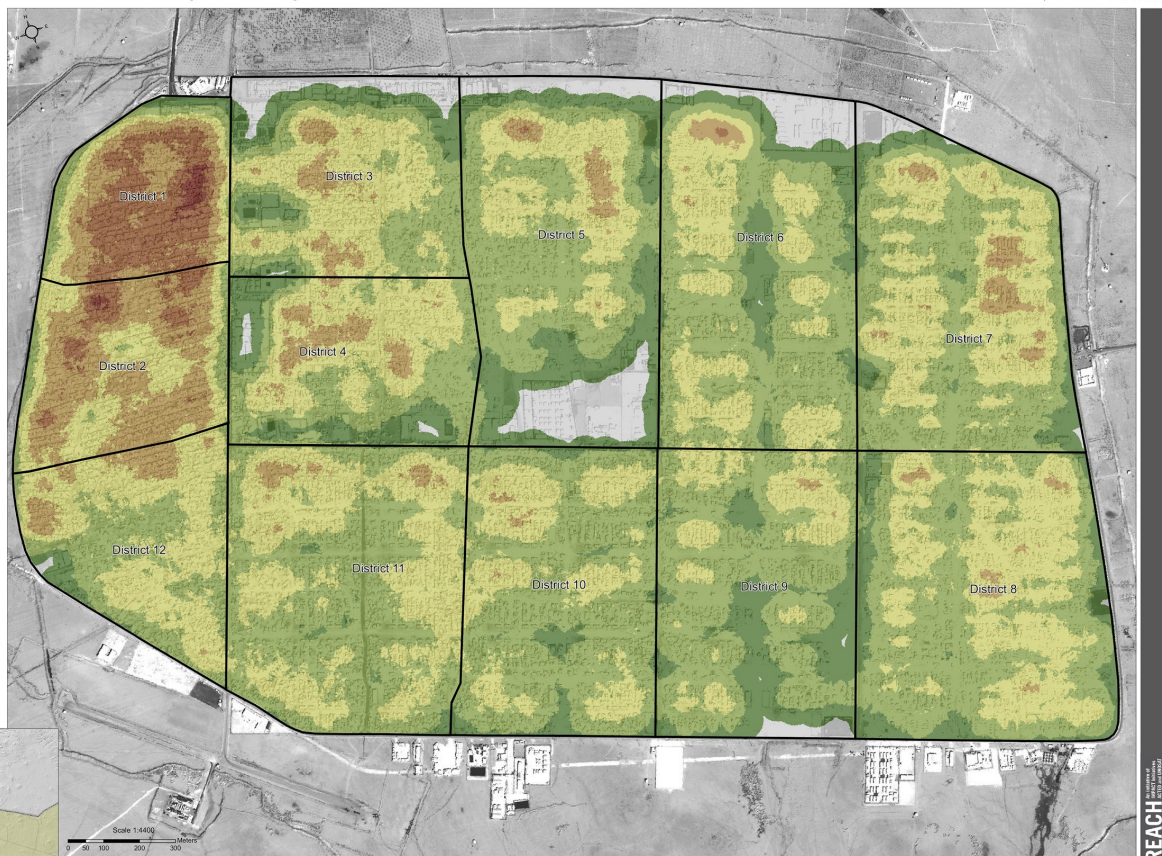
District	Number of Households
1	1190
2	1230
3	897
4	843
5	1034
6	1269
7	1373
8	1550
9	907
10	1126
11	1520
12	963
Total	13927

Data Source:
Population data - REACH
Dec 2014-Jan 2015
Camp Boundaries - UNHCR

Satellite Acquisition Date:
11/11/2015
Provider by UNOSAT

Projection: WGS 1984 UTM Zone 37N
File: REACH_JOR_Map_Zaatri_M0V_HouseholdDensity_28Jan2015_A1
Contact: reach.mena@impact-initiatives.org

Note: Data, designations and boundaries contained on this map are not warranted to be error-free and do not imply acceptance by the REACH partners, associates or donors mentioned on this map.



REACH
Impact Initiatives



JORDAN - Al Za'tari Refugee Camp Shelter Type of Households - January 2015

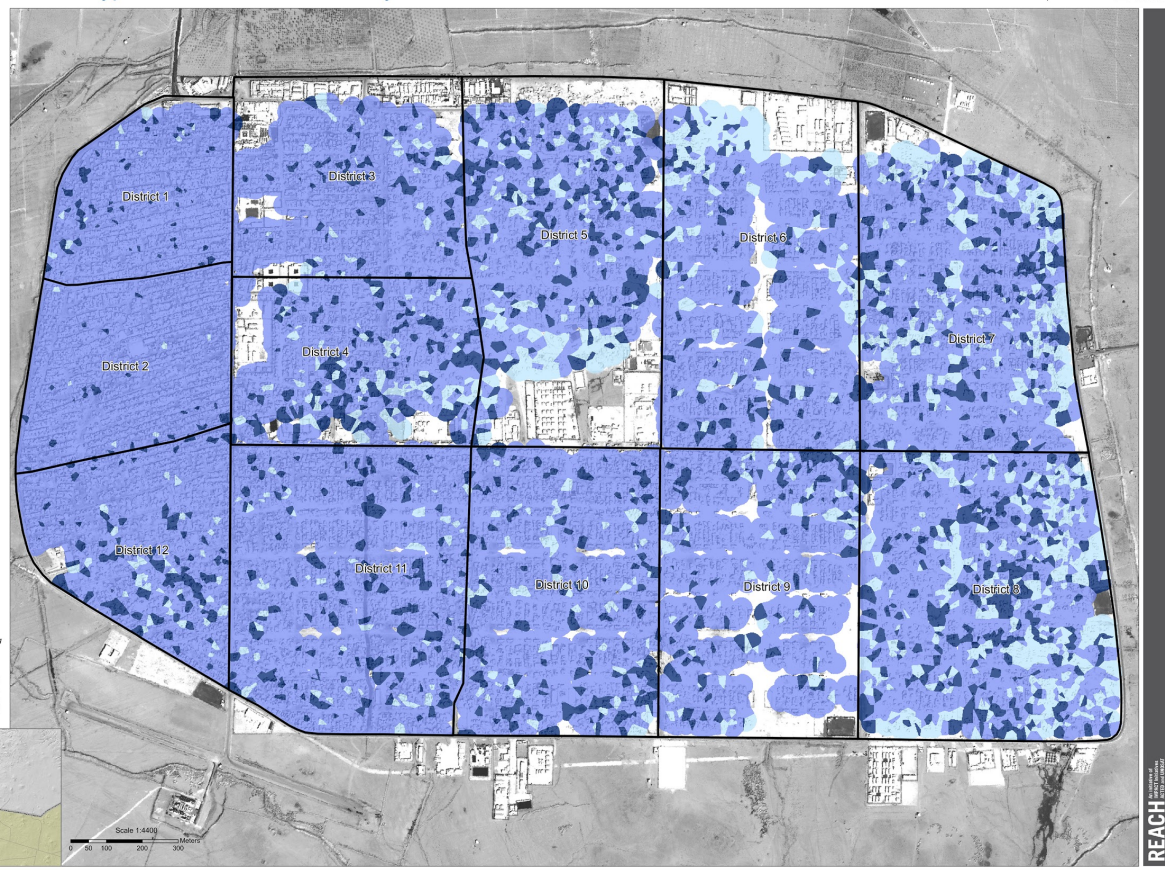
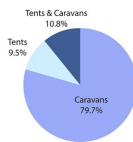
For Humanitarian Purposes Only
Production Date: 2 February 2015

For more information scan
to visit the Open
Street Map
Portal



Household Shelter Type

- Caravans
- Tents
- Tents and Caravans
- District Boundary



Data visualization: Thiessen polygons
Creates polygons out of point locations to better represent the area that a point contains one point that is closer in location to any other point feature.

Data Source:
Population Data - REACH
Dec 2014-Jan 2015
Camp Boundaries - UNHCR
Satellite Acquisition Date:
11/11/2014
Provider: UNOSAT
Projection: WGS 1984 UTM Zone 37N

File: REACH_JOR_Map_Za'atari_CCM_ShelterType_2Feb2015_A1
Contact: reach.mena@impact-initiatives.org

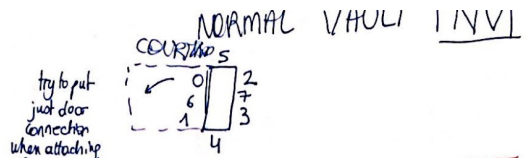
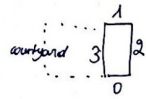
Note: Data, designation, and boundaries contained on this map are not intended to be error-free and do not imply acceptance by the REACH partners, associates or donors mentioned on this map.



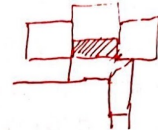
REACH
Impact Initiatives

Appendix A Computational PaperWork

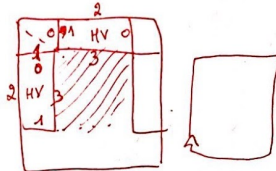
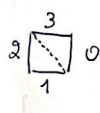
HALF VAULT MODULE HV1



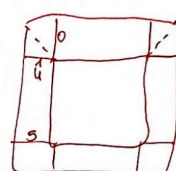
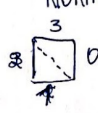
+ CREATE ANOTHER NORMAL VAULT
not for circulation
but internal connection.
(w/o colliders)



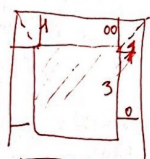
HALF VAULT CORNER RIGHT HCR



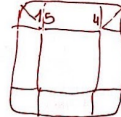
NORMAL VAULT RIGHT CORNER NCR



HALF VAULT CORNER LEFT HCL

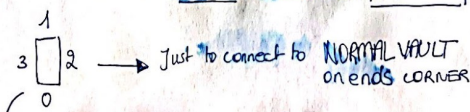


NORMAL VAULT LEFT CORNER NCU



NORMAL VAULT CONNECTION NVI

HALF VAULT MODULE WITHOUT COLLIDER HVN



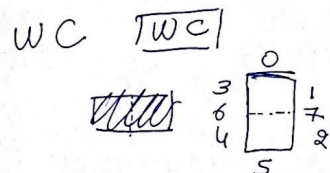
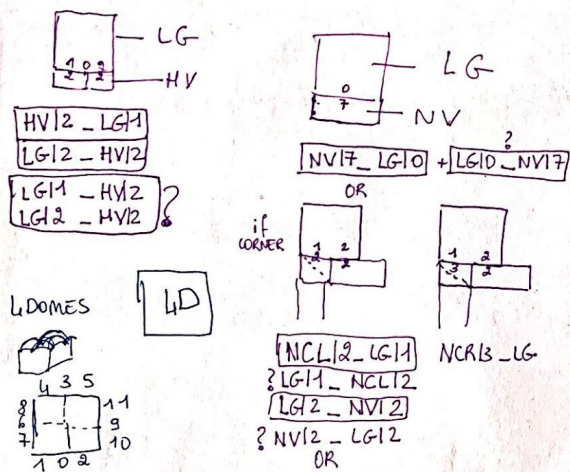
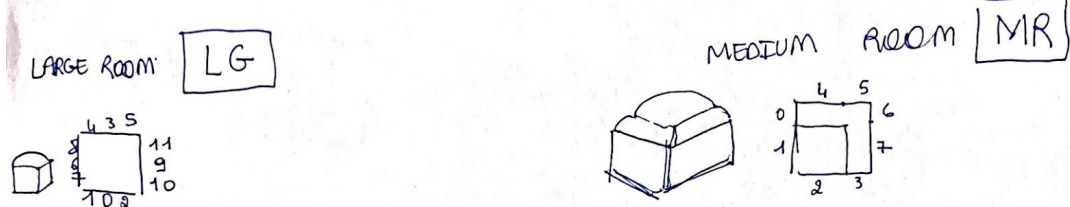
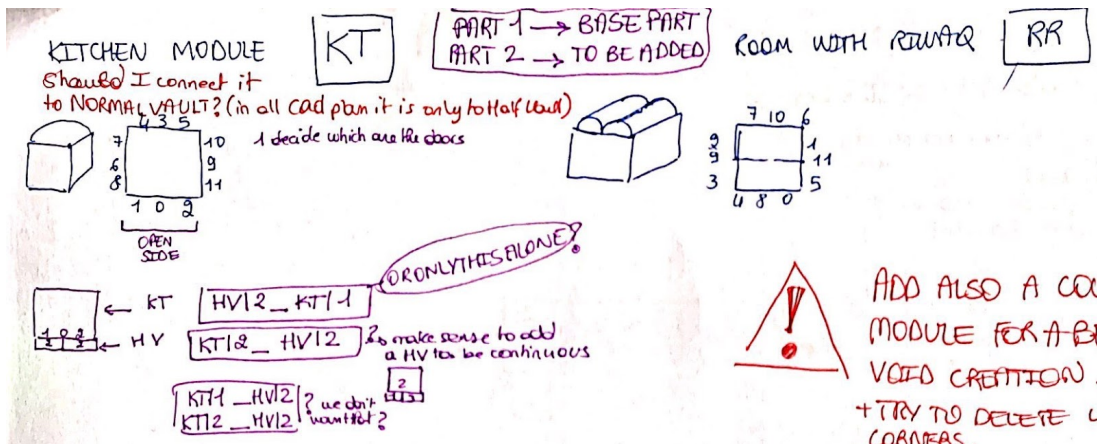
HVN - 3 / NV - 5 + HVN - 1

Scanned with
CamScanner

▲ The way I would connect CORNERS] may be BETTER.
is in one direction

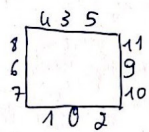
▲ the way Shenin connected them

Allows for more variation.



↑ I am just connecting open spaces and not CLOSED PART
↳ AT THE END CONNECT CLOSED FOR SOME PART ONLY TO GET A CLUSTER NON STOP GROWING.

LARGE ROOM [LG] WITH [HV] OR [NV]



LARGE ROOM

↳ should I connect closed part too? No because it won't make sense! close to close will start evolving which is not what we want

CASE 1

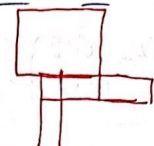


HV1 - LG1
HV2 - LG2

LG1 - HV1
LG2 - HV2

?

Yes?
No?



→ issue

CASE 2



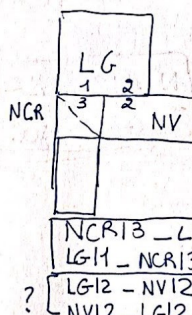
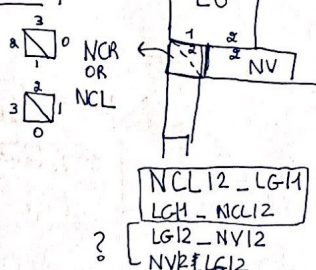
NV17 - LG10

LG10 - NV17

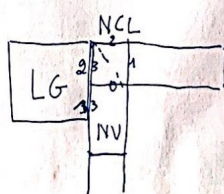
?

Yes?
No?

CASE 3

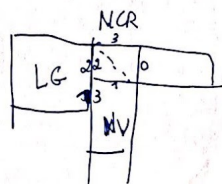


CASE 4



?

LG11 - NV13
NV13 - LG14



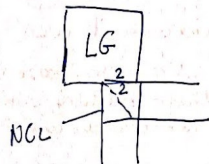
?

LG11 - NV13
NV13 - LG11

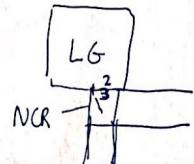


Scanned with
CamScanner

CASE 5

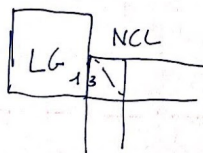


~~NCL12 - LG12
LG12 - NCL12~~



~~NCR13 - LG12
LG2 - NCR13~~

CASE 6



~~NCL13 - LG11
LG11 - NCL13~~



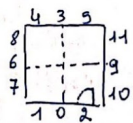
~~NCR12 - LG11
LG11 - NCR12~~

because

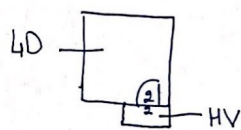


Scanned with
CamScanner

4 DOMES

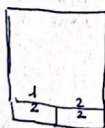


CASE 1



$HV12 - 4D12$
 $4D12 - HV12$?

IF

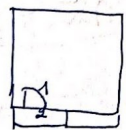


ADD

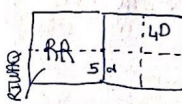
$4D11 - HV12$
 $HV12 - 4D11$

NEED
FOR
MIRRORED
ROOM

TRY IT



CASE 2



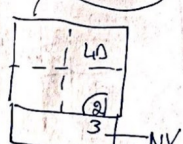
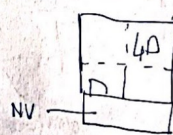
$4D12 - RR15$
 $RR15 - 4D12$

IN OUR PLAN



check this corner
if need to add
CLOSED MXT
BUT PROBABLY NOT.

CASE 3



SAME?

$NV13 - 4D12$
 $4D12 - NV13$

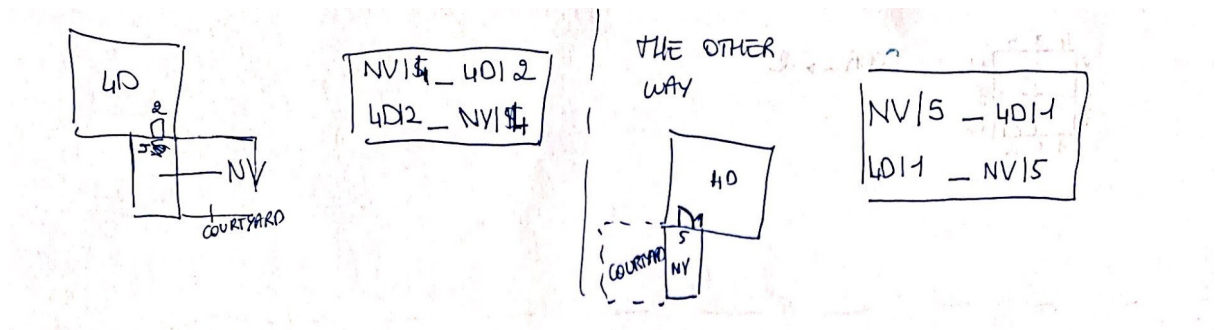
PUT JUST THIS

OK SO USE
WITH MIDPOINT TO MIRROR IT?

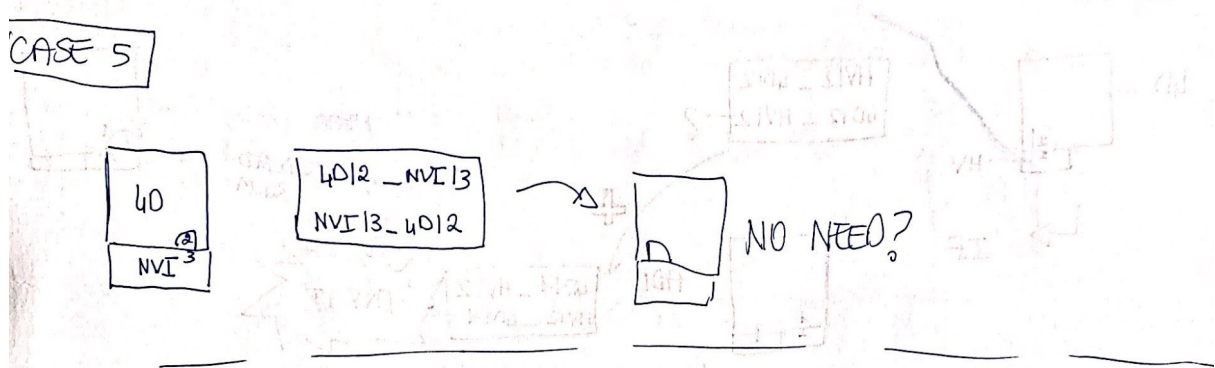
$NV17 - 4D10$
 $4D10 - NV17$



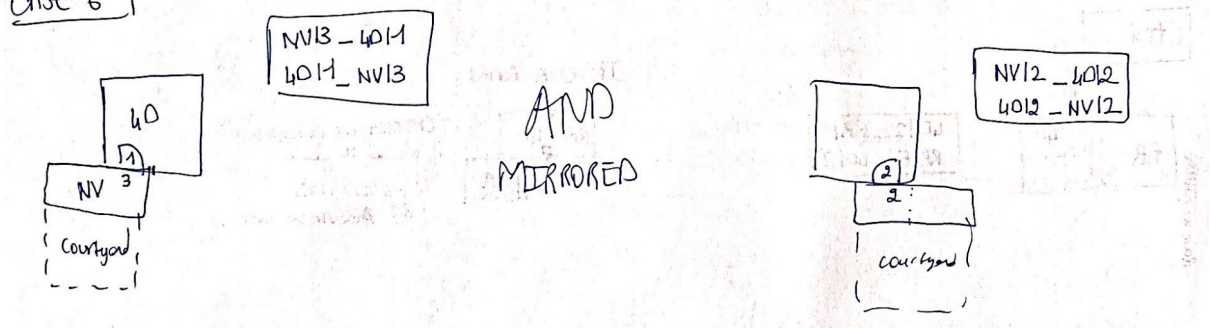
Scanned with
CamScanner



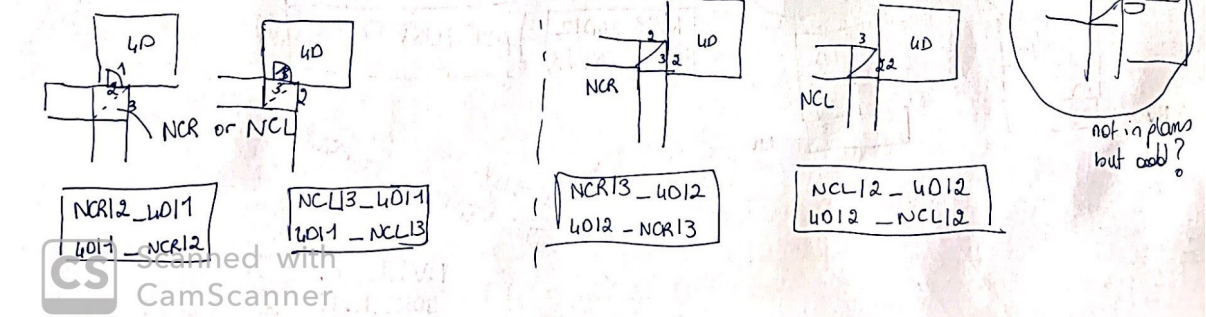
CASE 5



CASE 6

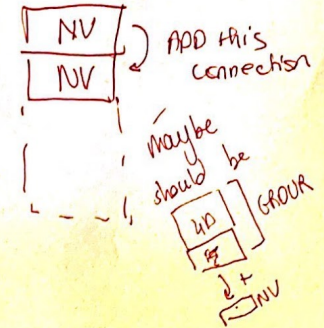
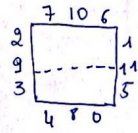


CASE 7

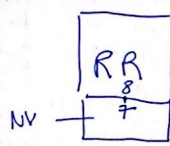


ROOM WITH RIWAQ

[RR]



CASE 1



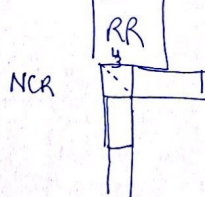
RR18 - NV17
NV17 - RR18

FOR LOP i did also
the side not mid point only? which better?

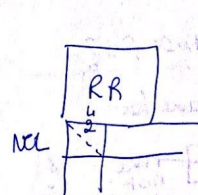
MID point?

mid point to mid point?

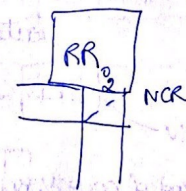
CASE 2



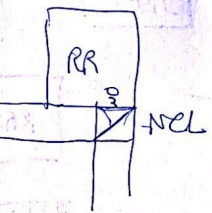
RR14 - NCR13
NCR13 - RR14



RR14 - NCL12
NCL12 - RR14



RR10 - NCR12
NCR12 - RR10

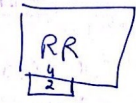


RR10 - NCL13
NCL13 - RR10

CASE 3



OR



RR14 - HV12
HV12 - RR14

CS

Scanned with
HV12-SR10

CASE 6

~~RR
WC10~~

~~RR13_WC10
WC10 - RR13~~

CASE 5

~~RR 17 MR~~

~~RR11 - MR17
MR17 - RR11~~

CASE

~~RR 40~~

ALREADY APPED w/ 40 paper.

CASE 6

~~RR 5b HV~~

~~RR15 - HV113
HV113 - RR15~~

create new module first?

→ use the same for

~~NV HV1
not HVnormal~~

MIRRORS

~~HV 33 RR~~

~~RR13 - HV113
HV113 - RR13~~

CASE 7

~~AR 54 NV~~

OR

~~NV513 RR~~

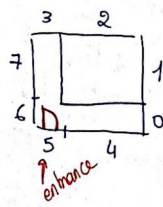
~~RR13 - NV5
NV5 - RR13~~



Scanned with
CamScanner

MEDIUM ROOM

| M R |



CASE 1



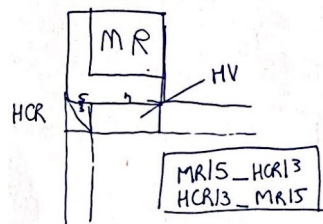
PISABLE
CONNECTION
IF TOO MANY

because DOOR IS ON

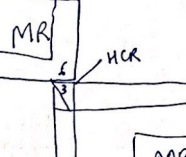
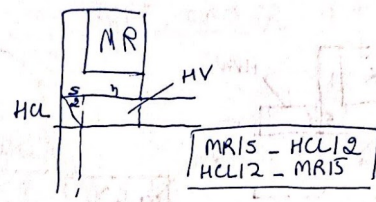
| # 5 |

↓
NOT

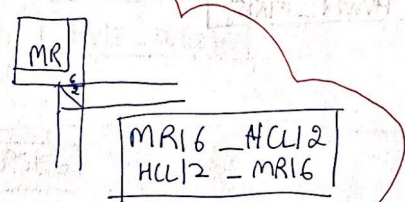
6



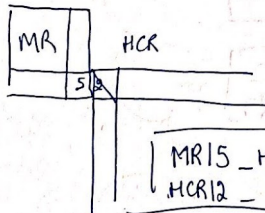
OR



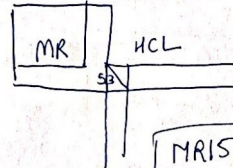
OR



CASE 3



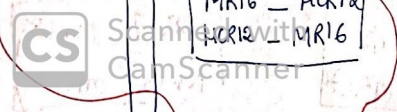
OR



CASE 4

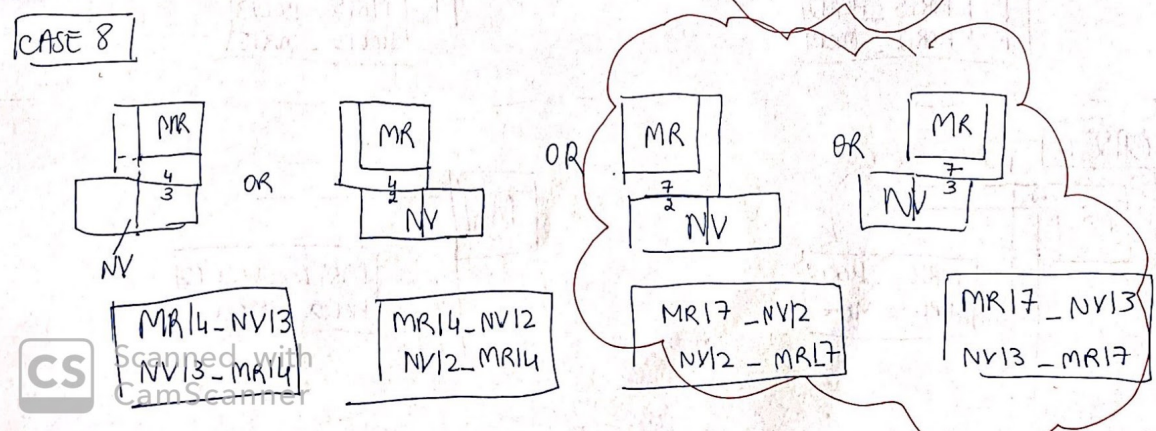
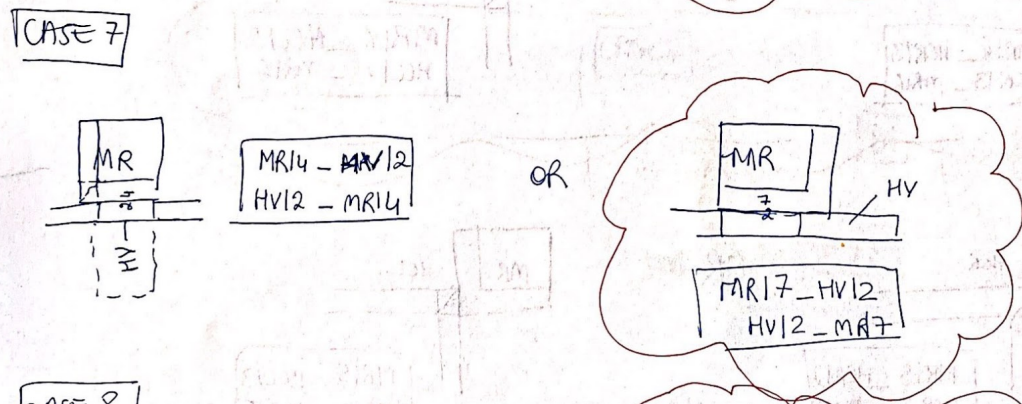
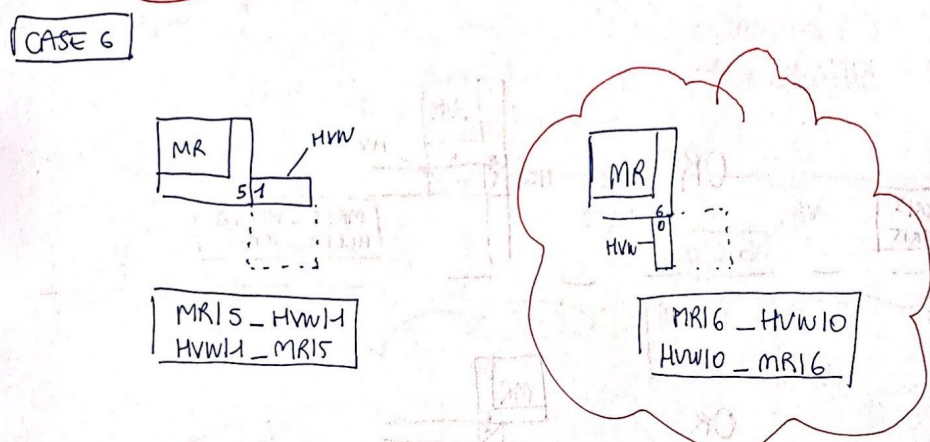
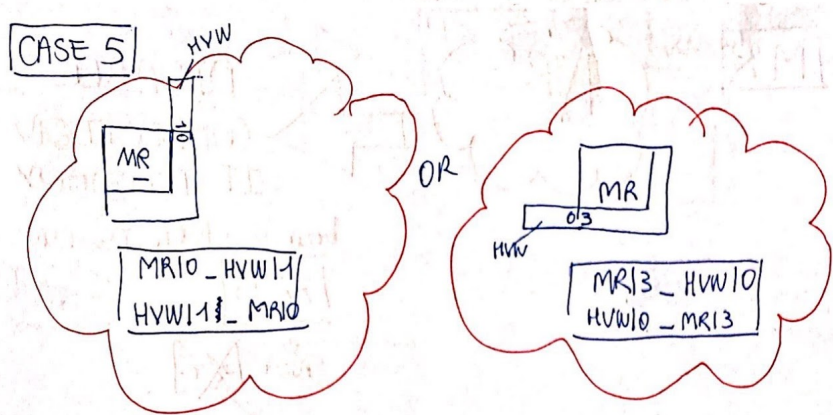
CS

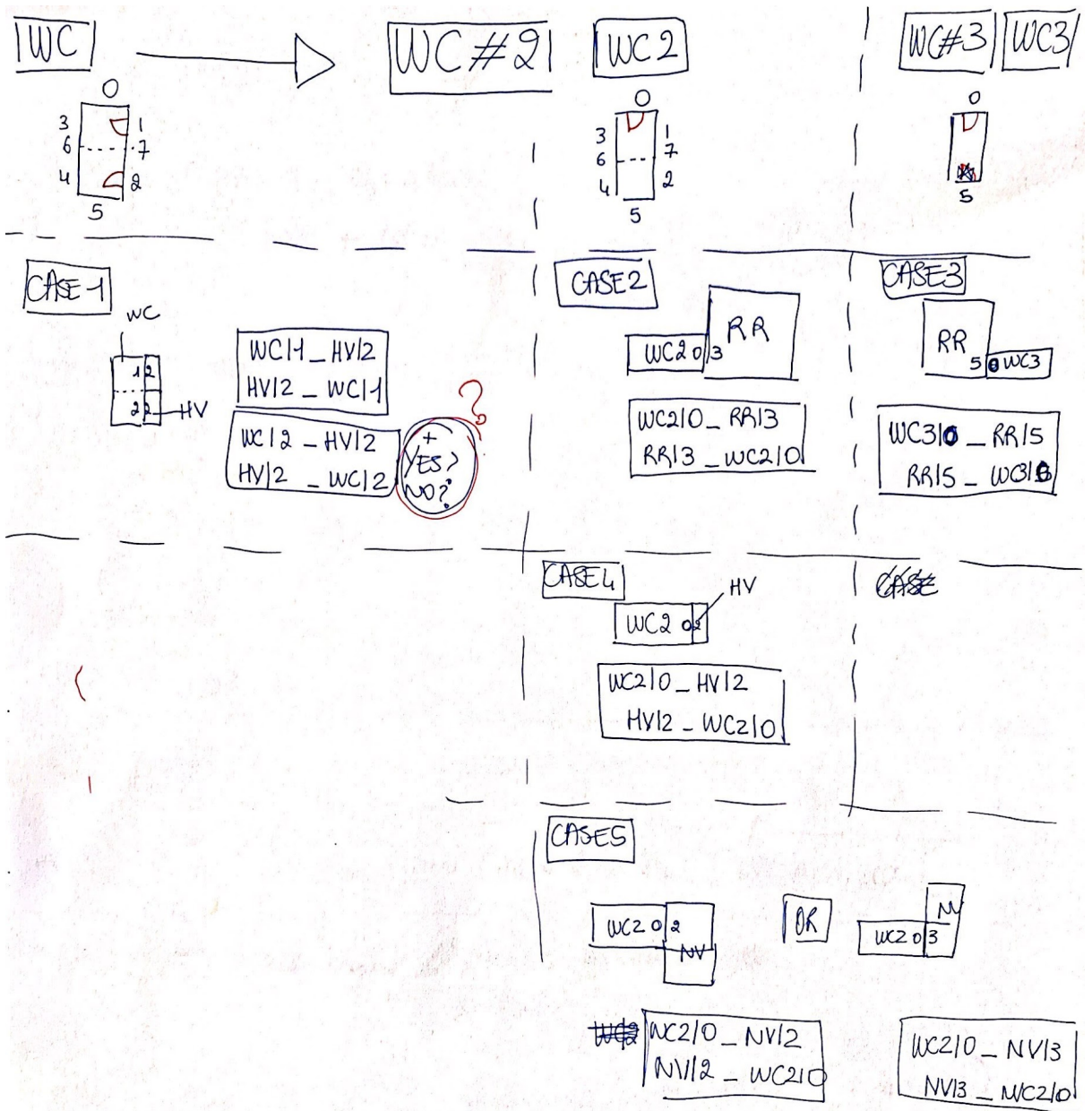
Scanned
CamScanner



OR







Scanned with
CamScanner

Appendix B - Analysis of Adobe Bricks

1. INTRODUCTION

Historically, earth has been utilized widely as a construction material since it is available in most regions of the world, especially in dry hot climate areas where other natural materials such as wood are rare. In these cases, earth is molded to create handmade sun-dried bricks known as adobe bricks to realize masonry buildings [1] [3].

Usually, adobe bricks are obtained by mixing clay, silt, sand and sometimes larger aggregates in different percentages. However, the composition of the soil from which the materials are extracted vary depending on the location and therefore affect the mechanical properties of the obtained bricks. Moreover, additive materials such as fibers and straws are added to the mixture to increase binding force and to improve the structural performance [1] [3]. Although, the additive materials utilized are different based on their availability in the area.

The aim of the report is to test how bricks produced with different composition and additive materials respond to a compression test in order to generate a reliable estimation of their compressive strength. Therefore, the results of a uniaxial compression test performed on various brick specimens are analyzed to determine which combination is more suitable for masonry construction.

2. METHODOLOGY

This paper analyses the mechanical properties of adobe bricks realized with a basic composition named as “control” to which are subsequently added various additive materials. Moreover, two sizes of bricks are evaluated to determine how the shape of the brick influences the results since earth is a heterogeneous material [2]. Multiple compression tests are performed on the different samples to assess the behavior of the mixtures and to compare their results.

Firstly, the production process of both the various mixtures and the specimens is explained. Afterwards, the uniaxial compression test procedure is described. Lastly, conclusions and reflections are drawn.

2.1 Mixing Procedure

The composition of the control mixture consists in a combination of clay, fine sand, coarse sand and water. The ratio of materials that compose the control batch is as follow: 40% coarse sand, 30% fine sand, 30% clay and the water supplemented consists in 10% of the total weight of the mixture. Afterwards, an electric blender machine is utilized to amalgam the composite.

Initially, a considerable batch of the mixture is produced to guarantee that the specimens are realized with a uniform material. Afterwards, the same batch is divided into smaller sets to which are supplemented the additive materials. Indeed, this decision facilitates to identify the influence of the added materials on the mechanical properties of the bricks since they differ only in them. Various materials are supplemented to the batches, such as wheat straw, 100% cotton cloth, wood chips, hemp, egg yolk and cornstarch.

More in depth, the straw and the hemp utilized are cut in smaller pieces of approximately 4-5 cm, while the cotton cloth is reduced to strips of 2 cm x 7-8 cm. The wood chips are composed of smaller parts with a diameter of less than 1 cm, while a single egg yolk is added to the mixture and blended with it. Also, the corn starch is weighted and added to another batch. In table 1 are listed the mixture compositions and the weight of the principal materials utilized, while in table 2 are listed the ratio of the principal and of the additive materials.

It is important to notice that a brick of the mixture C06 is realized with the composite C01 and subsequently wrapped in the cotton cloth. Hence, it is considered part of the batch C06 since the additive material is the same, but the cloth is not blended in the mixture as in the other specimens.



Figure 1: Specimens obtained from the various mixtures and additive materials combinations.

Mixture Code	Big Bricks [-]	Small Bricks [-]	Clay [Kg]	Fine Sand [Kg]	Coarse Sand [Kg]	Water [l]	Additive material [-]
C01	6	6	3,6	3,6	4,8	1,2	-
C02	1	1	0,4	0,8	0,8	0,2	Fine Sand
C03	1	1	0,8	0,4	0,8	0,2	Clay
C04	1	1	0,5	0,5	1,0	0,2	Coarse Sand
C05	5	1	2,4	2,4	3,2	0,8	Straw
C06	0	2*	0,6	0,6	0,8	0,2	Cloth
C07	0	1	0,6	0,6	0,8	0,2	Wood Chips
C08	0	1	0,6	0,6	0,8	0,2	Hemp
C09	1	0	0,6	0,6	0,8	0,2	Corn Starch
C10	1	0	0,6	0,6	0,8	0,2	Egg Yolk + Wood Chips
C11	1	1	0,6	0,6	0,8	0,2	Straw + Wood Chips
C12	1	0	0,6	0,6	0,8	0,2	Egg Yolk + Corn Starch + Wood Chips

Table 1: Quantity of materials utilized for the mixture compositions

Mixture Code	Big Bricks	Small Bricks	Clay	Fine Sand	Coarse Sand	Water	Quantity of Additive material
C01	6	6	30%	30%	40%	+10%	-
C02	1	1	20%	40%	40%	+10%	Fine Sand
C03	1	1	40%	20%	40%	+10%	Clay
C04	1	1	25%	25%	50%	+10%	Coarse Sand
C05	5	1	30%	30%	40%	+10%	10% Straw
C06	0	2*	30%	30%	40%	+10%	10% Cloth
C07	0	1	30%	30%	40%	+10%	10% Wood Chips
C08	0	1	30%	30%	40%	+10%	5% Hemp
C09	1	0	30%	30%	40%	+10%	50 g Corn Starch
C10	1	0	30%	30%	40%	+10%	1 Egg Yolk + 10% Wood Chips
C11	1	1	30%	30%	40%	+10%	10% Straw + 10 % Wood Chips
C12	1	0	30%	30%	40%	+10%	1 Egg Yolk + 50 g Corn Starch + 10 % Wood Chips

Table 2: Materials ratio utilized for the mixture compositions.

2.2 Specimens Preparation

Initially, two plastic molds of different dimensions were supplied, a small one (10,5 cm x 7,5 cm x 2,5 cm) and a big one. However, they rose problems while performing the specimen preparation process. Indeed, the mixture was sticking to their walls and it was difficult to extract from both molds, affecting the final integrity of the brick. Hence, few holes were cut in the small mold to facilitate the procedure, but it was not possible to apply this solution to the bigger form due to its thickness. Therefore, a new wooden mold (17,5 cm x 8,5 cm x 4 cm) is built. Since the sides of the wood have a

smooth finish, the mixture slides carefully on the walls of the form, facilitating the extraction procedure. In table 3 are listed the produced bricks, the utilized mixture and their dimensions. To prepare the specimens, the mold is placed on a plastic sheet and it is filled with the mixture. Afterwards, the composite is pressed by hand to close the air gaps within the brick.



Figure 2: The final molds utilized for the preparation of the specimens. The small one (left) and the big one (right)

Brick Code	Mixture Code	Size	Width [mm]	Lenght [mm]	Thickness [mm]	Area [mm ²]
B01	C01	Big	85,0	175,0	50,0	14875,0
B02	C01	Big	85,0	175,0	50,0	14875,0
B03	C01	Big	85,0	175,0	50,0	14875,0
B04	C01	Big	85,0	175,0	50,0	14875,0
B05	C01	Big	85,0	175,0	50,0	14875,0
B06	C01	Big	85,0	175,0	50,0	14875,0
B07	C01	Small	75,0	105,0	30,0	7875,0
B08	C01	Small	75,0	105,0	30,0	7875,0
B09	C01	Small	75,0	105,0	30,0	7875,0
B10	C01	Small	75,0	105,0	30,0	7875,0
B11	C01	Small	75,0	105,0	30,0	7875,0
B12	C01	Small	75,0	105,0	30,0	7875,0
B13	C02	Big	85,0	175,0	50,0	14875,0
B14	C02	Small	75,0	105,0	30,0	7875,0
B15	C03	Big	85,0	175,0	50,0	14875,0
B16	C03	Small	75,0	105,0	30,0	7875,0
B17	C04	Big	85,0	175,0	50,0	14875,0
B18	C04	Small	75,0	105,0	30,0	7875,0
B19	C05	Big	85,0	175,0	50,0	14875,0
B20	C05	Big	85,0	175,0	50,0	14875,0
B21	C05	Big	85,0	175,0	50,0	14875,0
B22	C05	Big	85,0	175,0	50,0	14875,0
B23	C05	Big	85,0	175,0	50,0	14875,0
B24	C05	Small	75,0	105,0	30,0	7875,0
B25	C06	Small	75,0	105,0	30,0	7875,0
B26	C06	Small	75,0	105,0	30,0	7875,0
B27	C07	Small	75,0	105,0	30,0	7875,0
B28	C08	Small	75,0	105,0	30,0	7875,0
B29	C09	Big	85,0	175,0	50,0	14875,0
B30	C10	Big	85,0	175,0	50,0	14875,0
B31	C11	Big	85,0	175,0	50,0	14875,0
B32	C11	Small	75,0	105,0	30,0	7875,0
B33	C12	Big	85,0	175,0	50,0	14875,0

Table 3: List of bricks dimensions, relative mixture utilized and their area.

In the end, the excessive material is removed from the form with a spatula and the mold is taken out. Afterwards, the bricks are left drying for one week from September 25th to October 2nd in a close environment to protect them from the atmospheric precipitations and to speed up the drying process as the air humidity can influence this procedure [1] [4]. Furthermore, the bricks are turned on one side on the second drying day (September 27th) to facilitate the evaporation of the moisture collected in the bottom of the blocks. At the end of the drying process, the bricks are measured again with a millimetric ruler to determine if the blocks shrink due to the water evaporation. However, the bricks seemed to have maintained their initial dimensions, thus the expected shrinking was negligible.



Figure 3: Bricks turned on the side on the second day of the drying process.

2.3 Testing Procedure

The main purpose of the experimentation described in this paper is to determine the mechanical properties of the mixtures utilized to produce the specimens. However, nowadays there are no standard methods to evaluate these characteristics in most of the countries around the world. Indeed, the only settlements available are related more to the quality of the specimens rather than the quality of the material. Therefore, in order to determine the mechanical properties, it is necessary to refer to the test performed on stone materials since they present similar characteristics [2][5].



Figure 4: The uniaxial compressive testing machine in action

The material test performed in this experimentation is a uniaxial compression test. More in depth, the assessment consists in a controlled displacement test that compresses the specimens with a hydraulic press perpendicularly to its largest surface area. Therefore, this method allowed to assess the maximum force that the specimen can withstand before failing. Hence, the maximum compressive strength can be determined since the cross-section area of the brick is known. Moreover, the deflection is assessed as well to determine the strain of the specimen and to determine the Young's modulus E of the material.

3. TESTING

The specimens were tested under the same environmental conditions at the 3ME material test laboratory of TU Delft. A Zwick Z100 uniaxial compressive testing machine was utilized to perform the experiment. Firstly, the specimens are listed in a table and named based on their shape and the mixture utilized. Afterwards a wood board is set under the head of the machine to be used as a base to position the specimens. Hence, the samples are set one by one into position and a steel plate is placed on top of them (only on top of the big samples) in order to distribute the force on the entire cross section area of the brick.

Finally, the test is performed and the results are recorded in a computer connected to the testing machine. More in depth, a graph of force and displacement is plotted automatically by the computer, while the deformation at the failure and the maximum force applied are recorded to determine the mechanical properties of the mixtures.

To conclude, it is important to notice that the order of testing presented in this paper is not the actual order followed during the experimentation. Indeed, the big specimens were tested before the smaller ones to accelerate the procedure. Thus, the loading head of the machine has to be set into position every time that the dimensions of the sample change.



Figure 5: Preparation of the specimens for the uniaxial compression test

4. EVALUATION AND DISCUSSION OF RESULTS

The results of the experimentation consist in a force-deformation graph showing the behavior of the specimens during the uniaxial compression test. All the 33 samples graphs are retrieved and analyzed to determine which bricks perform better and to determine the most suitable mixture to utilize in the structural analysis. All the results are listed in Appendix B. It is notable that the results of specimen B08 are not available since the machine did not record both the

deflection and the maximum force sustained due to a malfunction during the experimentation.

The graphs enlighten how the adobe bricks have an unpredictable behavior due to various aspects. Indeed, since adobe is a heterogeneous material, its mechanical properties are extremely dependent on the preparation procedure and on the shape and dimensions of the tested specimens [2] [5]. As can be seen in figure 6-7, the graphs show how two bricks prepared with the control mixture C01, but with different dimensions behave differently. On the one hand, the graph of the big brick shows how it is about to fail when the compressive force is around 12000 N but suddenly the slope increases and the brick finally fails at 19000 N. On the other hand, in the graph of the small brick the force and the displacement increase exponentially failing at almost 80000 N. This difference in behavior could be identified due to the porosity of the material caused by the evaporation of the water during the drying process and in the compactness of the mixture during the preparation procedure.

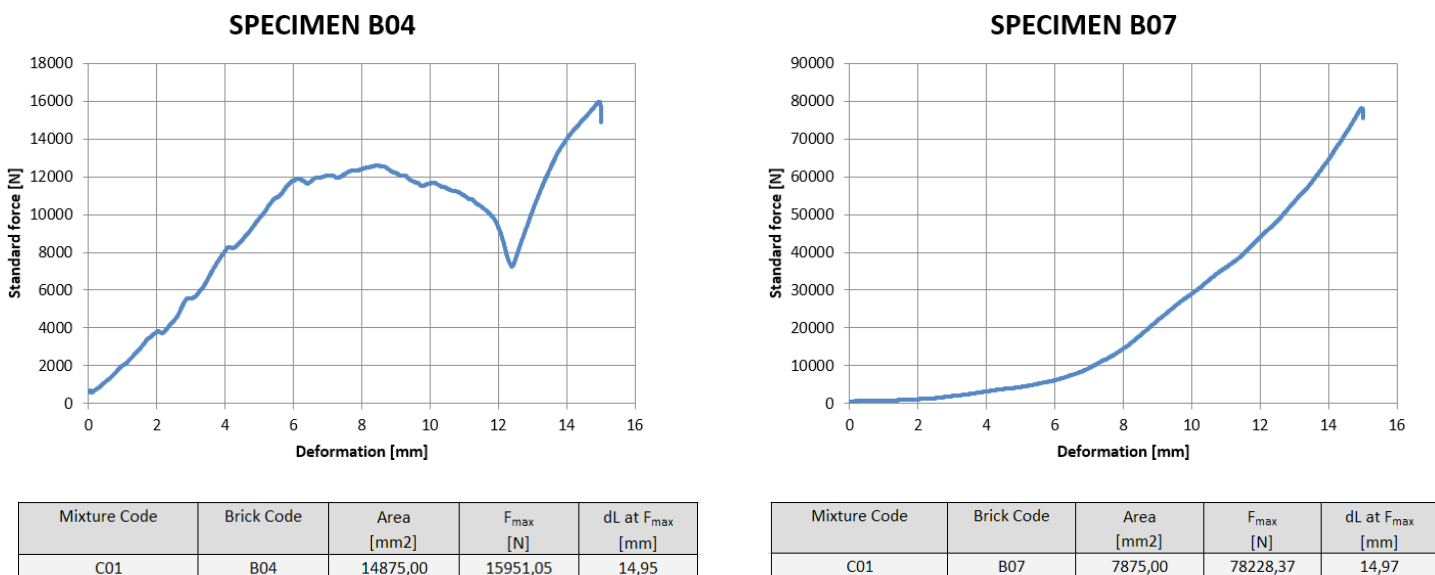


Figure 6-7: Graph of the behavior of specimens B04 and B07.

Indeed, the sample B04 seems to fail because the compression force causes the pores inside the brick to close and therefore increasing the density of the block and giving it the possibility to withstand a higher compression force. This behavior is identified as compactable behavior and it increases the ductility of the material since it undergoes deformation before collapsing [2]. However, the specimen B07 is smaller and most likely it has been compacted more during the preparation procedure. Hence, its graph shows a continuous increase of both the force and the displacement until reaching the failure load unlikely the specimen B04.

Considering the graphs of the specimens B20 and B24 (Figure 8-9), it is notable that their behavior is similar even though the slope of the small specimen B24 is steeper. Indeed, both the specimens' graphs show a continuous increment in both the force and the displacement until the failure point is reached. This comparison enlightens how the additional material added to the mixture improves the compactness of the specimen. Indeed, the straw supplemented in the mixture allows the absorption of the water during the drying process of the specimen and therefore reducing the porosity of the material giving it the possibility to withstand a higher compressive force [1].

Hence, the addition of materials capable of absorbing the moisture during the drying period can improve the characteristics of the composites. However, the graphs cannot always be approximated to a linear behavior typical of other construction materials. Therefore, it is important to determine an appropriate value as a safety factor to overcome the unpredictability of a material such as adobe.

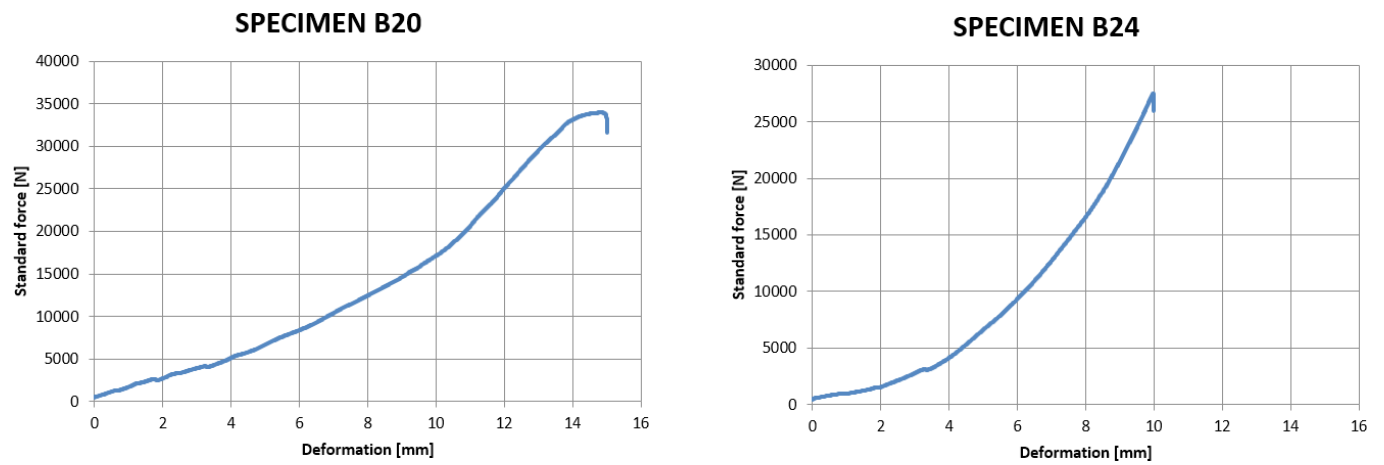


Figure 8-9: Graph of the behavior of specimens B20 and B24

4.1 Failure Behaviour

As previously explained, the main characteristic notable from the failure behavior of the specimens is the plastic deformation few of them undergo to. Initially, the samples present the formation of vertical cracks along the edges that starts gradually to detach from the central part of the specimens. Hence, few samples seem to fail before withstanding more compressive force before collapsing. However, this behavior is less likely to happen in the small samples and in the ones with additive materials due to the less porosity. Indeed, on the one hand the additive materials absorb the moisture during the drying time reducing the formation of voids within the bricks [3]. On the other hand, the small samples are easier to compact during the preparation procedure. This condition is notable in these specimens after the test since they are not fully disaggregated. The failure behavior of all the specimens are shown in appendix A.

To conclude, the additive materials help to keep together the samples and to redistribute more the forces within them causing less cracks to form and increasing the value of the compressive force they can withstand.

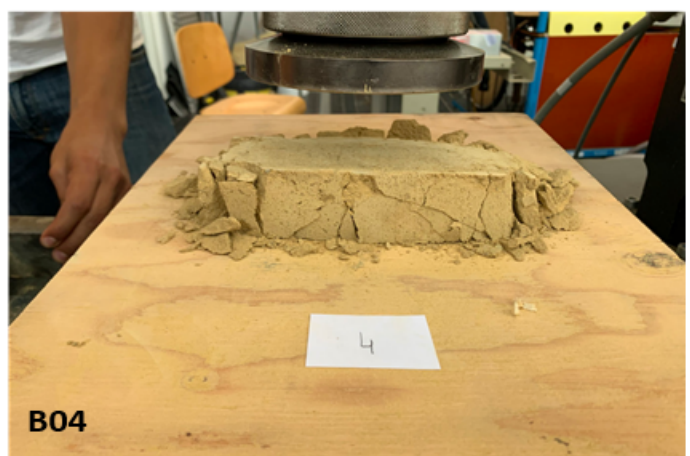
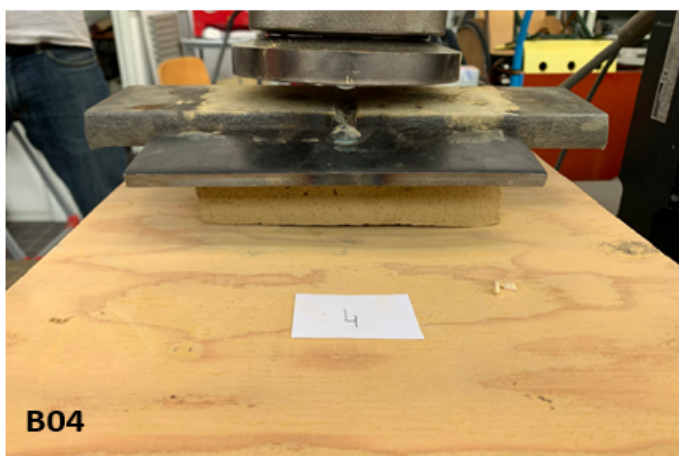


Figure 10-11: Failure behavior of specimen B04



Figure 12-13: Failure behavior of specimen B07

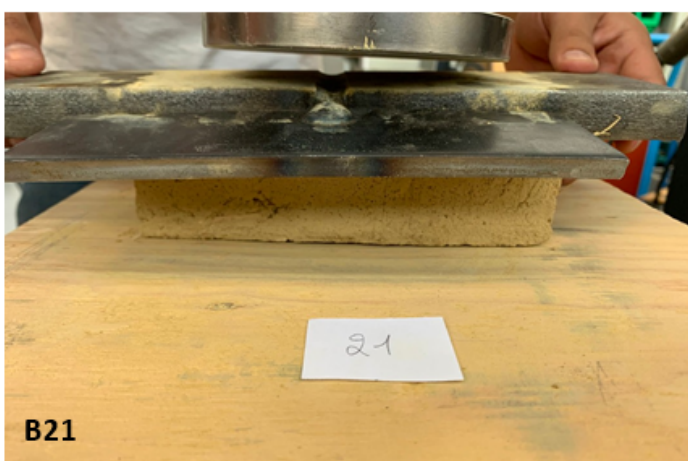


Figure 14-15: Failure behavior of specimen B21



Figure 16-17: Failure behavior of specimen B24

4.2 Compressive Strength

As previously mentioned, adobe is a heterogeneous material with an unpredictable behavior and thus multiple problems can rise in assessing accurately the characteristic of this material. Indeed, various factors as the shape of the specimens, the preparation procedure, the drying time and the components of the mixtures can influence largely the mechanical properties as can be seen from the results of the experimentation listed in table 4. Moreover, except for mixture C01 and C05, at maximum two bricks were prepared with the composites and therefore the reliability of their results is reduced.

Firstly, confronting the compressive strength values of the bricks produced with different mixtures, it can be noticed that the range results to be extremely wide with a minimum of 0.733 Mpa for B14 and a maximum of 11.162 Mpa for B10. Although this outcome is expected since the quantity of materials utilized in the mixtures varies, the range of values appears to be wide also for the specimens produced with the same composite.

Considering mixture C01, the size of the bricks appears to influence greatly the results, as the values range from 0.837 Mpa for B01 to 11.162 Mpa for B10. However, also same sized samples have largely different values for the compressive strength, as the values range from 3.703 Mpa for B09 to 11.162 Mpa for B10. Overall, the small sized bricks have higher values for the compressive strength compared to the bigger specimens. Moreover, the mixtures produced with additive materials as C05 result in an increment of the values compared to the basic composite C01, even though this observation is related exclusively to the big specimens. However, this outcome could be influenced by the amount of additive materials utilized in the mixtures. Indeed, a larger amount of straw in a small brick could affect the cohesion of the mixture instead of increasing it and therefore reducing the amount of force they can withstand.

Lastly, it is notable that all the specimens undergo a deformation of at least 0.214 (21.4%) for the C01 mixture, while it rises to a maximum of 0.5 (50%) for the samples containing additive materials as mixture C05. However, a large value for deformation is not recommended for a material to be utilized in a construction process since it can affect the stability of the structure [5]. Hence, it will be advisable to set a limit of allowed deformation and to determine the compressive strength from it. Nonetheless, according to the specifications of the course, it seems preferable to take this consideration into account during the assessment of the safety factor.

Mixture Code	Brick Code	Area [mm ²]	F _{max} [N]	dL at F _{max} [mm]	F _{max} /Area [N/mm ²]	Δl/l [-]
C01	B01	14875,00	12457,81	11,32	0,837	0,226
C01	B02	14875,00	13624,26	9,26	0,916	0,185
C01	B03	14875,00	13027,70	11,29	0,876	0,226
C01	B04	14875,00	15951,05	14,95	1,072	0,299
C01	B05	14875,00	19770,12	8,56	1,329	0,171
C01	B06	14875,00	21831,98	10,02	1,468	0,200
C01	B07	7875,00	78228,37	14,97	9,934	0,499
C01	B09	7875,00	29158,42	15,00	3,703	0,500
C01	B10	7875,00	87904,19	14,99	11,162	0,500
C01	B11	7875,00	30334,93	15,00	3,852	0,500
C01	B12	7875,00	79126,34	14,98	10,048	0,499
C02	B13	14875,0	18749,35	11,70	1,260	0,234
C02	B14	7875,0	5772,04	9,95	0,733	0,332
C03	B15	14875,0	32743,46	10,80	2,201	0,216
C03	B16	7875,0	42718,99	9,96	5,425	0,332
C04	B17	14875,0	18634,59	11,45	1,253	0,229
C04	B18	7875,0	10378,99	7,66	1,318	0,255
C05	B19	14875,0	36592,63	14,94	2,460	0,299
C05	B20	14875,0	33957,98	14,79	2,283	0,296
C05	B21	14875,0	56105,79	14,94	3,772	0,299
C05	B22	14875,0	51784,55	14,93	3,481	0,299
C05	B23	14875,0	56502,25	14,94	3,798	0,299
C05	B24	7875,0	27459,32	9,97	3,487	0,332
C06	B25	7875,0	20726,14	9,97	2,632	0,332
C06	B26	7875,0	37088,25	11,97	4,710	0,399
C07	B27	7875,0	43293,21	11,96	5,498	0,399
C08	B28	7875,0	76151,38	11,97	9,670	0,399
C09	B29	14875,0	37139,72	13,87	2,497	0,277
C10	B30	14875,0	45827,04	14,95	3,081	0,299
C11	B31	14875,0	59666,73	10,25	4,011	0,205
C11	B32	7875,0	44791,19	11,96	5,688	0,399
C12	B33	14875,0	83444,94	14,95	5,610	0,299

Table 4: Compressive Strength and Strain of Bricks

4.3 Safety Factor

The main aspects that have to be considered in the assessment of the safety factor are mainly the typology of the designed structure and the material utilized to construct it. In this case, a masonry framework is determined and adobe is selected as the main building material. However, little literature is available regarding safety factor for adobe masonry structures. Indeed, regulations as EN 1996-1-1 Eurocode 6 does not cover cases regarding adobe [5]. Usually, a safety factor of 3 is considered for masonry construction since the utilized materials and their interactions are often vague, which is the case of adobe, while a safety factor of 2 is applied to the building materials that compose the building. Considering these aspects and taking into account that the range of values retrieved from the experimentation is wide, the safety factor should be adequate in order to ensure the stability of the structure, but without restraining further the mechanical properties of adobe, which are already low.

Another important aspect that must be considered in the evaluation of the safety factor is the strain. Indeed, a large deformation in the bricks can cause instability in the structure and it can bring it to fail, even though the maximum stress in the samples has not been reached yet. Hence, the total deformation of each specimen is the value utilized to assess the safety factor. Therefore, the maximum allowed strain of all the specimens is set to a peak value of 0.15 (15%). The ratio between the strain of the samples and this value provides the safety factor of each brick, which is then utilized to assess the maximum compressive strength value to be utilized for the structural analysis of the design.

In table 6 are listed the calculated safety factors for each specimen along with the maximum allowed compressive strength. In the next section, the bricks are grouped based on the mixture utilized for the production to assess an average value of each composite. Afterwards, the best performing brick and the mixture will be selected.

Mixture Code	Brick Code	Area [mm ²]	F _{max} [N]	dL at F _{max} [mm]	F _{max} /Area [N/mm ²]	Δl/l [-]	E [N/mm ²]	Safety Factor [-]	Maximum Compressive σ [N/mm ²]	Maximum Allowed Strain ε [-]
C01	B01	14875,00	12457,81	11,32	0,837	0,226	3,700	1,5	0,555	0,150
C01	B02	14875,00	13624,26	9,26	0,916	0,185	4,947	1,2	0,742	0,150
C01	B03	14875,00	13027,70	11,29	0,876	0,226	3,880	1,5	0,582	0,150
C01	B04	14875,00	15951,05	14,95	1,072	0,299	3,587	2,0	0,538	0,150
C01	B05	14875,00	19770,12	8,56	1,329	0,171	7,766	1,1	1,165	0,150
C01	B06	14875,00	21831,98	10,02	1,468	0,200	7,327	1,3	1,099	0,150
C01	B07	7875,00	78228,37	14,97	9,934	0,499	19,903	3,3	2,985	0,150
C01	B09	7875,00	29158,42	15,00	3,703	0,500	7,405	3,3	1,111	0,150
C01	B10	7875,00	87904,19	14,99	11,162	0,500	22,344	3,3	3,352	0,150
C01	B11	7875,00	30334,93	15,00	3,852	0,500	7,704	3,3	1,156	0,150
C01	B12	7875,00	79126,34	14,98	10,048	0,499	20,121	3,3	3,018	0,150
C02	B13	14875,0	18749,35	11,70	1,260	0,234	5,388	1,6	0,808	0,150
C02	B14	7875,0	5772,04	9,95	0,733	0,332	2,211	2,2	0,332	0,150
C03	B15	14875,0	32743,46	10,80	2,201	0,216	10,194	1,4	1,529	0,150
C03	B16	7875,0	42718,99	9,96	5,425	0,332	16,345	2,2	2,452	0,150
C04	B17	14875,0	18634,59	11,45	1,253	0,229	5,472	1,5	0,821	0,150
C04	B18	7875,0	10378,99	7,66	1,318	0,255	5,164	1,7	0,775	0,150
C05	B19	14875,0	36592,63	14,94	2,460	0,299	8,235	2,0	1,235	0,150
C05	B20	14875,0	33957,98	14,79	2,283	0,296	7,720	2,0	1,158	0,150
C05	B21	14875,0	56105,79	14,94	3,772	0,299	12,626	2,0	1,894	0,150
C05	B22	14875,0	51784,55	14,93	3,481	0,299	11,662	2,0	1,749	0,150
C05	B23	14875,0	56502,25	14,94	3,798	0,299	12,715	2,0	1,907	0,150
C05	B24	7875,0	27459,32	9,97	3,487	0,332	10,489	2,2	1,573	0,150
C06	B25	7875,0	20726,14	9,97	2,632	0,332	7,917	2,2	1,188	0,150
C06	B26	7875,0	37088,25	11,97	4,710	0,399	11,808	2,7	1,771	0,150
C07	B27	7875,0	43293,21	11,96	5,498	0,399	13,784	2,7	2,068	0,150
C08	B28	7875,0	76151,38	11,97	9,670	0,399	24,229	2,7	3,634	0,150
C09	B29	14875,0	37139,72	13,87	2,497	0,277	9,003	1,8	1,350	0,150
C10	B30	14875,0	45827,04	14,95	3,081	0,299	10,306	2,0	1,546	0,150
C11	B31	14875,0	59666,73	10,25	4,011	0,205	19,573	1,4	2,936	0,150
C11	B32	7875,0	44791,19	11,96	5,688	0,399	14,271	2,7	2,141	0,150
C12	B33	14875,0	83444,94	14,95	5,610	0,299	18,766	2,0	2,815	0,150

Table 6: List of the calculated safety factors for each specimen and the correspondent maximum compressive strength

5. CONCLUSIONS

5.1 Typologies and Values of Bricks

The experimentation ran on the specimens showed the unpredictable behavior of adobe. Indeed, its heterogeneous nature rose difficulties in the assessment of its mechanical behavior. In total, 33 samples produced with 12 different mixtures were realized and tested. Initially, a control composite made of coarse sand, clay, fine sand and water was produced, to which were supplemented various additive materials such as straw, wood chips, cloth, corn starch and egg yolk in different combinations. Two main sizes of brick were tested.

In general, it is notable from the results that the additive materials improved the mechanical properties of the brick resulting in higher values for the maximum compressive stress that can be sustained by these bricks. However, this aspect is mainly reflected by the big samples, while the small specimens produced with the control mixture C01 resulted to be the strongest. Nevertheless, the quantity of additive materials supplemented to the mixtures utilized to produce the small bricks could have been excessive, resulting in less compact samples. Hence, these specimens could have performed worse due to the disaggregation of the mixture. It would have been interesting to test small sized bricks with a lower concentration of additive materials to gain more insight on this aspect. In order to choose the most suitable brick type and mixture to utilize for the construction and the structural analysis, only the samples produced with the composite C01 and C05 were compared and analyzed further. Indeed, considering the heterogeneous nature of adobe and since they have the largest batches among the mixtures, the results are considered more reliable.

It can be noticed that the small bricks produced with the composite C01 have a large deformation, which is of 50% against a maximum of 30% for the big specimens produced with the same mixture. Even though the safety factor applied to the results is of 3.3, the values for the maximum compressive strength and the maximum tensile stress, which is calculated as 1/10 of the maximum compressive strength [6] [7], are still arguably the best among the whole tested specimens. However, their trapezoidal shape and their dimensions could have played a role in the determination of these mechanical properties. Therefore, since the bricks implemented in the design have dimensions more related to the big tested specimens, the results of the small samples are not considered for the structural analysis of the buildings.

Hence, comparing the results of the specimens produced with the mixtures C01 and C05, the straw composite offered higher values. Therefore, this typology of brick is considered to be utilized in the design. Lastly, it is important to notice that the results of the single small specimen produced with the mixture C05 is neglected while calculating the average Compressive strength and Young's Modulus due to the different dimensions.

Mixture Code	Brick Code	Area [mm ²]	F _{max} [N]	dL at F _{max} [mm]	F _{max} /Area [N/mm ²]	Δl/l [-]	E [N/mm ²]
C01	B01	14875,00	12457,81	11,32	0,837	0,226	3,700
C01	B02	14875,00	13624,26	9,26	0,916	0,185	4,947
C01	B03	14875,00	13027,70	11,29	0,876	0,226	3,880
C01	B04	14875,00	15951,05	14,95	1,072	0,299	3,587
C01	B05	14875,00	19770,12	8,56	1,329	0,171	7,766
C01	B06	14875,00	21831,98	10,02	1,468	0,200	7,327

Table 7a: Group of big specimens produced with the control mixture C01

Safety Factor [-]	Maximum Compressive σ [N/mm ²]	Maximum Allowed Strain ϵ [-]	Maximum Tensile σ [N/mm ²]	Average Maximum Compressive σ [N/mm ²]	Average Maximum Tensile σ [N/mm ²]	Average E [N/mm ²]
1,5	0,555	0,15	0,06	0,78	0,078	5,201
1,2	0,742	0,15	0,07			
1,5	0,582	0,15	0,06			
2,0	0,538	0,15	0,05			
1,1	1,165	0,15	0,12			
1,3	1,099	0,15	0,11			

Table 7b: Calculated safety factor and maximum allowed value for the big specimens produced with control

Mixture Code	Brick Code	Area [mm ²]	F_{max} [N]	dL at F_{max} [mm]	$F_{max}/Area$ [N/mm ²]	$\Delta l/l$ [-]	E [N/mm ²]
C01	B07	7875,00	78228,37	14,97	9,934	0,499	19,903
C01	B09	7875,00	29158,42	15,00	3,703	0,500	7,405
C01	B10	7875,00	87904,19	14,99	11,162	0,500	22,344
C01	B11	7875,00	30334,93	15,00	3,852	0,500	7,704
C01	B12	7875,00	79126,34	14,98	10,048	0,499	20,121

mixture C01

Table 8a: Group of small specimens produced with the control mixture C01

Safety Factor [-]	Maximum Compressive σ [N/mm ²]	Maximum Allowed Strain ϵ [-]	Maximum Tensile σ [N/mm ²]	Average Maximum Compressive σ [N/mm ²]	Average Maximum Tensile σ [N/mm ²]	Average E [N/mm ²]
3,3	2,985	0,15	0,30	2,32	0,232	15,495
3,3	1,111	0,15	0,11			
3,3	3,352	0,15	0,34			
3,3	1,156	0,15	0,12			
3,3	3,018	0,15	0,30			

Table 8b: Calculated safety factor and maximum allowed value for the small specimens produced with control mixture C01

Mixture Code	Brick Code	Area [mm ²]	F_{max} [N]	dL at F_{max} [mm]	$F_{max}/Area$ [N/mm ²]	$\Delta l/l$ [-]	E [N/mm ²]
C05	B19	14875,0	36592,63	14,94	2,460	0,299	8,235
C05	B20	14875,0	33957,98	14,79	2,283	0,296	7,720
C05	B21	14875,0	56105,79	14,94	3,772	0,299	12,626
C05	B22	14875,0	51784,55	14,93	3,481	0,299	11,662
C05	B23	14875,0	56502,25	14,94	3,798	0,299	12,715
C05	B24	7875,0	27459,32	9,97	3,487	0,332	10,489

Table 9a: Group of big and small specimens produced with the mixture C05 (Straw)

Safety Factor [-]	Maximum Compressive σ [N/mm ²]	Maximum Allowed Strain ϵ [-]	Maximum Tensile σ [N/mm ²]	Average Maximum Compressive σ [N/mm ²]	Average Maximum Tensile σ [N/mm ²]	Average E [N/mm ²]
2,0	1,24	0,15	0,12	1,59	0,159	10,591
2,0	1,16	0,15	0,12			
2,0	1,89	0,15	0,19			
2,0	1,75	0,15	0,17			
2,0	1,91	0,15	0,19			
2,2	1,57	0,15	0,16			

Table 9b: Calculated safety factor and maximum allowed value for the specimens produced with mixture C05 (Straw)

5.2 Limitations

Considering the preparation procedure, the mixture was manually poured and pressed roughly into the molds. Even though this method is most likely to be employed in the context of Jordan, using an appropriate tool could have improved the compression of the bricks and therefore it could have provided better performing samples. Furthermore, the drying process has also to be taken into account as a limitation. In this case, the samples were kept drying for only 7 days in a closed humid environment with an average temperature of 15° C, while the advised drying period for unbaked adobe bricks is usually of 30 to 40 days under the action of sun [4]. Most likely, the weather conditions of the Jordan context will be more effective and could improve the quality of the samples. Lastly, the mold utilized for the small specimens was a plastic container with an irregular trapezoid shape. Since the shape appears to influence the results of the test, it would have been interesting to evaluate this aspect further to determine the degree of influence on the mechanical properties of adobe. For example, a big trapezoidal mold could have been realized to compare its results with the rectangular ones.

Concerning the testing procedure, all 33 specimens produced with 12 different mixtures were evaluated. Usually, this solution provides more values for a comparison of the results. However, the unpredictable behavior of adobe requires for large batches of specimens produced with the same composition to obtain more reliable results, which is the case of only mixtures C01 and C05. Even though the values of the analysis of other groups were available, they could not be compared since the ratios of the principal and additive materials were different and therefore not relevant. Another limitation of the testing procedure concerns the determination of the failure point of the specimens due to the large deformation ranging from 21.4% to 50% of the bricks. Indeed, the large strain rose few problems in the determination of the maximum allowed compressive stress, resulting in the application of higher safety factors for the structural analysis.

Considering this aspect, the little literature available reduced the evaluation of the safety factors to a simplistic estimation based on the maximum allowed strain of the bricks. Moreover, the samples were realized with various mixtures and dimensions, which did not allow for a statistical evaluation of the safety factor. Indeed, the estimation is performed with a more qualitative approach than a quantitative one. Lastly, masonry is a construction method that foresees the iteration of multiple components such as mortar and reinforcement material, which were neither analyzed nor considered for the evaluation of the safety factors.

6. PERSONAL REFLECTIONS

The experimentation gave an insight of the characteristics and mechanical properties of adobe bricks and their preparation method. However, the applicability of these results in the perspective of the Al Zaatari refugee camp is limited. Indeed, the context of Jordan is extremely different from the one in which this experiment was run and therefore the outcome on the real site may be different. Hence, the processes

explained in this paper could be considered more as a manual of tips to provide the refugees useful information about adobe bricks and their preparation method to overcome possible problems during the construction of the design.

Another aspect that has to be taken into account is the availability of the additive material such as straw or other fibers on site. However, various construction activities and initiatives took place in the camp or in the surrounding areas in which the refugees had the possibility to utilize materials retrieved on site to build facilities or to sculpt object [8] [9]. Hence, it could be safe to estimate the applicability of this production method in the area using these materials since there is proof of their availability.

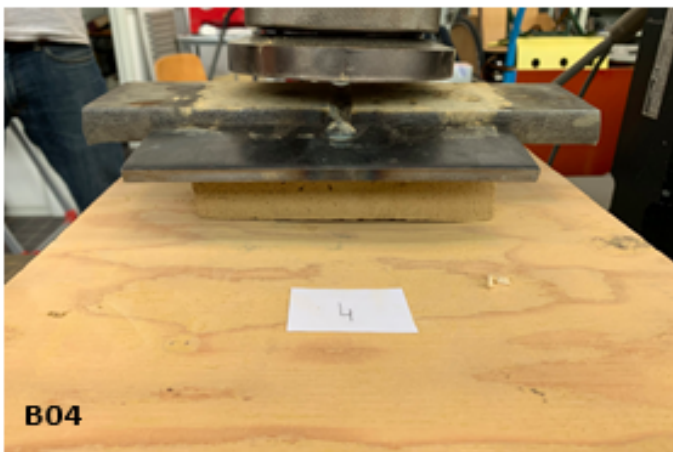
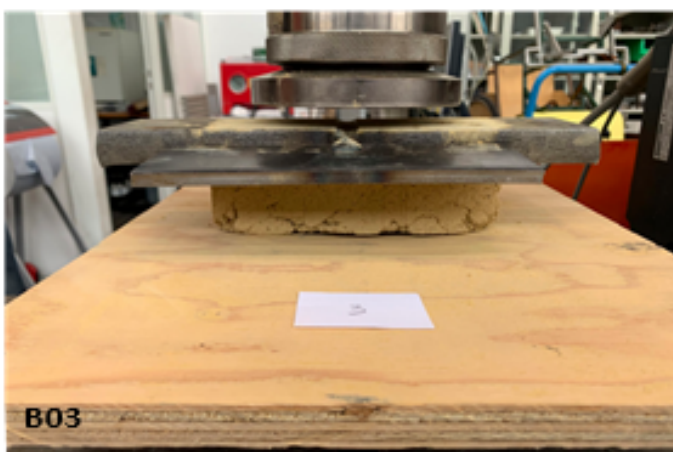
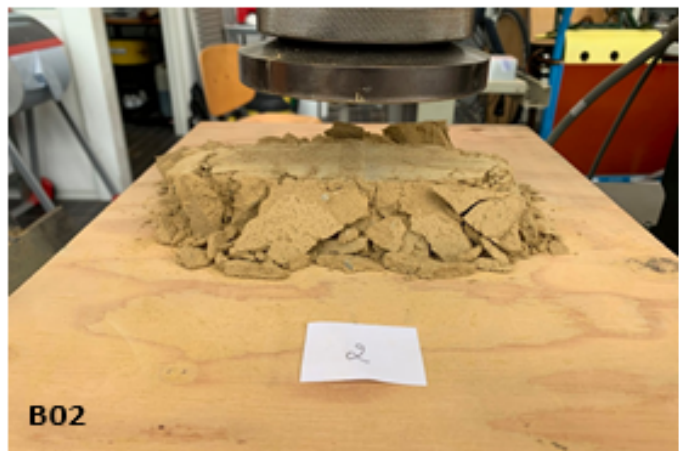
7. BIBLIOGRAPHY

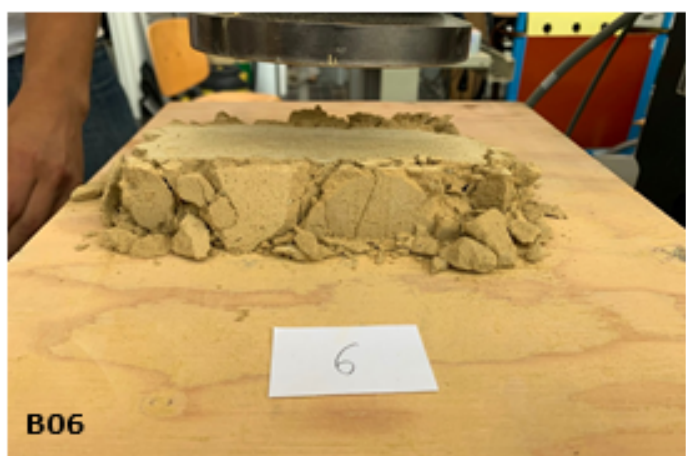
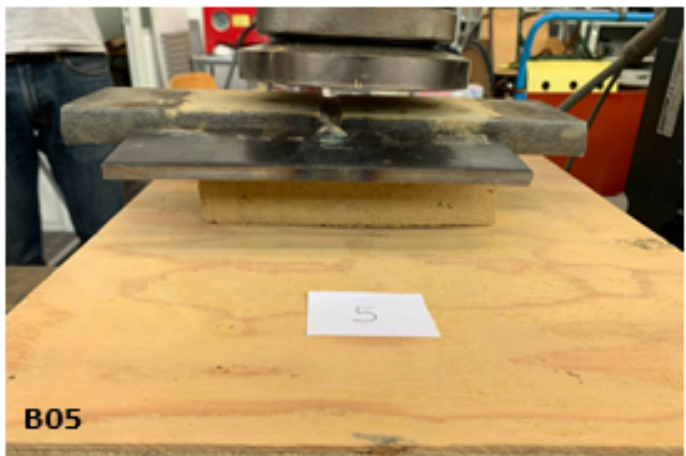
- [1] Minke Gernot (2006), Building with Earth: Design and Technology of a Sustainable Architecture.
doi: https://ia800306.us.archive.org/13/items/Gernot_Minke-Building_With_Earth/Gernot_Minke-Building_With_Earth.pdf
- [2] Lotti Giuseppe, Mecca Saverio (2008), Earth/Lands: Earthen Architecture in Southern Italy/Architettura in terra nell'Italia del Sud.
doi: <https://issuu.com/dida-unifi/docs/earth-lands>
- [3] Quagliarini Enrico, Lenci Stefano (2010), The influence of natural stabilizers and natural fibres on the mechanical properties of ancient Roman adobe bricks.
doi: <https://doi.org/10.1016/j.culher.2009.11.012>
- [4] Tarque Ruiz Sabino Nicola (2011), Numerical modelling of the seismic behaviour of adobe buildings.
doi: <https://pdfs.semanticscholar.org/d42f/2de9bcb290c0fd12ef8fbcd9585df21b5af2.pdf>
- [5] R. Illampas, I. Ioannou & D. C. Charmpis (2011), A study of the mechanical behaviour of adobe masonry.
doi: https://www.researchgate.net/publication/271492466_A_study_of_the_mechanical_behaviour_of_adobe_masonry
- [6] Gubasheva Samal (2017), Adobe bricks as a building material
doi: <https://dspace.cvut.cz/bitstream/handle/10467/69500/F1-BP-2017-Gubasheva-Samal-priloha-ADOBEPDF.pdf?sequence=3&isAllowed=y>
- [7] Wencil Brown Paul, Clifton James R. (1978), Adobe. I: The Properties of Adobe
doi: [10.2307/1505842](https://doi.org/10.2307/1505842) <https://www.jstor.org/stable/1505842>
- [8] Noor al-Saleh in Amman (2013), Zaatari village classroom wins architecture award, Al-Mashareq
doi: http://almashareq.com/en_GB/articles/cnmi_am/features/2018/03/13/feature-01
- [9] Segal Corinne (2016), Using only materials from a refugee camp, artists recreate Syria's lost treasures, PBS News Hour
doi: <https://www.pbs.org/newshour/arts/using-only-materials-from-a-refugee-camp-artists-recreate-syrias-lost-treasures>

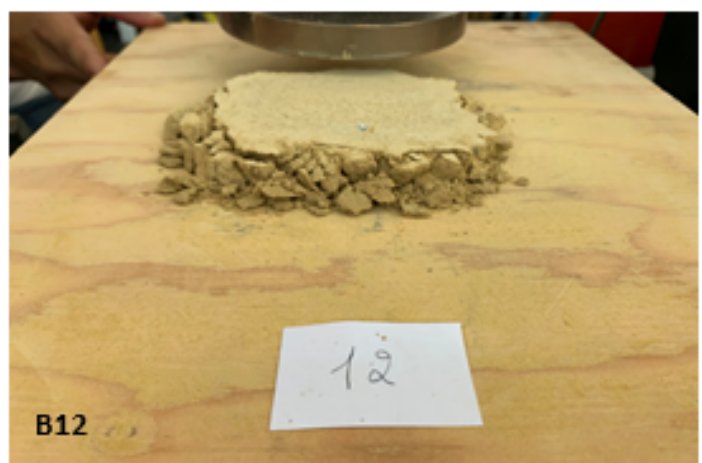
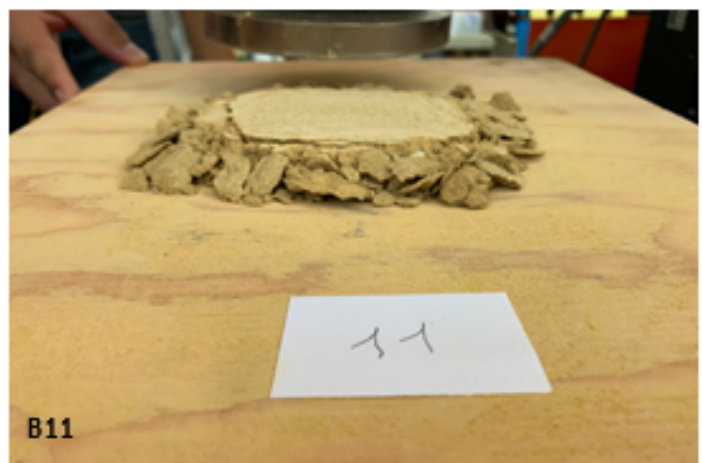
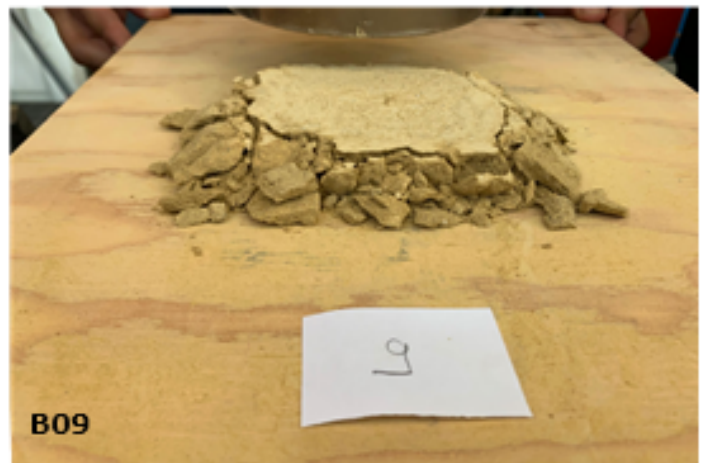
APPENDIX B1 - Failure Behavior of Specimens

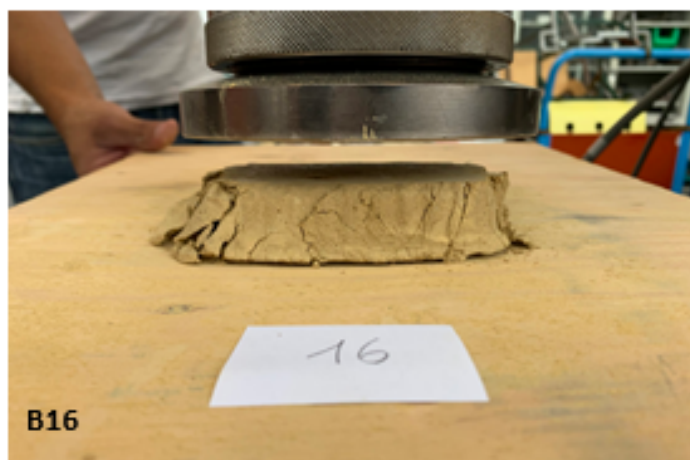
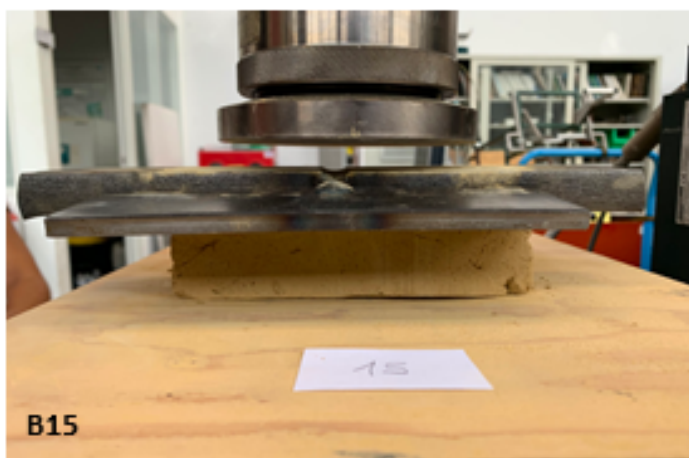
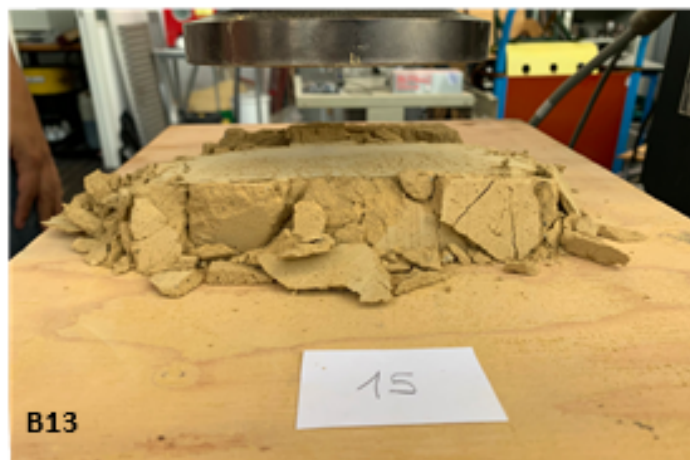
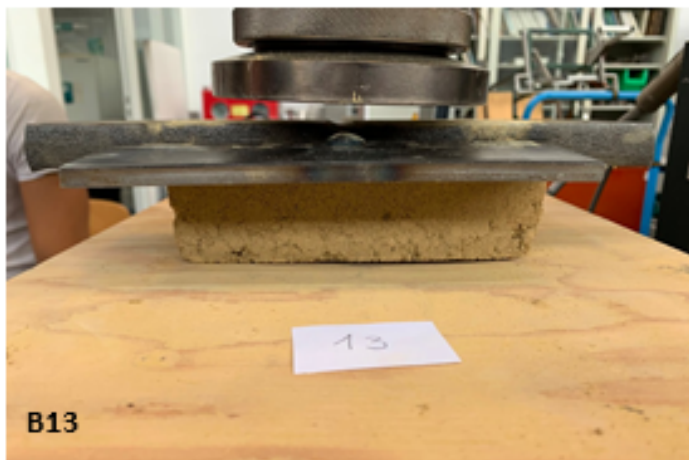
Specimens Before Test

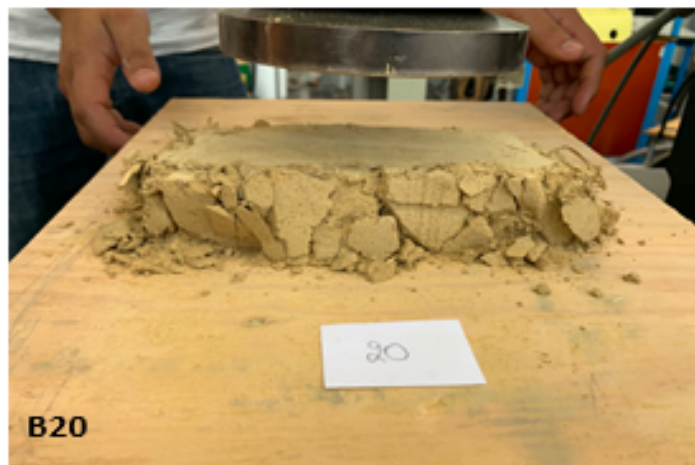
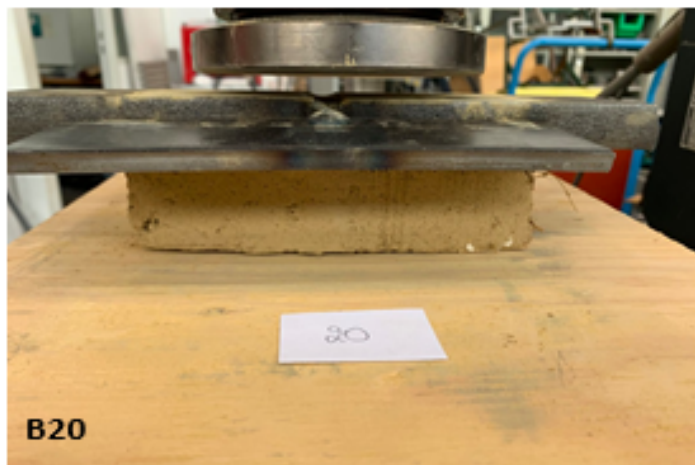
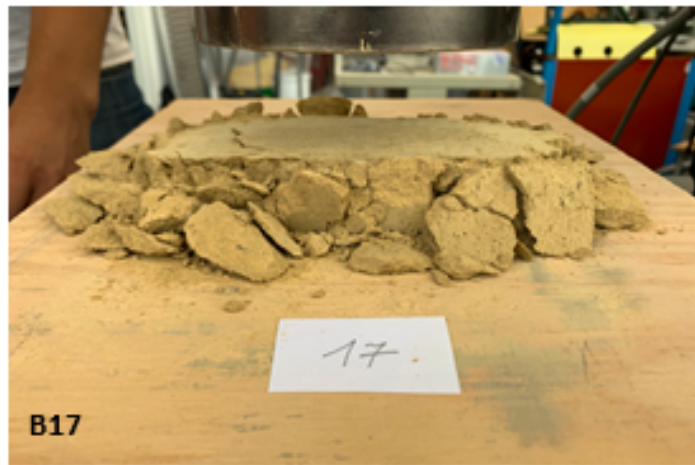
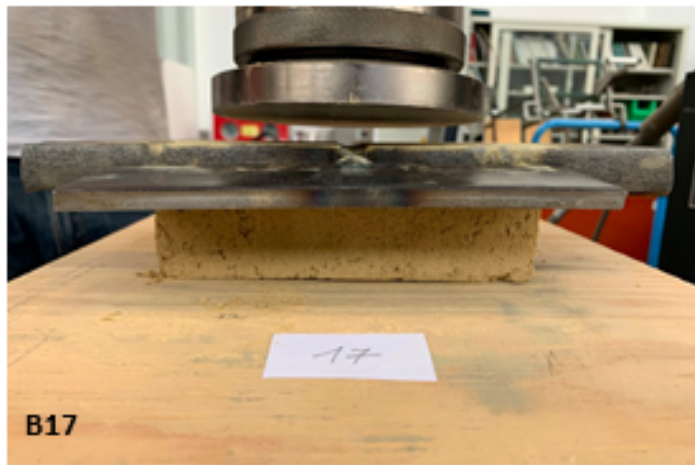
Specimens After Test

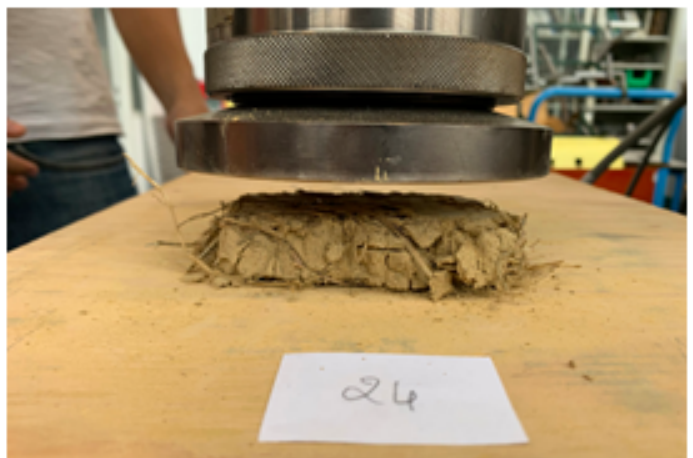
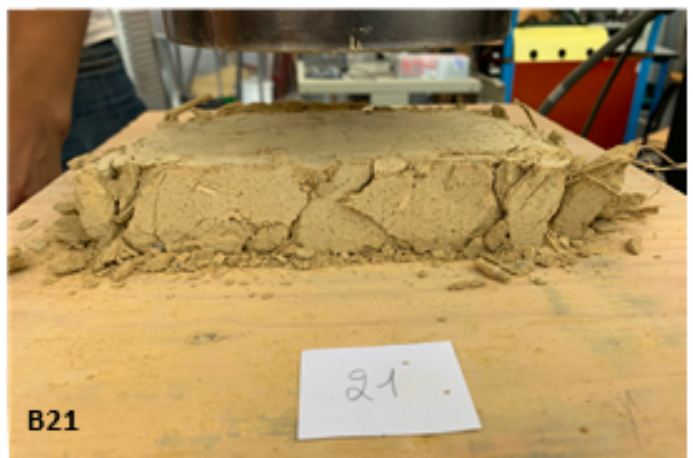
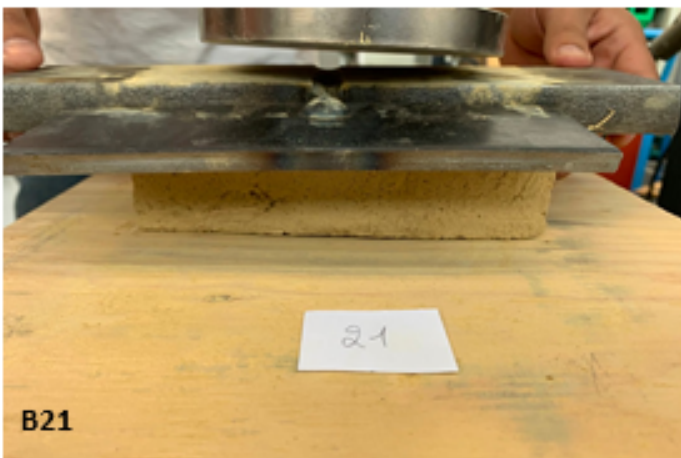


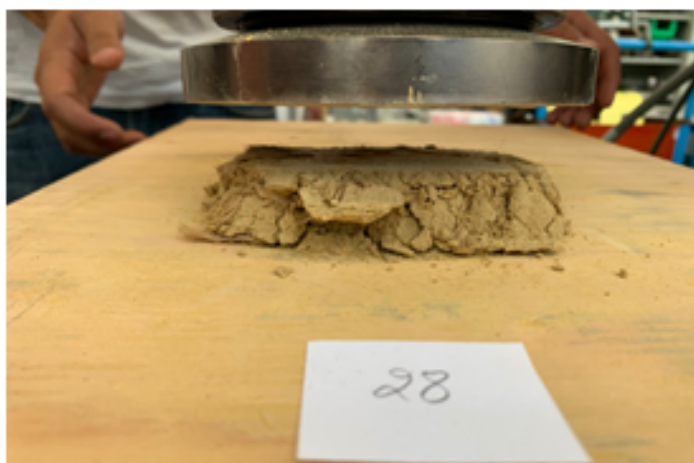
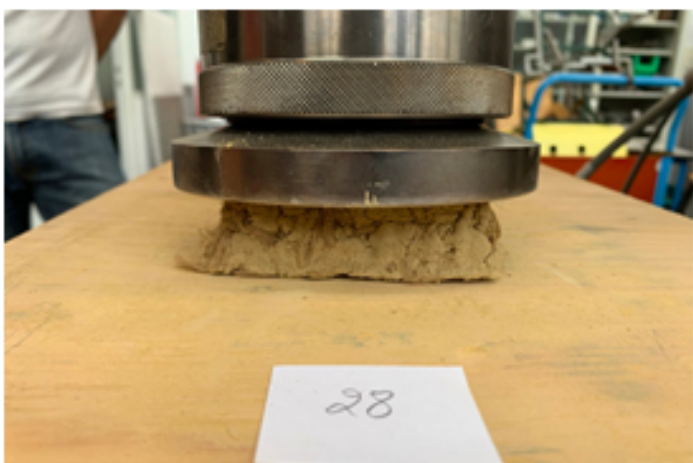




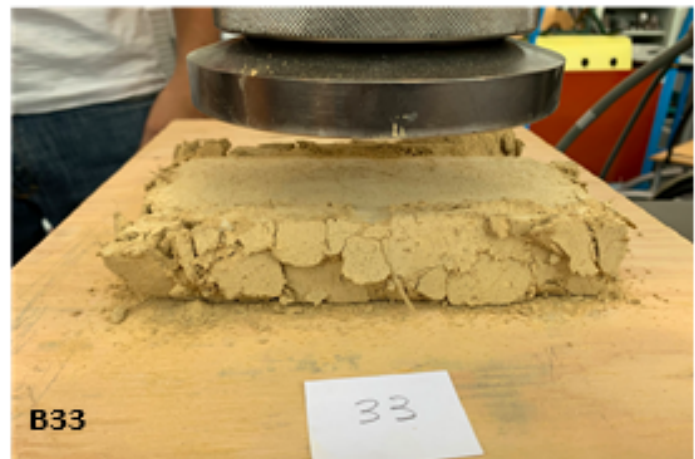
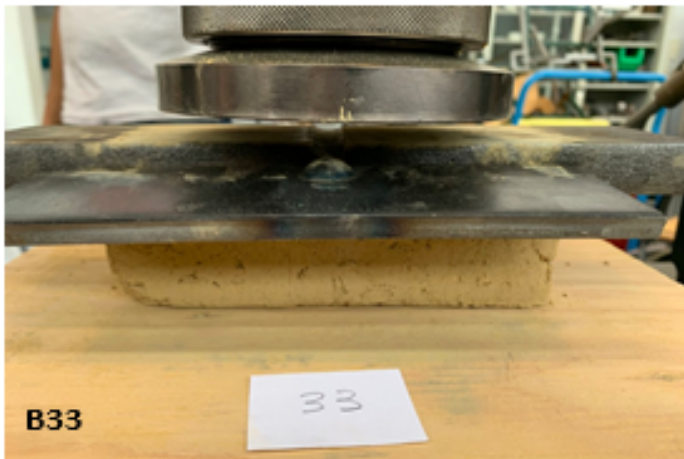










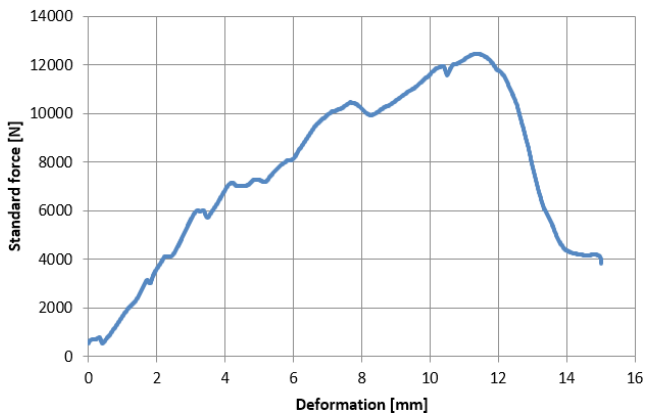


APPENDIX B2 - Force and Displacement Diagrams of Tested Specimens

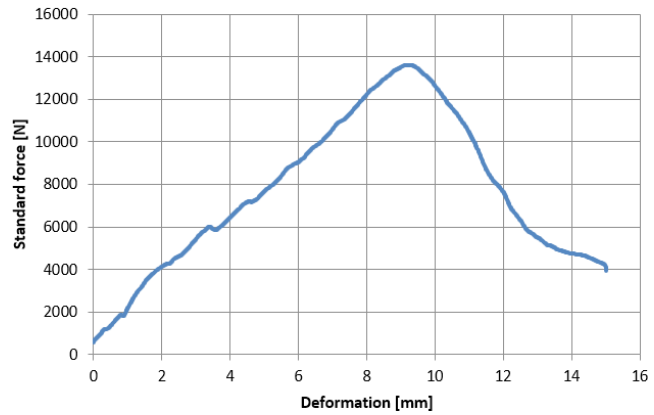
Mixture Code	Brick Code	Area [mm ²]	F _{max} [N]	dL at F _{max} [mm]	F _{max} /Area [N/mm ²]	Δl/l [-]	E [N/mm ²]
C01	B01	14875,00	12457,81	11,32	0,837	0,226	3,700
C01	B02	14875,00	13624,26	9,26	0,916	0,185	4,947
C01	B03	14875,00	13027,70	11,29	0,876	0,226	3,880
C01	B04	14875,00	15951,05	14,95	1,072	0,299	3,587
C01	B05	14875,00	19770,12	8,56	1,329	0,171	7,766
C01	B06	14875,00	21831,98	10,02	1,468	0,200	7,327
C01	B07	7875,00	78228,37	14,97	9,934	0,499	19,903
C01	B09	7875,00	29158,42	15,00	3,703	0,500	7,405
C01	B10	7875,00	87904,19	14,99	11,162	0,500	22,344
C01	B11	7875,00	30334,93	15,00	3,852	0,500	7,704
C01	B12	7875,00	79126,34	14,98	10,048	0,499	20,121
C02	B13	14875,0	18749,35	11,70	1,260	0,234	5,388
C02	B14	7875,0	5772,04	9,95	0,733	0,332	2,211
C03	B15	14875,0	32743,46	10,80	2,201	0,216	10,194
C03	B16	7875,0	42718,99	9,96	5,425	0,332	16,345
C04	B17	14875,0	18634,59	11,45	1,253	0,229	5,472
C04	B18	7875,0	10378,99	7,66	1,318	0,255	5,164
C05	B19	14875,0	36592,63	14,94	2,460	0,299	8,235
C05	B20	14875,0	33957,98	14,79	2,283	0,296	7,720
C05	B21	14875,0	56105,79	14,94	3,772	0,299	12,626
C05	B22	14875,0	51784,55	14,93	3,481	0,299	11,662
C05	B23	14875,0	56502,25	14,94	3,798	0,299	12,715
C05	B24	7875,0	27459,32	9,97	3,487	0,332	10,489
C06	B25	7875,0	20726,14	9,97	2,632	0,332	7,917
C06	B26	7875,0	37088,25	11,97	4,710	0,399	11,808
C07	B27	7875,0	43293,21	11,96	5,498	0,399	13,784
C08	B28	7875,0	76151,38	11,97	9,670	0,399	24,229
C09	B29	14875,0	37139,72	13,87	2,497	0,277	9,003
C10	B30	14875,0	45827,04	14,95	3,081	0,299	10,306
C11	B31	14875,0	59666,73	10,25	4,011	0,205	19,573
C11	B32	7875,0	44791,19	11,96	5,688	0,399	14,271
C12	B33	14875,0	83444,94	14,95	5,610	0,299	18,766

Table xx: Results of Uniaxial Compression Test

SPECIMEN B01



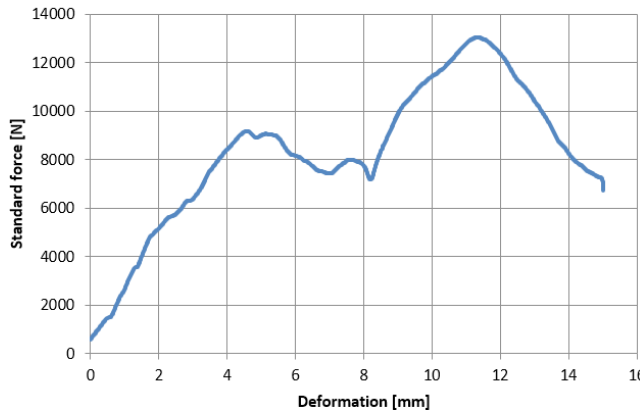
SPECIMEN B02



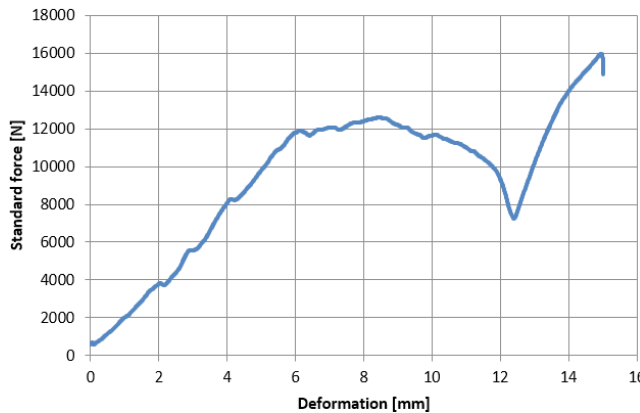
Mixture Code	Brick Code	Area [mm ²]	F _{max} [N]	dL at F _{max} [mm]
C01	B01	14875,00	12457,81	11,32

Mixture Code	Brick Code	Area [mm ²]	F _{max} [N]	dL at F _{max} [mm]
C01	B02	14875,00	13624,26	9,26

SPECIMEN B03



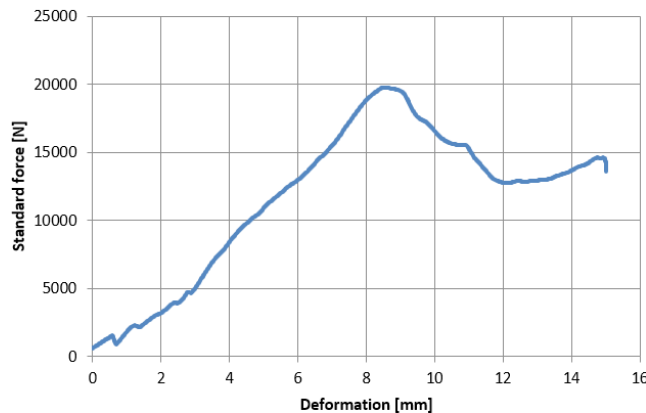
SPECIMEN B04



Mixture Code	Brick Code	Area [mm ²]	F _{max} [N]	dL at F _{max} [mm]
C01	B03	14875,00	13027,70	11,29

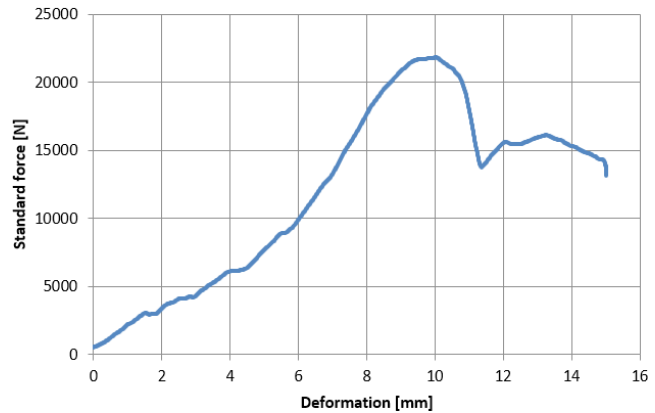
Mixture Code	Brick Code	Area [mm ²]	F _{max} [N]	dL at F _{max} [mm]
C01	B04	14875,00	15951,05	14,95

SPECIMEN B05



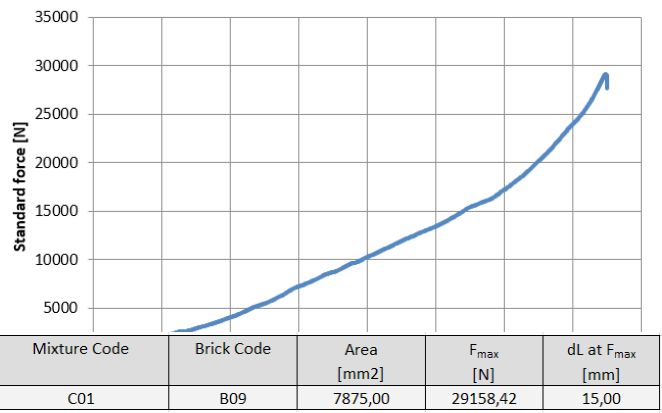
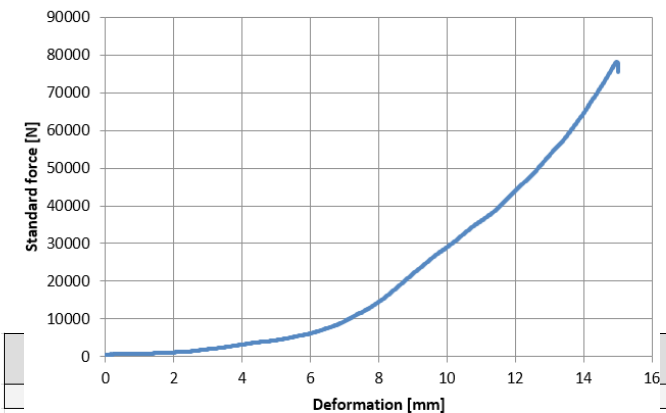
Mixture Code	Brick Code	Area [mm ²]	F _{max} [N]	dL at F _{max} [mm]
C01	B05	14875,00	19770,12	8,56

SPECIMEN B06

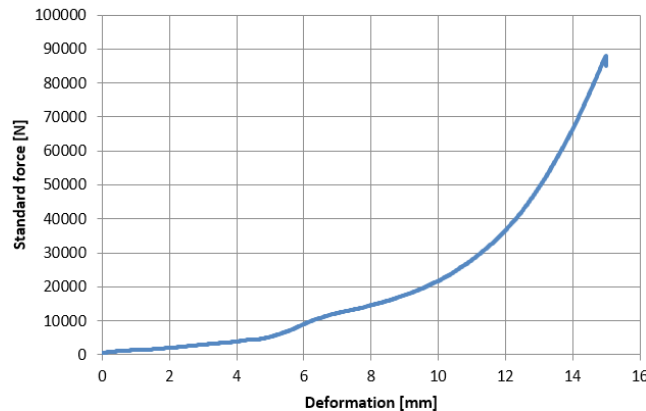


Mixture Code	Brick Code	Area [mm ²]	F _{max} [N]	dL at F _{max} [mm]
C01	B06	14875,00	21831,98	10,02

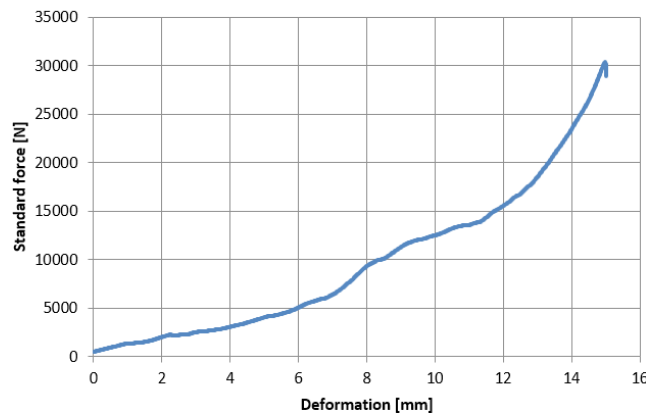
SPECIMEN B07



SPECIMEN B10



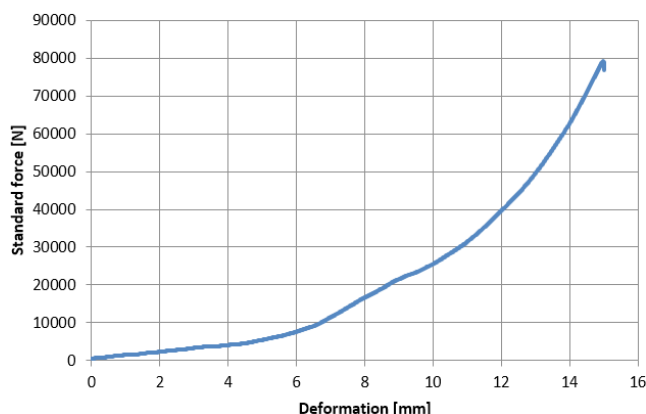
SPECIMEN B11



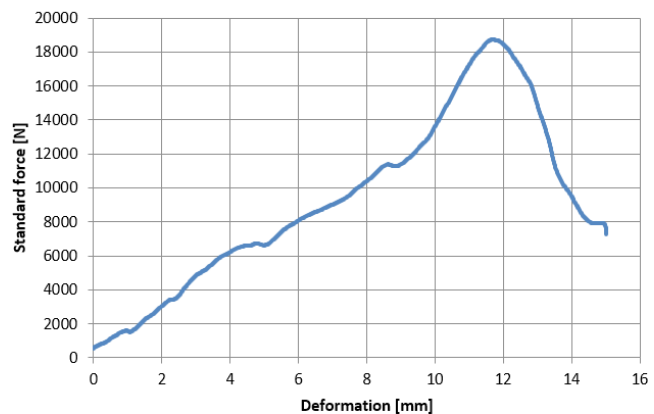
Mixture Code	Brick Code	Area [mm ²]	F _{max} [N]	dL at F _{max} [mm]
C01	B10	7875,00	87904,19	14,99

Mixture Code	Brick Code	Area [mm ²]	F _{max} [N]	dL at F _{max} [mm]
C01	B11	7875,00	30334,93	15,00

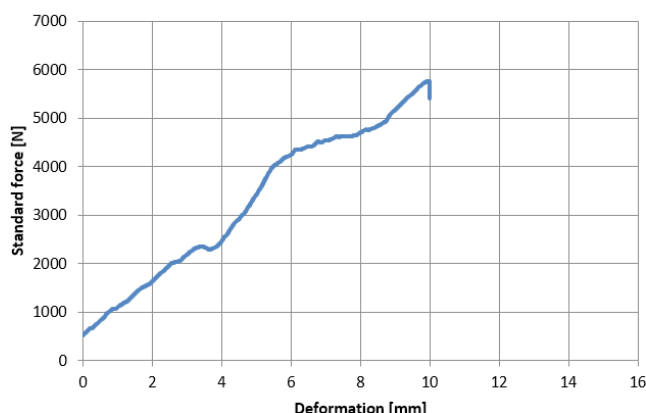
SPECIMEN B12



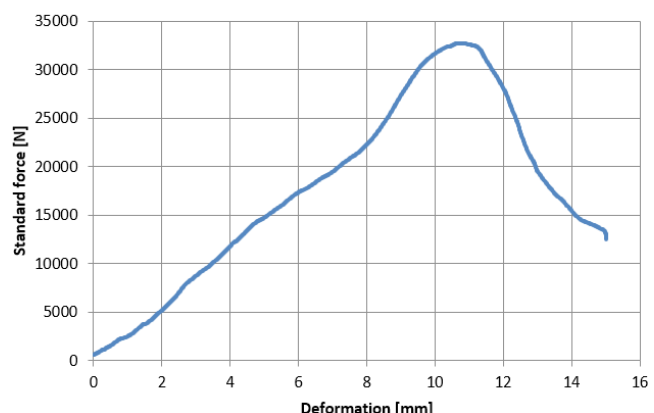
SPECIMEN B13



SPECIMEN B14

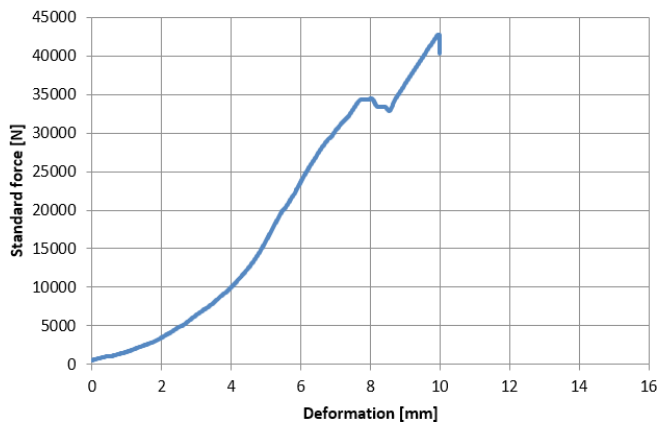


SPECIMEN B15



Mixture Code	Brick Code	Area [mm ²]	F _{max} [N]	dL at F _{max} [mm]
C01	B12	7875,00	79126,34	14,98

SPECIMEN B16

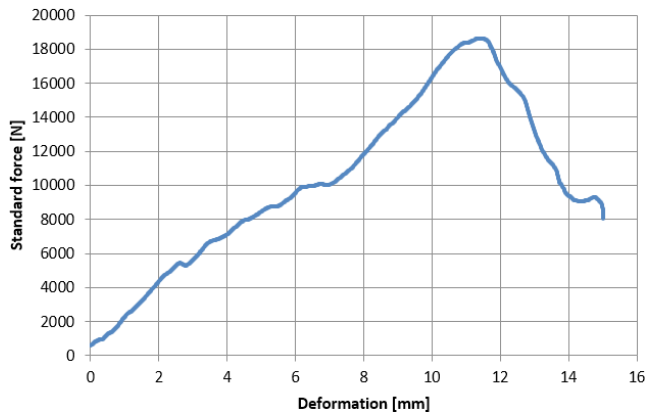


Mixture Code	Brick Code	Area [mm ²]	F _{max} [N]	dL at F _{max} [mm]
C02	B13	14875,0	18749,35	11,70

Mixture Code	Brick Code	Area [mm ²]	F _{max} [N]	dL at F _{max} [mm]
C02	B14	7875,0	5772,04	9,95

Mixture Code	Brick Code	Area [mm ²]	F _{max} [N]	dL at F _{max} [mm]
C03	B15	14875,0	32743,46	10,80

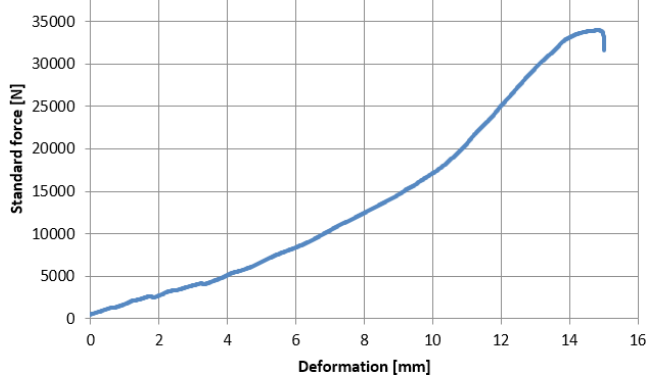
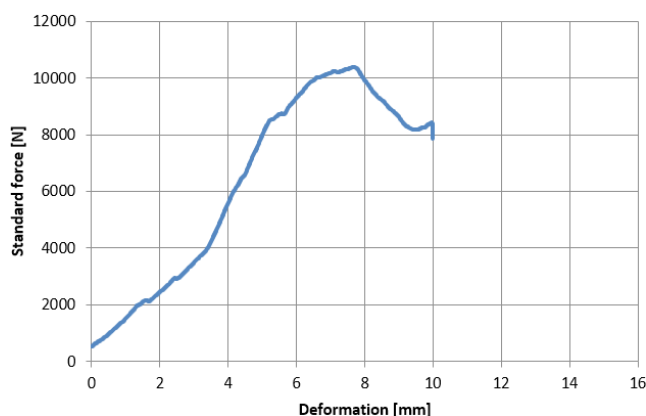
SPECIMEN B17



Mixture Code	Brick Code	Area [mm ²]	F _{max} [N]	dL at F _{max} [mm]
C03	B16	7875,0	42718,99	9,96

Mixture Code	Brick Code	Area [mm ²]	F _{max} [N]	dL at F _{max} [mm]
C04	B17	14875,0	18634,59	11,45

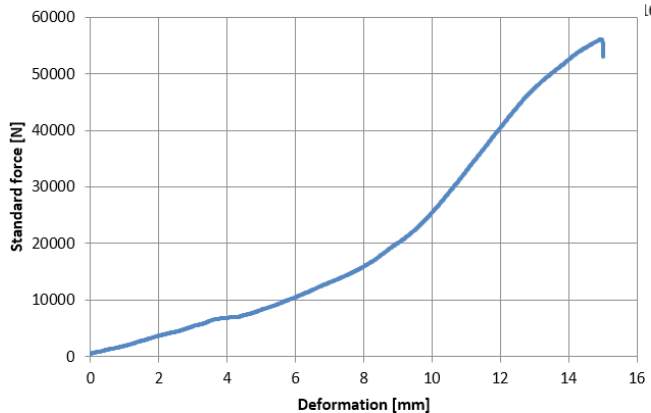
SPECIMEN B18



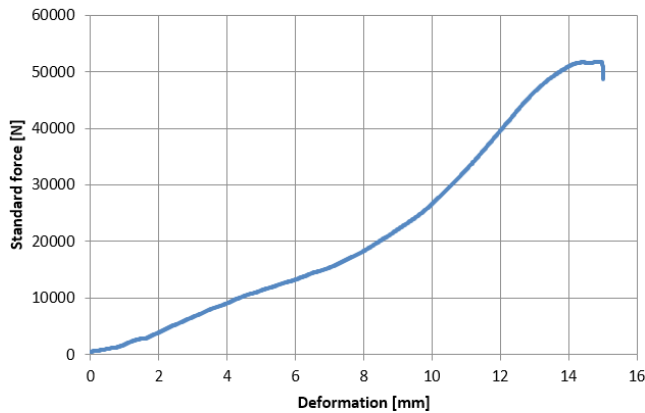
SPECIMEN B19



SPECIMEN B21

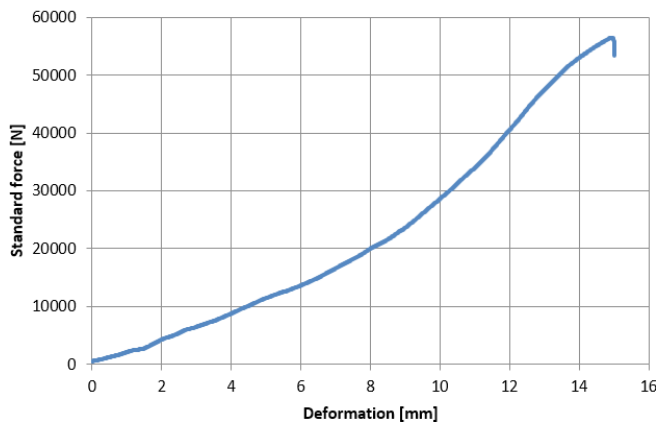


SPECIMEN B22



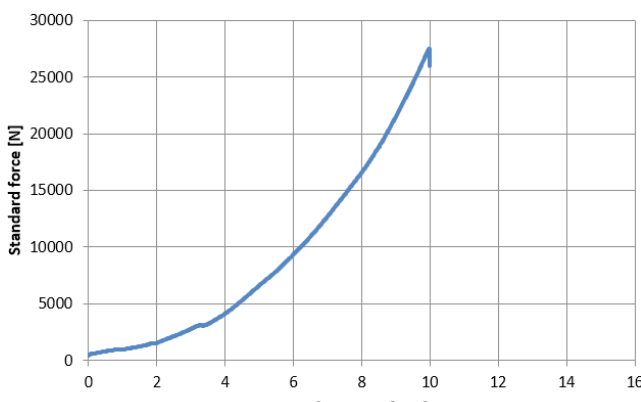
Mixture Code	Brick Code	Area [mm ²]	F _{max} [N]	dL at F _{max} [mm]
C05	B19	14875,0	36592,63	14,94

SPECIMEN B23

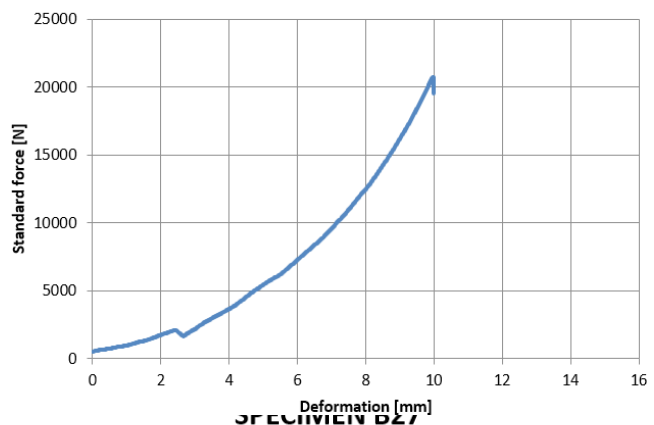


Mixture Code	Brick Code	Area [mm ²]	F _{max} [N]	dL at F _{max} [mm]
C05	B23	14875,0	56502,25	14,94

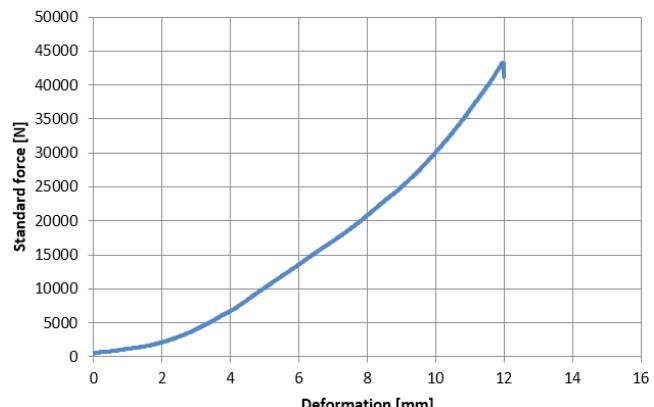
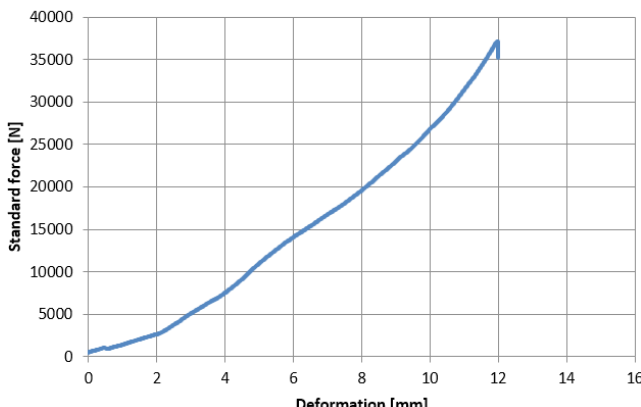
SPECIMEN B24



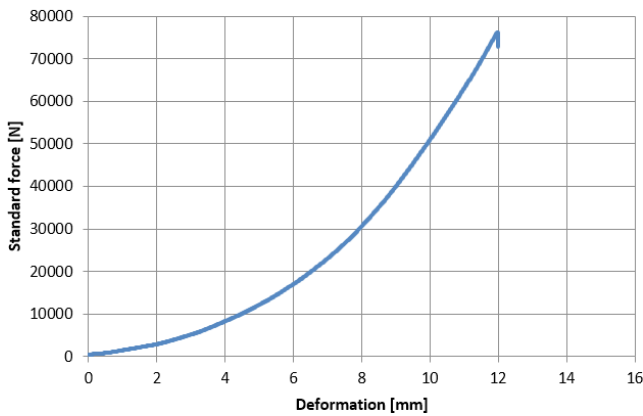
SPECIMEN B25



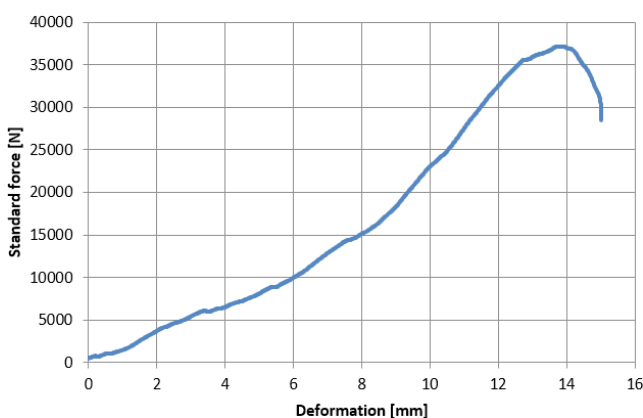
SPECIMEN B26



SPECIMEN B28

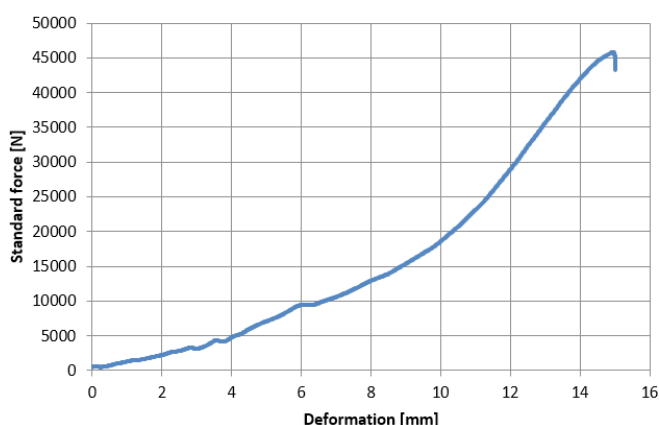


SPECIMEN B29



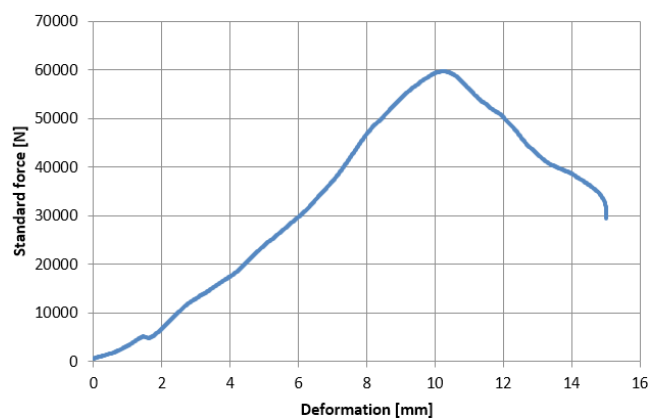
Mixture Code	Brick Code	Area [mm ²]	F _{max} [N]	dL at F _{max} [mm]
C06	B25	7875,0	20726,14	9,97

SPECIMEN B30

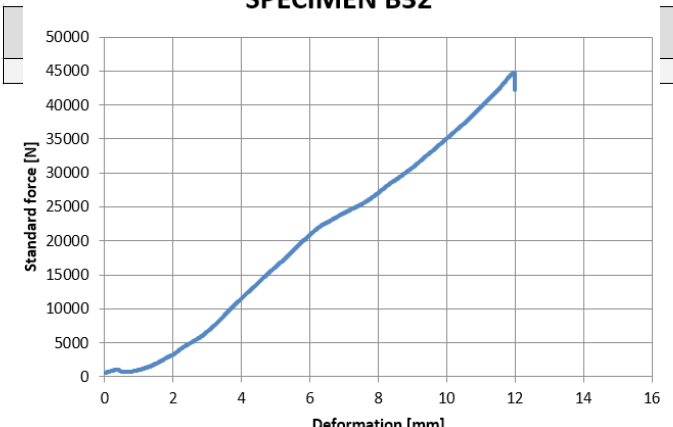


Mixture Code	Brick Code	Area [mm ²]	F _{max} [N]	dL at F _{max} [mm]
C09	B29	14875,0	37139,72	13,87
C07	B27	7875,0	43293,21	11,96

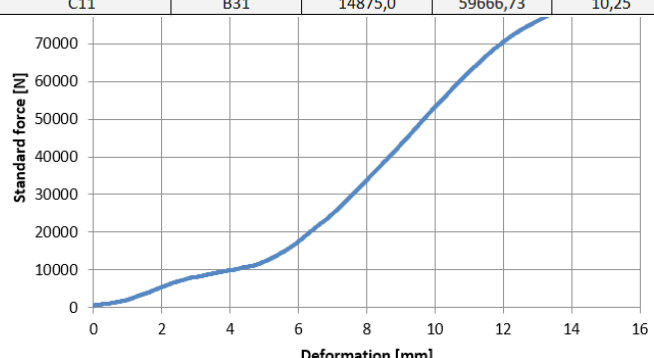
SPECIMEN B31



SPECIMEN B32



Mixture Code	Brick Code	Area [mm ²]	F _{max} [N]	dL at F _{max} [mm]
C11	B31	14875,0	59666,73	10,25



Mixture Code	Brick Code	Area [mm ²]	F _{max} [N]	dL at F _{max} [mm]
C11	B32	7875,0	44791,19	11,96

Mixture Code	Brick Code	Area [mm ²]	F _{max} [N]	dL at F _{max} [mm]
C12	B33	14875,0	83444,94	14,95